Mechanisms of muscle-tumor crosstalk:

Altered iron metabolism in the skeletal muscle promotes wasting and cancer progression

Thesis submitted for the degree of Doctor of Philosophy

in Biomedical Sciences and Oncology (XXXIIIrd cycle)

Universita degli studi di Torino

Candidate: Myriam Hsu

Supervisor: Prof. Paolo Ettore Porporato

Committee : Profs. Vincenzo Calautti, Massimiliano Mazzone, Giorgio Merlo, Valeria Poli

External Reviewers: Profs. Dario Coletti, Nicoletta Filigheddu

Academic Years: 2017-2021

Contents

Abbreviations

ABCB7 ATP-Binding Cassette sub-family B member 7
ACO Aconitase
ACOT1 Acyl-CoA Thioesterase 1
Akt Protein kinase B
ALAS Amino-Levulinic Acid Synthase
ALP Autophagy-Lysosomal Pathway
AMPK AMP-activated protein kinase
BMP Bone-Morphogenetic Protein
BNIP3 BCL2 Interacting Protein 3
BPS Bathophenanthroline Disulfonic Acid
CAF Cancer-Associated Fibroblast
CAT Catalase
CD Cluster of Differentiation
CDK1 Cyclin-Dependent Kinase 1
CM Conditionned Medium
CoQ10 Coenzyme Q10
COX Cyclooxygenase
CP Ceruloplasmin
CPT1b Carnitine Palmitoyl-Transferase 1b
CSA Cross-Sectional Area through
CXCL C-X-C Motif Chemokine Ligand
C/EBP CCAAT/Enhancer Binding Protein
DFO Deferoxamine
DMT1 Divalent Metal Transporter 1
DOHH Deoxyhypusine Hydroxylase
Dycb Duodenal Cytochrome b
DRP1 Dynamin Related Protein 1
ECM Extracellular Matrix
EMT Epithelial to Mesenchymal Transition
ETC Electron Transport Chain
ERFE Erythroferrone
ERK Extracellular Signal Regulated Kinase
FeCM Ferric Carboxymaltose
FBXL15 F-Box and Leucine Rich Repeat Protein 15
FLVCR1 Feline Leukemia Virus Receptor1
FoxO Forkhead Box Protein
FSP1 Ferroptosis Suppressor Protein 1
FTX Frataxin
FT Ferritin
FTH Ferritin Heavy Chain
FTL Ferritin Light Chain
FPN Ferroportin
GPX4 Glutathione Peroxidase 4
HCP1 Heme Carrier Protein 1
HNK Hinokitiol

HPA Hypothalamic-Pituitary-Adrenal
HRG1 Heme-Responsive Gene 1
HEPC Hepcidin
HEPH Hephestin
HIF Hypoxia-Inducible Factor
HO1 Heme Oxygenase 1
IFN-γ Interferon -Gamma
IGF Insulin-like Growth Factor
IL Interleukin
IRE Iron Responsive Element
IRP Iron Regulatory Protein
ISC Iron-Sulfur Cluster
ISCU ISC Assembly Enzyme
JAK Janus Kinase
KRAS Kirsten Rat Sarcoma Viral Oncogene Homologue
LCN2 Lipocalin2
Lf Lactoferrin
LIP Labile Iron Pool
LLC Lewis Lung Carcinoma
MAPK Mitogen Activated Protein Kinase
MCD Malonyl-CoA Decarboxylase
MCU Mitochondrial Calcium Uniporter
MFRN Mitoferrin
MMP Matrix Metallo-Proteinase
mTOR Mechanistic Target Of Rapamycin
MuRF1 Muscle RING-Finger protein1
NCOA4 Nuclear Receptor Coactivator 4
NF-κB Nuclear Factor Kappa-Light-Chain-Enhancer of Activated B Cells
NFS1 Cysteine Disulfurase 1
NO Nitric Oxide
NOS NO Synthase
NRF2 Nuclear Factor Erythroid 2-Related Factor 2
NTBI Non-Transferrin Bound Iron
OCR Oxygen Consumption Rate
OPA1 Optic Atrophy 1
PGC1-α Peroxisome Proliferator-Activated Receptor-Gamma Coactivator 1-Alpha
PI3K Phosphatidylinositol 3-Kinase
PHD Prolyl Hydroxylase
PDAC Pancreatic Ductal Adenocarcinoma
RBC Red Blood Cells
REDD1 Regulated in Development and DNA Damage Responses 1
ROS Reactive Oxygen Species
SCARA5 Scavenger Receptor Class A Member 5
SDH Succinate Dehydrogenase
STAT Signal Transducer and Activator of Transcription
STEAP Six-Transmembrane Epithelial Antigen of Prostate
TAM Tumor-Associated Macrophages

TBI Transferrin-Bound Iron
Tf Transferrin
TFR Transferrin receptor
TGF-β Transforming Growth Factor -Beta
TCA cycle Tricarboxylic Acid Cycle/ Krebs Cycle
TLR Toll-Like Receptor
TNF-α Tumor Necrosis Factor-Alpha
UCP Uncoupling Protein
UPS Ubiquitin-Proteasome System
VEGF Vascular Endothelial Growth Factor
XOR Xanthine Oxido-Reductase

Abstract

Cancer research has been globally focused on the intrinsic changes of cells that initiate tumorigenesis and sustain tumor progression. Contrariwise, how cancer reprograms systemic metabolism, and how alterations occurring in the host abet tumor growth have been poorly understood. Importantly, a systemic wasting syndrome also known as cachexia is highly prevalent in cancer patients and accounts for at least 20% of deaths. Noteworthy, cancer cells typically require higher amount of iron to support proliferation, but iron deficiency is also a common comorbidity in cancer patients. Whether and how cancer induces changes in iron metabolism in the skeletal muscle is unknown despite its significant pool of iron that could be mobilized. Herein, we found that iron homeostasis is strongly perturbed in the skeletal muscle of several models of tumor-bearing mice as well as in pancreatic and colorectal cancer patients, which are characterized by a strongly downregulated transferrin receptor 1 (TFR1) and ferritin upregulation. Reduction of iron either by genetic means (*e.g.* silencing of TFR1) or by selective chelation *in vitro* consistently induced myotube atrophy. Coherently, fiber-specific TFR1 silencing led to fiber atrophy, whereas its overexpression led to hypertrophy in healthy mice, indicating that iron availability controls directly muscle mass. Specifically, mitochondrial iron deficiency impairs mitochondrial metabolism and ATP generation that ultimately lead to AMPK activation and muscle atrophy in C26 tumor-bearing mice. Promisingly, iron supplementation prevented atrophy both *in vitro* and in tumor-bearing mice (despite no difference in tumor growth), and even prolonged survival. Furthermore, iron supplementation significantly increased strength in a cohort of colorectal and pancreatic cancer patients. Since tumor-bearing mice present significantly reduced heme levels in the skeletal muscle, we further investigated whether and how muscular heme metabolism can contribute to cancer progression using transgenic mice. Complementary to the previous findings, selective knockout of the heme exporter FLVCR1a in the skeletal muscle impacted tumor metastasis in LLC tumor bearing mice, without affecting tumor growth. Strikingly, muscle-specific FLVCR1a silencing significantly reduced neutrophil count of the primary tumor, suggesting a modulation of the immune landscape by the skeletal muscle during cancer progression. Altogether, cancer induces alterations in skeletal muscle iron metabolism, which can in turn favor cancer progression, and targeting iron trafficking or normalizing iron levels are potential therapeutic strategies for cancer-induced cachexia.

General introduction

Cancer is a leading cause of mortality and morbidity worldwide. Although research in oncology has made significant advances in understanding tumor metabolism, cancer remains a global growing burden, notably in developing countries (WHO report 2020). Cancer includes all diseases that are characterized by the growth of potentially invasive cells that jeopardize normal physiology of the organ or host where they reside. Common abnormalities underlying malignant transformation and tumor progression have been increasingly clear. Notably, cancer cells undergo considerable metabolic changes to foster unbridled proliferation in a hostile environment characterized by nutrient deprivation, inefficient perfusion, and competitive immune infiltrates (*1*). While metabolic reprogramming has been recognized as a hallmark of cancer, the role of micronutrients in shaping such adaptations remains scarcely investigated. In particular, the broad electron-transferring abilities of iron makes it a versatile cofactor that participate in a myriad of biochemical reactions vital to cellular homeostasis, including cell respiration and DNA replication. Although iron itself can readily participate in redox reactions enabling these processes, its reactivity also contributes the formation of reactive oxygen species (ROS).

Approximately one third of cancer related deaths is caused by a multi-organ wasting condition termed cachexia. However, this metabolic syndrome is often considered as a mere epiphenomenon of the primary pathology hence overlooked upon medical diagnosis. Similarly, research in oncology mainly focuses on the tumor, while how systemic changes occurring in the host influence tumor onset and growth remain largely unexplored. Skeletal muscle atrophy is the main feature of cachexia that debilitates cancer patients and strongly reduces their quality of life. Altered iron metabolism is one of the most common systemic changes in cancer patients. Noteworthy, iron deficiency is highly prevalent in patients afflicted with pancreatic or gastro-intestinal cancers, which are also the most susceptible to cachexia.

Albeit lacking functional properties, tumors are structurally similar to organs as they are complex unit of abnormal epithelial or glandular cells, stromal cells (including mesenchymal cells, vascular cells), and immune cells (in particular neutrophils, T and B lymphocytes, macrophages) joint by an extracellular matrix (**Fig. 1**) (*2*). Consequently, the process of tumor development is highly dependent on the surrounding environment, which can directly contribute to the growth and invasion of cancer cells in the same way as during organogenesis. Both intrinsic factors such as (epi)genetic changes and extrinsic factors including nutrient availability, extracellular matrix (ECM) stiffness, oxygen and pH

gradient strongly influence cancer cell gene expression and metabolism, resulting in highly heterogeneous cell populations with variable metabolic features within the same tumor (*3*).

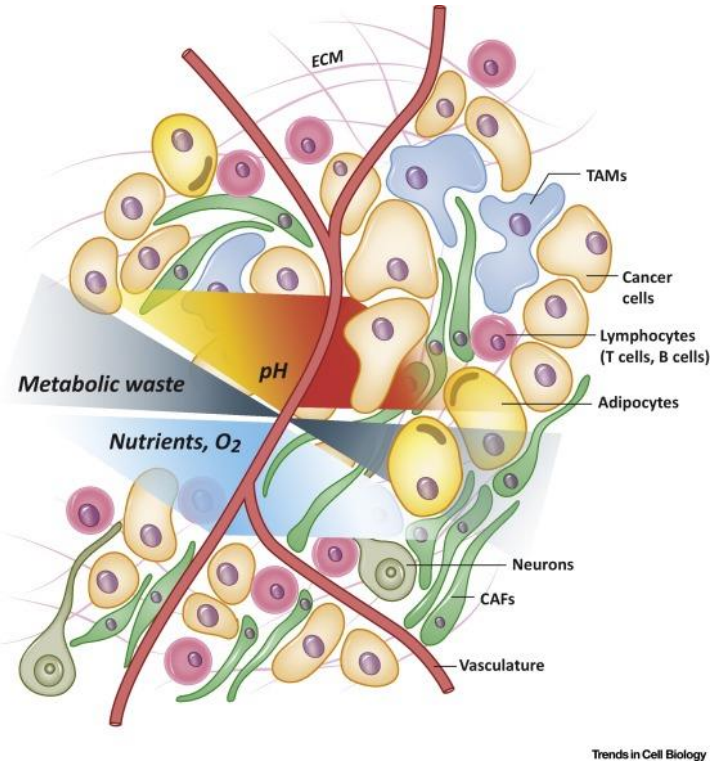

Figure 1. Tumors are composed of different cell populations giving rise to metabolic heterogeneity (*3*)
Tumor growth is supported by cancer-associated fibroblasts (CAF), adipocytes, blood vessels, and nerves within the extracellular matrix (ECM). Infiltration of immune cells such as T and B cells, neutrophils, and tumor associated macrophages (TAM) further reshape the tumor microenvironment. Consequently, gradients of metabolites, oxygen tension and pH define the metabolic features of tumors.

Cancer cells reside in an overall hostile environment characterized by physical pressure, oxidative stress, nutrient shortage, immune invasion, hypoxia, and acidosis (*3*). However, they can also communicate and hijack the surrounding non-cancer cells to adopt a pro-tumoral phenotype. For instance, squamous cell carcinoma cells secrete glutamate to fuel the production of aspartate by surrounding fibroblasts, which feed aspartate back to cancer cells for nucleotide synthesis (*4*). Ovarian cancer cells release *N*-acetylaspartate which stimulates glutamine synthetase expression in macrophages, causing their polarization to M2, pro-tumoral phenotype (*5*). Moreover, the tumor microenvironment also influences the efficacy of anticancer therapies. Notably, the abnormal organization of the tumor characterized by increased distance between cancer cells and capillaries leads

to poor drug distribution. The overall acidic extracellular space due to hypoxia also decreases the efficacy of several chemotherapeutic drugs and radiotherapy while upregulating survival signals in cancer cells (*e.g.* Bcl-xL and heat shock proteins through HIF1-α) (*6*). Finally, stromal cells (such as vasculature cells or cancer-associated fibroblasts) can also secrete signals that sustain cancer cell stemness by activating Notch signaling (*7, 8*), indirectly contributing to tumor relapse.

Beyond the tumor microenvironment, further crosstalk between cancer cells and distant organs have been less studied and evidenced only recently. In a mouse model, advanced glycation end products (glycated proteins or lipids) derived from lung adenocarcinoma cells were shown to instruct bone osteoblasts to supply specific pro-tumoral neutrophils (*9*). Similarly, such "trialogue" was described with cancer-associated fibroblasts through C-X-C Motif Chemokine Ligand 12 (CXCL12) secretion, triggering the release of hematopoietic progenitors from the bone marrow, which in turn support metastatic growth (*10*). Intriguingly, in prostate tumor-bearing mice, brain-derived neural progenitors were found to reach through circulation the primary tumor and metastases, where they finally differentiate into adrenergic neurons that are known to support tumorigenesis (*11*). These studies underscore that long range interactions between malignant cells and other organs are pivotal to tumor progression, and novel anticancer strategies should aim at breaking the network. In addition, understanding how tumor progression drives alterations in the host can provide potential therapeutic options to alleviate the disease.

Cancer-induced systemic changes

Cancer is a systemic disease, not only because cancer cells can enter blood and lymphatic circulation before reaching distant organs where they form metastases, but they also alter the metabolism and immunity of the organ and even the whole organism. Noteworthy, immunodeficiency, stroke due to thromboembolism, and organ failures are amidst the direct cause of deaths in cancer patients, rather than the tumor itself (*12*). Factors secreted by tumors can exert far-reaching effects that impact not only the microenvironment but also systemically. These include notably growth factors and cytokines: Vascular endothelial growth factor (VEGF), platelet-derived growth factor (PDGF), angiopoietins, angiogenin, hepatocyte growth factor, fibroblast growth factor, transforming growth factor-beta (TGF-β), growth-related oncogene-alpha (CXCL1), as well as other hormones such as leptin (*13*). Most of these factors are amplified during cancer progression and cachexia, which will be discussed in detail hereafter.

1. Chronic inflammation

Cancer causes chronic and systemic inflammation, which is known to abet cancer initiation and progression, creating a vicious cycle. Roughly 20% of human cancers are related to sustained inflammation resulting from microbial infections (*e.g.* Epstein-Barr lymphomas, human papilloma virus in cervix cancer, helicobacter pylori in gastric cancer), chronic exposure to irritants (*e.g.* asbestos for mesothelioma, smoke for lung cancer, dietary heme or acrylamide for colorectal cancer), or autoimmune diseases (*14*). In cancer patients, inflammation is markedly present both within the tumor stroma and systemically, with increased circulating cytokines including IL-1, IL-6, and IL-18, that correlate with poor prognosis (*15, 16*).

Oncogenic transcription factors such as nuclear factor kappa-B (NF-κB), signal transducer and activator of transcription 3 (STAT3) or hypoxia-inducible factor 1 alpha (HIF1-α) also mediate the expression of cytokines and chemokines in the tumor. Some cytokines favor tumor progression (TGF-β, interleukins 6, 17, 23, FAS ligand, tumor necrosis factor-alpha (TNF-α)), while others have anti-tumor properties (IL-12, IFN-γ) (*14*). Noteworthy, immune cells and fibroblasts are able to produce cytokines, growth factors and chemokines at much higher levels than tumor cells (*17-19*). Therefore, systemic inflammation is mainly driven by the host's response to the tumor, rather than by the malignancy itself.

Indeed, several tissues contribute to the excessive inflammation. The liver plays a key role in mediating systemic inflammation by secreting acute-phase proteins, including C-reactive protein (CRP), amyloid A, alpha 1 antitrypsin, and alpha 1 acid glycoprotein (*20*). Notably, cytokines secreted by Kupffer cells strongly induce systemic inflammation, and the absence of hepatic and splenic macrophages is sufficient to prevent death in mice challenged with zymosan, a potent inducer of sterile inflammation (*21*).

Interestingly, the gut microbiota also controls inflammation both within the tumor microenvironment and systemically. Antibiotic-treated or germ-free tumor bearing mice have impaired innate immune response to immunotherapy and oxaliplatin, characterized by lower cytokine production and tumor necrosis (*22*). Another study showed that cyclophosphamide, a chemotherapeutic drug, alters the composition of microbiota in the small intestine and stimulates the generation of a subset of T helper cells that promote adaptive immune response (*23*).

The degree of inflammation generally correlates with tumor aggressiveness and poor prognosis.Specifically, in lung and gastrointestinal cancer patients, chronic systemic inflammation (denoted by increased serum levels of acute phase proteins such as C reactive protein) along with elevated circulating gamma-glutamyl transferase and alkaline phosphatase activity correlated with advanced stage (*24*). Inhibitors of inflammatory cytokines (TNF-a, IL-6, IL8) have shown however only limited outcome in clinical trials on cancer patients (*25*), suggesting a complex irreversible phenomenon.

2. Immuno-deficiency

Cancer severely suppresses immunity, thereby increasing dramatically patient mortality. Although the impact on immunity is not always obvious in early-stage cancer patients, immunodeficiency develops with tumor progression and chemotherapies. Circulating myeloid-derived suppressor cells can increase up to 10-fold in cancer patients (*26*). Cancer-induced immunosuppression is mainly characterized by functional impairment of T-cell, accumulation of T-reg and decreased antibody production, disabling the rejection of allogenic tumors in mice (*27*).

Indeed, both pro-tumoral and anti-tumoral inflammation shape the evolution of tumors, and cancer immunotherapy is a highly active area of research. Several mechanisms of immune evasion and inhibition have been characterized. For instance, metastatic cells can upregulate the secretion of

programmed death-ligand 1 (PD-L1) to suppress CD8 T-cell function (*28*). Pancreatic cancer cells also release miR-203 through exosomes that downregulates toll-like receptor 4 (TLR4) and downstream inflammatory cytokines expression by dendritic cells (*29*). Intriguingly, immune cells including macrophages, T-reg cells, neutrophils and natural killer cells may have both antitumoral and pro-tumoral properties. The correlation between their number and patient prognosis can be therefore highly variable from one context to another (*30*).

3. Neuro-endocrine changes

During cancer progression, inflammatory cytokines such as IL-1β, IL-6, and TNF-α are amplified within the hypothalamus, causing central nervous system inflammation and consequently alterations of activity or weight-modulating pathways (*31, 32*). In addition, cancer has been generally associated chronic stress, which is characterized by upregulated release and signaling of catecholamines by the sympathetic nervous system (adrenal-medullary axis) that normally mediates the fight-or-flight reflex in normal conditions. Clinical studies have also found elevated circulating levels of cortisol in cancer patients (including colorectal, prostate, and breast cancers) (*33-35*), which is known to mediate immunosuppression, depression, or even muscle atrophy (discussed hereafter) (*36*). In most cases, the increase correlated with IL-6 levels, indicating that inflammation is the key trigger for excessive hypothalamic-pituitary-adrenal (HPA) activity.

Primary and secondary lymphoid organs are innervated by sympathetic nerves, while lymphocytes and monocytes also express receptors for the stress hormones (including adrenocorticotropic hormone ACTH and cortisol, secreted by the HPA axis) (*37*). Therefore, cancer can also alter the immune system through the activation of nervous stress response which indirectly promotes tumor progression. In melanoma and colon cancer mouse models, an enriched housing environment significantly reduced leptin secretion by adipose tissue, leading to decreased tumor growth and increased remission (*38*). In line with this finding, epidemiological studies have shown that prostate adenocarcinoma patients on androgen deprivation therapy treated with non-selective beta-blockers have lower cancer-caused mortality (*39*). Likewise, in female patients with melanoma or breast cancer, beta-blockers administration significantly increased survival (*40, 41*). From the mechanistic standpoint, norepinephrine upregulates the production of MMP2, MMP9, and VEGF in human nasopharyngeal carcinoma (*42*), while β-Adrenergic receptor inhibition on human melanoma cell lines suppressed VEGF, IL-8, and IL-6 expression (*43*).

In contrast to the sympathetic nervous system, the role of parasympathetic nervous system in cancer has been less documented. However, both muscarinic and nicotinic receptors that bind acetylcholine and the downstream signaling seem to initiate cytokine synthesis by immune cells (*44*). In gastric and prostate tumor-bearing mice, parasympathetic denervation, genetic knockout, or pharmacological inhibition of muscarinic receptors inhibited tumor growth and metastasis, respectively (*45, 46*). However, cholinergic inhibition can indirectly stimulate adrenergic pathway as both axes influence each other. Nevertheless, since many cancers show nerve outgrowth, targeting neurotropic growth factors secreted by cancer cells would be a promising alternative approach (*47*).

4. Hemodynamic abnormalities

Roughly half of cancer patients (especially those with metastases) present high risk of thromboembolism. This susceptibility mainly results from an imbalance between coagulative and fibrinolytic factors within the tumor where cancer cells, endothelial cells, immune cells, and platelets interact and contribute to thrombosis (*48*). Both cancer cells and the surrounding stromal cells (especially macrophages and endothelial cells) can express or release pro-coagulant factors that initiate hemostasis by binding factors of the coagulation cascade (*48*). Angiogenesis is also linked to increased coagulation as VEGF signaling stimulates tissue factor secretion by endothelial cells (*49*). Moreover, the pro-thrombotic state is amplified by systemic inflammation as inflammatory cytokines stimulates the secretion of tissue factor by immune cells (notably eosinophils and monocytes) (*50, 51*).

Multi-organ wasting or cancer-induced cachexia

The etymology of cachexia stems from the Greek words “kakos” and “hexis”, which literally mean bad condition (*52*). Cachexia is defined as a systemic, multifactorial syndrome characterized by a loss of skeletal muscle mass, with or without loss of fat mass, that cannot be fully reversed by conventional nutritional support and leads to progressive functional impairment. In consequence, patients present intolerance to chemotherapy, complications from surgery and overall decreased prognosis. Clinical diagnosis is made when the patient (with a normal body mass index) has lost at least 5% of their total body weight in the previous six months without fasting, diet, or lifestyle change (*53*).

Cachexia affects approximately 9 million patients afflicted with advanced chronic diseases worldwide; including heart failure, kidney failure, chronic obstructive pulmonary disease, acquired immunodeficiency syndrome (AIDS), and notably cancer. There is a clear association of cachexia with most life-threatening chronic diseases and its prevalence is uniformly high at the end of life (up to 80%). Current therapeutic approaches can only slow the rate of weight loss (which occurs regardless of energy intake) and physical decline. When cachexia becomes refractory, interventions are often futile and increasingly invasive, patients are emaciated and typically die within a few months (*53, 54*).

Roughly half of the global cancer deaths are attributed to cancer types that are associated with high prevalence of cachexia (**Fig. 2**), including pancreatic, esophageal, gastric, colorectal, pulmonary, and hepatic cancers (0.33, 0.4, 0.72, 0.69, 1.59, and 0.75 million deaths, respectively) (WHO 2020). This association likely results from the diagnosis at late-stage, the physical impact of tumor on digestion and absorption, as well as specific cancer-induced hormonal and metabolic alterations. Besides these cancer types, additional factors can increase the susceptibility to developing cachexia, including sex (male patients being more susceptible), age, genetic factors, other comorbidities and/or treatments that have catabolic side effects. For instance, cardiac failure increases the risk of cachexia in cancer patients (*55*), while sorafenib (a tyrosine kinase inhibitor) and glucocorticoids (treatment of chronic inflammatory diseases or palliative care of cancer patients) promote catabolism in the skeletal muscle (*56*). Importantly, patients that are underweight prior to cancer diagnosis present higher risk of weight loss, morbidity, and mortality (*57*), but higher BMI does not confer absolute protection as massive weight loss can still occur in obese patients (*58*). In fact, muscle mass and strength were shown to accurately predict the prognosis in cancer-associated cachexia, regardless of total body weight (*58*). Indeed, patients with early-stage cancer can also present cachexia, that is reversible upon successful cure of the

underlying cancer (*59*). Contrariwise, some patients maintain or even gain weight (including muscle and fat) during cancer progression (*60*), cachexia is therefore not an inevitable outcome of cancer. Noteworthy, in a mouse model of colon cancer, the reversal of cachexia significantly prolonged survival despite consistent tumor growth, indicating that cachexia should be considered as a separate, distinct pathology rather than a complication of cancer (*61*).

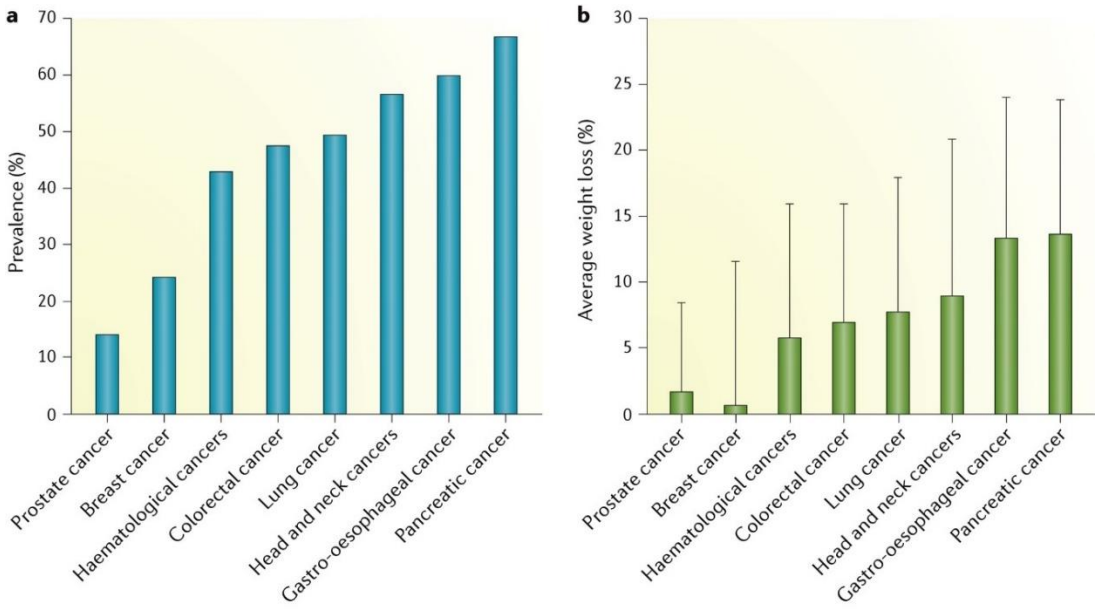

Figure 2. Prevalence of cachexia and the average loss of weight in patients according to the cancer type (*62*)
The prevalence of cachexia can reach up to 70% in patients afflicted with pancreatic, head and neck, gastro-intestinal, or lung cancers (left). Noteworthy, the degree of weight loss also correlates with the prevalence of cachexia (right).

Pathophysiology of cancer-induced cachexia

The syndrome of cachexia is mainly driven by a combination of reduced food intake (anorexia), aberrant systemic metabolism characterized by elevated energy expenditure, and chronic inflammation. Cachexia can be potentially mediated by factors deriving directly from cancer cells, cells of the tumor microenvironment, or far-reaching host tissues (*63*). These factors include inflammatory cytokines TNF-α, IL-1β, IL-6, IFN-γ, members of the transforming growth factor TGF-β superfamily (*e.g.* activins, myostatin), eicosanoids (prostaglandins and thromboxane) (*64*), and heat-shock proteins (HSP70, HSP90) (*65*) that are commonly elevated in the serum of cachectic patients. They can directly activate catabolism in target organs or induce metabolic shifts and signaling pathways in others to

increase overall energy expenditure (*63*, *66*). Consequently, the intricate combination of humoral, neural, and behavioral effectors induces catabolism, primarily in skeletal muscle, adipose tissue, and cardiac muscle along with multi-organ dysfunction (**Fig. 3**) (*63*, *66*, *67*).

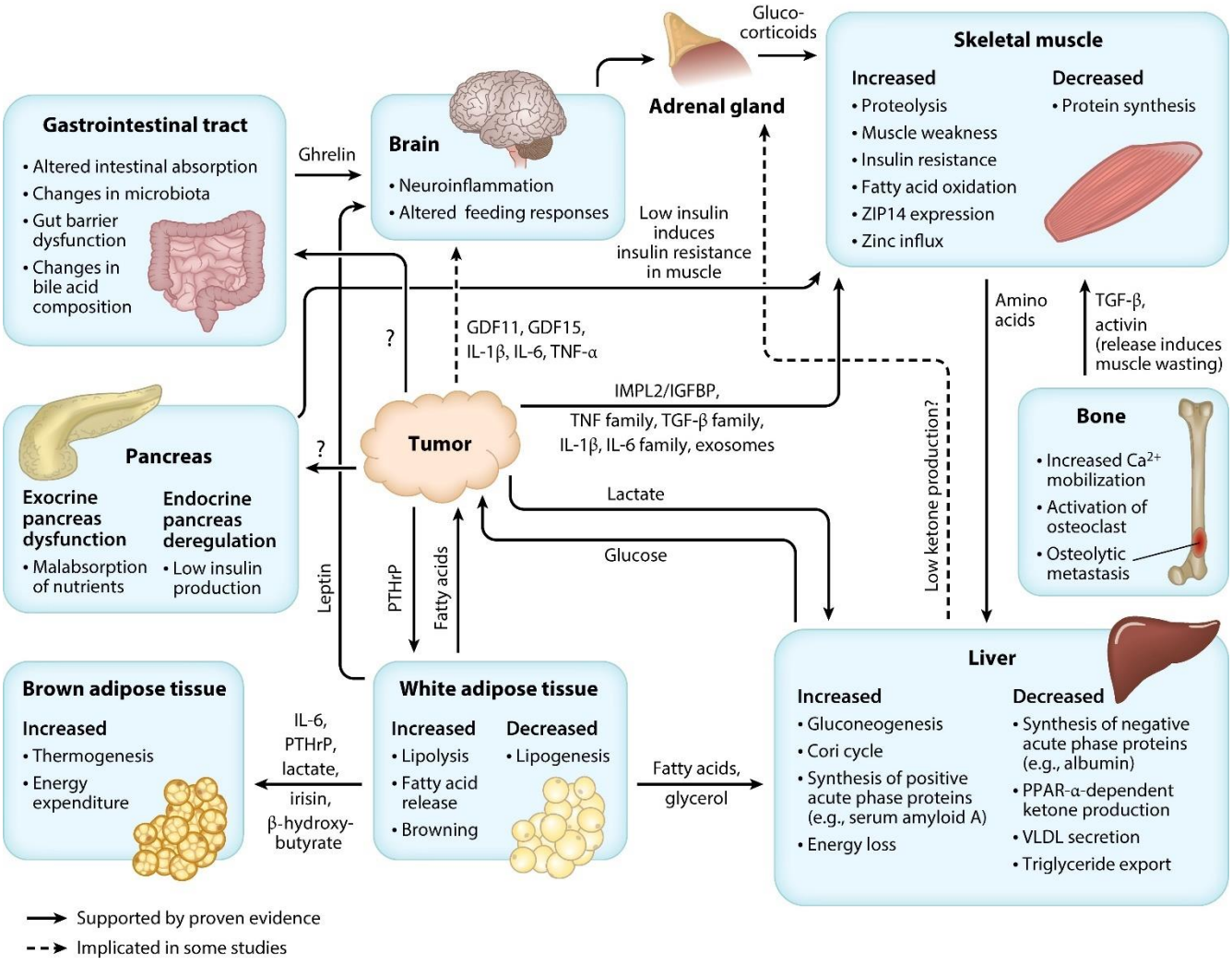

<u>Figure 3. Overview of systemic alterations occurring during cancer-induced cachexia</u> (*68*)
Cancer cachexia represents a whole-body wasting syndrome resulting from both tumor-host and inter-organ interactions. Most organs including the brain, gastro-intestinal tract, pancreas, liver, bone, adipose tissue, and especially skeletal muscle show strongly altered metabolism.

1. Role of central nervous system, feeding behavior, and HPA axis in cachexia

Cancer-induced inflammation alters CNS homeostasis, enhancing sympathetic nervous system and adrenal corticosteroids secretion to amplify the catabolism of carbohydrates, proteins, and lipids in peripheral tissues as well as anorexia (*69*).

Intracerebral administration of IL-1β is sufficient to trigger rapid atrophy in the skeletal muscle though glucocorticoid signaling (*31*). Importantly, the hypothalamus regulates appetite, which is abnormally decreased in cancer patients and exacerbates cachexia. Appetite-suppressing (anorexigenic) function is mediated by the ventromedial hypothalamus, whereas appetite-enhancing (orexigenic) function is regulated by the lateral hypothalamus. Their outputs are primarily driven by anorexigenic proopiomelanocortin (POMC) neurons and orexigenic neuropeptide Y (NPY)/agouti-related peptide (AgRP) neurons (*70*). Peripheral tissues also interact with these neurons to modulate feeding behavior. For example, the adipose tissue-derived hormone leptin exerts anorexigenic effects by activating POMC neurons and inhibiting the NPY/AgRP neurons (*70*). The opposite mechanisms mediate the orexigenic activity of the gut hormone ghrelin, which is paradoxically increased in cancer patients (*71*). Besides its orexigenic effect on the CNS, it also regulates blood glucose homeostasis, adiposity (*72*), reduces energy expenditure (*73*), and impedes muscle atrophy (*74*). However, cancer-associated cachexia is associated with resistance to ghrelin, and its increase has been considered as a compensatory mechanism of the body aiming at mitigating tissue wasting (*71*). Anamorelin, an oral ghrelin mimetic, improved both appetite and muscle mass in cancer patients (*75, 76*).

Another important neurotransmitter regulating feeding behavior is serotonin. Tumor bearing mice showed lower brain serotonin that inversely correlated with food intake (*77*). *In vitro*, serotonin repressed neuronal hypothalamic NPY secretion (*78*). In tumor-bearing rats, pharmacological activation of AMP-activated protein kinase (AMPK) in the hypothalamus reversed anorexia by mitigating inflammation and POMC signaling (*79*).

As discussed above, the hypothalamus-pituitary-adrenal (HPA) axis is also altered in cancer patients. Pro-inflammatory cytokines including TNF-α, IL-1β, and IL-6 stimulate the secretion of CRH (by the hypothalamus), ACTH (by the pituitary), and cortisol release from the adrenal glands (*80-82*). Glucocorticoids (*e.g.* cortisol) are hormones affecting multiple organs besides their anti-inflammatory effects (*83*). Importantly, glucocorticoids promote insulin resistance, gluconeogenesis, and lipogenesis, thereby increasing whole body energy expenditure (*84, 85*). Increased circulating glucocorticoids or HPA activity has been reported in several *in vivo* cachexia models (*35, 86-88*). Interestingly, *in situ* central nervous system inflammation activated HPA axis and elicited rapid muscle atrophy that can be otherwise spared with adrenalectomy in mice (*31*). Mechanistically, glucocorticoids drive muscle atrophy through the suppression of IGF-1 signaling while inducing myostatin production, resulting overall in reduced mTOR activation and increased FoxO signaling (*89-91*).

2. Adipose tissue wasting and browning

Adipose tissue can be composed of white, beige, or brown adipocytes that differ by their location and functions. The shade of the tissue is determined by the levels of uncoupling protein 1 (UCP-1), located in the inner mitochondrial membrane and responsible for the uncoupling of respiratory chain from ATP synthesis, generating heat. The primary role of WAT is to store energy in the form of triglycerides, and brown adipose tissue (BAT) mostly expends energy (*92*). Beige adipocytes function as brown adipocytes but are formed by the browning of WAT as a response to stress stimuli such as prolonged cold exposure and β adrenergic activation (*93*). This phenotypic switch is associated with increased energy expenditure and improved insulin sensitivity leading to body weight loss, hence represents a promising strategy to treat obesity (*94*). Nonetheless, WAT browning is rather detrimental in other pathological conditions such as cancer, kidney failure, or post-burn injury (*95, 96*). In tumor-bearing mice, enhanced lipolysis, elevated total energy expenditure, and BAT thermogenesis occur during early stage cachexia (*97*). One important cause of browning is inflammation, and neutralization of IL-6 reduced the severity of cachexia by decreasing UCP1 levels in several murine models (*98*). In a Lewis lung carcinoma model of cancer cachexia, tumor-derived parathyroid-hormone-related protein (PTHrP) was shown to drive the expression of genes involved in thermogenesis in adipocytes, and PTHrP inhibition prevented fat browning as well as muscle atrophy (*99*)**.** Similarly, the silencing of adipose triglyceride lipase (ATGL), the enzyme that catalyzes the first step of triacylglycerol hydrolysis, protected mice from both WAT and muscle wasting (*100*). These studies also indicate that WAT wasting typically precedes the one of skeletal muscle in cancer-induced cachexia, and intriguingly, altered metabolism in adipose tissue can cause muscle proteolysis.

Of note, carboxyl-metabolites such as lactate or β-hydroxybutyrate can also induce fat browning during redox changes (*101*). Therefore, skeletal muscle (*e.g.* after intensive exercise) or highly glycolytic tumors could promote thermogenesis through lactate release. Indeed, skeletal muscle metabolism affects WAT homeostasis as well. Peroxisome Proliferator-Activated Receptor-Gamma Coactivator 1-Alpha (PGC1-α) overexpression in the muscle led to increased UCP1 expression in WAT through a myokine known as irisin (FNDC5) (*102*). In addition, cell death–inducing DNA fragmentation factor alpha subunit-like effector A (CIDEA) is significantly increased in the adipose tissue of cancer patients (*103*). It was later shown that this protein induces lipolysis through AMPK dissociation independently of UCP1 levels, and constitutive active AMPK expression reduces lipid wasting in mouse models of cachexia (*104*).

3. Pancreatic dysfunction

Significant metabolic changes along with pancreatic dysfunction are implicated in the pathogenesis of cachexia. The pancreas plays fundamental roles in the control of digestion and glycemia through the secretion of digestive enzymes (exocrine function), insulin and glucagon (endocrine function) (*105*). Therefore, pancreatic failure and pancreatic tumors are typically associated with digestive disorders and weight loss. However, controversial data exist regarding the impact of altered exocrine pancreas function on patient survival. Although decreased exocrine pancreatic function promotes wasting of peripheral tissues in early stage of pancreatic cancer, correction by supplementing pancreatic enzymes only reduced WAT wasting without beneficial effects on muscle atrophy or survival (*106*).

In response to a rise of glycemia, pancreatic beta cells secrete insulin which activates the transport of glucose into cells and inhibits proteolysis (*107*). Cancer patients and animal models of cachexia commonly show a decrease in both insulin secretion and sensitivity in the skeletal muscle (*107*). Notably, in a murine model of cancer cachexia, insulin resistance preceded overt weight loss, which could be partially reversed by an insulin-sensitizing agent, rosiglitazone (*108, 109*). Another similar study in tumor-bearing rats showed that metformin mitigated protein wasting in the skeletal muscle (*110*).

4. Aberrant hepatic metabolism

The liver is a major metabolic hub that senses nutrient levels and adapt to supply the metabolic demands of peripheral tissues. It contributes tremendously to the pathogenesis of cancer-associated cachexia through several ways. First, the liver increases energy expenditure by the synthesis of acute-phase proteins at the expense of structural proteins (*111*). Second, it undergoes futile cycles and consumes energy to create glucose or amino acids, exacerbating energy wasting. It takes up circulating lactate produced by the tumor or peripheral organs (notably the skeletal muscle) to fuel gluconeogenesis, releasing glucose back to the circulation – a process known as Cori cycle. The latter is aberrantly increased in advanced stage cancer patients (*112-114*). Hepatic gluconeogenesis can also be fueled by amino acids (*e.g.* alanine) released from muscle proteolysis –a circuit termed Cahill cycle (*115, 116*). In contrast to these enhanced pathways, hepatic lipid metabolism is impaired during cancer-induced cachexia, which is marked by suppressed lipogenesis, and export of very low-density lipoprotein and triglyceride (*117*). However, very few studies have focused on the contribution of abnormal liver metabolism to cancer-associated cachexia. Besides its intrinsic metabolic function, the

liver also synthesizes bile acids that are essential in dietary lipid absorption and cholesterol catabolism. Importantly, administration of bile acids to mice increased energy expenditure in brown adipose tissue through the activation of cyclic-AMP-dependent thyroid hormone–activating enzyme D2, preventing obesity and resistance to insulin (*118*). A recent study has further shown that cancer-induced systemic inflammation alters bile acid metabolism and impairs hepatobiliary secretion, causing hepatic inflammation (*119*).

5. Bone-muscle interaction

Bone loss is also a feature of cancer cachexia that is often concomitantly observed with muscle atrophy (*120*). The relationship between bone and muscle is intimate with one influencing directly the homeostasis of the other (*121*). Skeletal indian hedgehog (Ihh) stimulate myogenesis and muscle growth by regulating myoblast cell cycle (*122*), and morphogenetic protein (BMP) signaling maintains muscle mass through Smad1/5/8 pathway which inhibits atrogene expression (*123*). In the other way around, muscle-derived factors IGF-1 (insulin-like growth factor 1) and FGF-2 (fibroblast growth factor 2) promote bone formation (*124-126*). Noteworthy, bone metastases (but not the primary tumor) were shown to increase the secretion of TGF-β from bone, which then induces muscle weakness in mice (*127*). Recent work has further shown that elevated circulating receptor activator of NF-kB ligand (RANKL) causes muscle atrophy and bone resorption in a mouse model of ovarian cancer, whereas bone preservation by bisphosphonates (used for the treatment of osteoporosis) or anti-RANKL prevents the loss of muscle mass and function (*128*).

6. Contribution of the gut microbiota

The gut microbiota plays a fundamental role in systemic metabolism and inflammation. Recent studies have explored the contribution of altered microbiota to the pathogenesis of metabolic diseases including obesity and cancer. The microbiota composition was found to differ significantly from obese, lean, to anorexic patients. For example, Lactobacillus species and *Methanobrevibacter smithii* were higher in obese and anorexic patients, respectively (*129*). Intriguingly, supplementation of *Lactobacillus reuteri* led to lower intestinal tumor burden and prevented muscle wasting in mice (*130*). Similarly, oral administration of *L. reuteri* and *L. gasseri* reduced pro-inflammatory cytokine levels as well as muscle atrophy in a mouse model of acute myeloid leukemia (*131*). In another wasting model driven by C26 colon cancer, the microbiota of tumor bearing mice showed an increase in *Klebsiella oxytoca* that is associated with IL-6-induced disruption of the gut barrier (*132*).

Moreover, the metabolites secreted by the gut microbiome can also directly influence cancer progression. Inulin-type fructans were shown to undergo gut fermentation into propionate, which inhibits leukemia cell proliferation in the liver tissue (*133*).

7. Cardiac and respiratory failure

Respiratory failure and cardiac arrest constitute two major causes of death in cancer patients. Proteolysis in the heart or diaphragm is directly linked to muscle wasting resulting from the syndrome of cachexia (*12*). Symptoms of fatigue, shortness of breath, and impaired exercise tolerance are often due to cardiac failure (*134*). Body weight loss is generally associated with decreased in heart weight in several murine models of cancer-cachexia (*135*) and in patients with lung, pancreatic, and gastrointestinal cancers (*136*). In addition, some chemotherapeutic agents (*e.g.* doxorubicin) can cause cardiac atrophy and diaphragm weakness as side effect, exacerbating cachexia (*137, 138*). Cardiac failure is associated with elevated oxygen consumption and heart rate as the heart tries to compensate for the insufficient output, causing increased energy expenditure and cardiac muscle wasting. In cancer patients, increased heart rate correlates with the increase in energy expenditure and predicts accurately mortality risk (*136, 139*).

From the mechanistic standpoint, similarly to muscle atrophy, inflammatory cytokines are the main drivers of cancer-related heart failure (*140*). Indeed, chronic inflammation, but also chemotherapy, and antioxidant deficiency lead to oxidative stress that contributes to heart failure (*141*). Noteworthy, the activation of sympathetic system also raises the heart rate and cardiac output, worsening cardiac wasting (*142*). Besides these features, the heart also exhibits aberrant hormonal secretion. High levels of circulating cardiovascular neuro-hormones have been reported in cancer patients, although whether these factors are involved in heart failure remains unclear. Interestingly, increased brain natriuretic peptide (BNP), a regulator of cardiac remodeling used as diagnostic marker in heart conditions (*143*), was found in cancer patients even without any cardiovascular symptoms (*144*). Finally, the renin–angiotensin system, which is a key regulator of blood pressure, is also altered in cachexia (*145*). Notably, angiotensin II levels are elevated in several types of cancers and has been proposed as a biomarker of cachexia (*146*). The molecular mechanisms mediating cardiac muscle proteolysis are very similar to the ones of skeletal muscle and will be discussed below.

Skeletal muscle wasting

The skeletal muscle allows one to move, speak, chew, and controls breathing, temperature homeostasis, and even vision. It is the largest reservoir of proteins accounting for roughly half of the total body weight, which can be broken down and mobilized to provide energy source (or precursors for protein synthesis) for other organs (*147*). Muscle mass and myofiber size can vary largely depending on the physiological and pathological conditions. Muscle mass increases during development, upon mechanical, or hormonal stimuli (*e.g.* strength training, testosterone, β2-adrenergic agonists). By contrast, its decrease can result from aging, disuse, denervation (or motor neuron disease), fasting, chronic use of corticosteroids (*e.g.* Cushing syndrome), and metabolic disorders including diabetes and cancer (*148*). Skeletal muscle atrophy is the hallmark of cachexia, and muscle mass accurately predicts the outcome of therapies and survival in cancer patients. General muscle physiology will be outlined briefly hereafter prior to the discussion of cancer-induced muscle atrophy.

Oxidative vs glycolytic fibers

The force generated by the skeletal muscle depends on its size and composition of fiber type, the latter also predicts the metabolism and response to stimulus of the muscle. In humans, most skeletal muscles express two major type of fibers: slow twitch (type 1) and fast-twitch (type 2), which include subtypes 2A, 2B and 2X depending on the isoform of myosin heavy chain (MHC) expressed (*149*). Skeletal muscles rich in slow-twitch fibers (*e.g.* soleus) are characterized by denser vascularization, mitochondrial saturation, higher expression of myoglobin, and primarily rely on mitochondrial oxidative metabolism. Consequently, they are more resistant to fatigue, and contract with little force for longer periods, allowing endurance exercises. Conversely, skeletal muscles that are richer in fast-twitch fibers (*e.g.* gastrocnemius) have less mitochondria and myoglobin, undergo faster contraction period that is sustained by anaerobic glycolysis, and are therefore more susceptible to fatigue. They allow short but powerful exercise such as sprint and weightlifting (*149*).

Conditions linked to muscle atrophy and their differences

The molecular changes that mediate skeletal muscle atrophy can vary largely depending on the stimulus. For instance, starvation causes caloric deficiency prior to the induction of a reversible muscle atrophy that is often associated with adipose tissue loss, without inflammation nor change in resting energy expenditure. Moreover, the wasting is a relatively short phenomenon compared to other types of

atrophy, and prolonged starvation paradoxically reduces protein catabolism (*150*). Atrophy also occurs in response to decreased or loss of neural input such as in motor neuron diseases or denervation, with similar characteristics as starvation-induced atrophy but both protein degradation and synthesis are increased (*151, 152*). Sarcopenia is the progressive loss of muscle mass and strength due to normal aging (*153*), which is characterized by reduced resting energy expenditure, normal or reduced protein catabolism, without systemic inflammation or any underlying pathological condition (*154*). Sarcopenia is mostly preventable or even reversible, especially by increasing physical exercise (*155*). In contrast to the stimuli above, skeletal muscle atrophy occurring in cachexia (*e.g.* due to COPD, chronic cardiac failure and especially cancer) is associated with tremendous increase in energy expenditure, inflammation, and protein catabolism, which cannot be reversed by nutritional supplementation (*156*).

Muscle mass regulation

Myofiber size is mainly regulated by two cellular processes: Protein turnover (balance between protein synthesis and degradation) and myonuclear turnover (fusion of satellite cells, or nuclear apoptosis). Of note, the metabolism and response to a stimulus can vary drastically according to the muscle fiber types present within the muscle. For instance, slow muscles (*e.g.* soleus) have higher rates of both protein synthesis and degradation, and are less susceptible to undergo to atrophy caused by starvation (*148*).

Myogenesis/myonuclear turnover

Myonuclear accretion that occurs during post-natal myogenesis or muscle regeneration depends essentially on the activity of satellite cells, or precursor of myoblasts. Upon stimulus (*e.g.* injury), satellite cells are activated and proliferate through symmetric and asymmetric cell division, which results in two distinct myoblast populations (**Fig. 4**): One population returns to quiescence, while the other further differentiate into myocytes and finally fuse with muscle fibers by nuclear accretion. Committed satellite cells are characterized by loss of Pax3 (marker of precursor cells) followed by Pax7 and MYF5 expression, which then decreases during differentiation. Meanwhile, MyoD expression regulates the proliferation of myoblast and their differentiation into myocytes. Finally, MyoG is a key regulator of late differentiation which consists in the fusion and formation of myofibers (or myotubes *in vitro*) (*157*). In pathological states (*e.g.* prolonged inflammation), satellite cell activation, proliferation, or differentiation can be compromised, causing muscle atrophy (*158*). Consistently, *in vivo* atrophy induced by C26 colon carcinoma featured upregulated Pax7 and reduced myogenin levels, reflecting impaired myogenesis (*159*). Another study on the same model further

showed that upon injury, cachectic mice fail to recruit mesenchymal progenitors, neutrophils, and macrophages (which normally infiltrate the damaged tissue) in the skeletal muscle, causing defective regeneration (*160*).

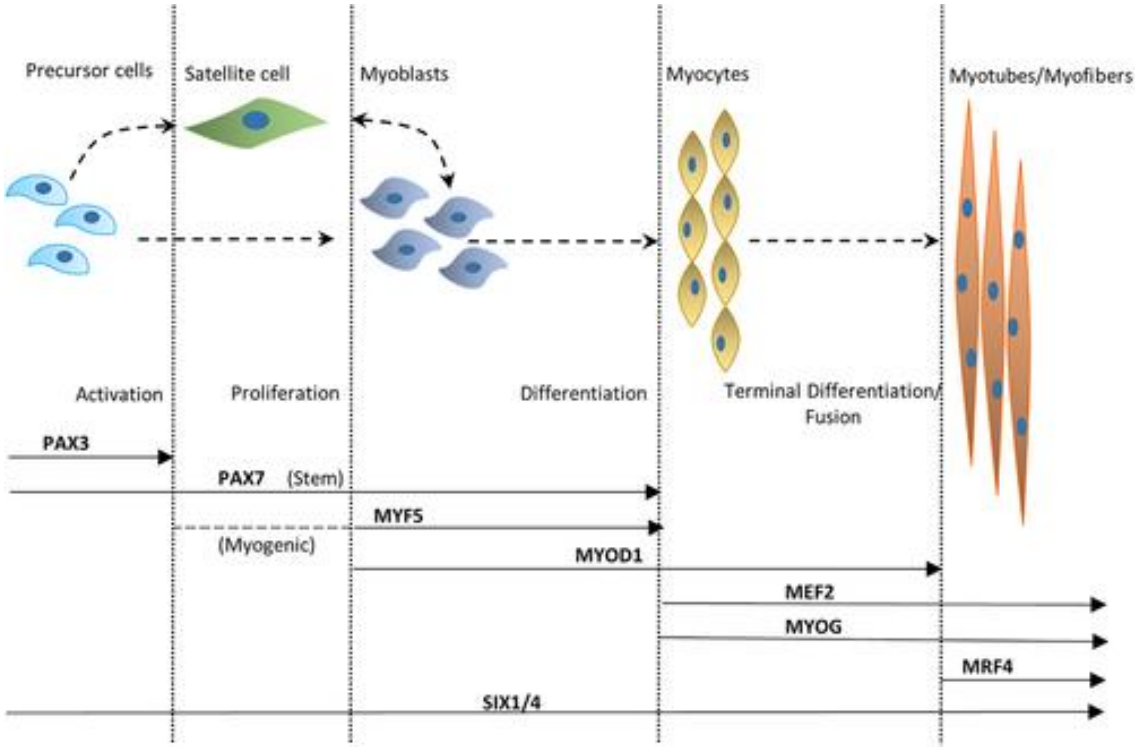

Figure 4. Chronological involvement of major transcription factors and markers across different stages of myogenesis (*149*)
Myonuclear fusion regulates muscle mass. During embryogenesis or post-natal regeneration, activated satellite cells proliferate and fuse, leading to increased number of myonuclei which contribute to muscle growth.

Protein homeostasis

Protein turnover is finely regulated by transcriptional, translational, and post-translational processes (*161*), and the balance between protein synthesis and degradation determines muscle mass. Protein synthesis is highly dependent on the pathway of phosphoinositide−3−kinase/protein kinase B/mechanistic target of rapamycin (PI3K- Akt-mTOR). Conversely, myofibrillar degradation is mainly mediated by the ubiquitin-proteasomal system (UPS), autophagy-lysosomal pathway (ALP), caspases, and calpains. Noteworthy, FoxO transcription factors are essential regulators of proteolysis as it activates both ubiquitin ligases and autophagy.

Insulin/IGF-1-AktT-mTOR axis

Insulin is a peptide hormone secreted by beta-cells of the pancreas, and insulin-like growth factor 1 (IGF-1) is mainly produced by the liver. These two hormones are important anabolic factors for muscle growth by activating a cascade of phosphorylative events through the mitogen-activated protein kinase/extracellular signal-regulated kinase (MAPK-ERK) and the PI3K-Akt-mTOR pathways. Importantly, muscle-specific overexpression of IGF-1 is sufficient to sustain muscle growth and regeneration in aged mice (*162*). However, only the activation of PI3K–AKT pathway (either constitutive or inducible), but not of ERK, could induce hypertrophy of myofibers without satellite cell activation (*163-165*).

Akt is a key mediator in preserving muscle mass as it stimulates protein synthesis through mTOR but also inhibits protein degradation by the phosphorylation of FoxOs, which impedes their nuclear translocation (*148*). Mechanistic target of rapamycin (mTOR) is a multiprotein complex that regulates cell metabolism, proliferation, and nutrient sensing. mTORC1 and mTORC2 are structurally and functionally distinct. mTORC1 (rapamycin-sensitive) is involved in anabolic signaling, protein synthesis, organelle biogenesis while mTORC2 plays a role in glucose and lipid metabolism. Indeed, selective inhibition of mTORC1 by rapamycin or genetic knock out impairs muscle growth *in vivo (164, 166, 167)*. However, inducible muscle-specific deletion of Raptor (subunit of mTORC1) does not fully suppress protein synthesis (*168*). Although significantly decreased, muscle growth is not completely blunted upon the expression of catalytically inactive mTOR, and autophagy is unexpectedly impaired rather than activated, contributing to severe myopathy (*167, 169*). Therefore, mTORC1 is mainly involved in the regulation of muscle growth, but its role is not exclusive as other mTOR-independent pathways also control protein synthesis and autophagy. Noteworthy, other pathways also converge on the mTOR pathway to stimulate protein synthesis, including β-adrenergic signaling. β2-adrenergic agonists (*e.g.* clenbuterol or formoterol) induces muscle hypertrophy through AKT phosphorylation which can be abolished by rapamycin (*170*).

Intracellular mechanisms of protein degradation

Myofibrillar degradation is mainly mediated by the ubiquitin-proteasomal system (UPS), autophagy-lysosomal pathway (ALP), caspases, and calpains. The UPS is responsible for the removal of targeted proteins for degradation. A sequential process of ubiquitin transfer by ubiquitin-activating enzymes (E1), conjugating enzymes (E2), and ligating enzymes (E3) marks specific proteins destined for

degradation (*171*). Polyubiquitinated proteins are then transferred to 26S proteasome complexes in which they are degraded. Muscle-specific E3 Ub-ligases are also known as atrogenes and serve as readout of skeletal muscle atrophy in experimental studies, including Atrogin-1 and MuRF1 (muscle RING-finger protein-1).

In physiological and catabolic conditions, the ALP plays a fundamental role in the clearance of misfolded, aggregated, damaged proteins or parts of cell organelles (*e.g.* mitochondria and endoplasmic reticulum) whose accumulation can cause cell toxicity. Therefore, impaired autophagy can cause also myofiber degeneration as toxic aggregates accumulate (*172*). Autophagy is triggered in response to nutrient starvation (notably of amino acids and glucose, sensed by mTOR and AMPK, respectively) as a recycling program to yield metabolites (*173*). Noteworthy, the skeletal muscle can undergo persistent autophagy continuing for days during starvation, unlike most tissues that show a rather transient activation lasting a few hours (*174*). The process of autophagy is initiated by the generation of double membrane intracellular vesicles that engulf parts of cytoplasm, organelles, or protein aggregates, forming a complex called autophagosomes, which are then fused with lysosomes for the degradation of their contents (*175*). These steps require the expression and complexation of kinases and core autophagy-related proteins (ATG) proteins, including the ULK1 (Unc-51-like kinase 1), phosphatidylinositol 3-kinase, catalytic subunit type 3 (PI3KC3, also known as VPS34), BCL2 Interacting Protein 3 (BNIP3), Beclin 1 (BECN1), microtubule-associated proteins light chain 3 (LC3) and γ-aminobutyric acid receptor-associated proteins (GABARAP) subfamily (*173, 175*). Importantly, the two latter are among the upregulated atrogenes encoding for proteins that are degraded during the fusion of autophagosomes and lysosomes (*172*).

To a lesser extent, protein degradation in the muscle can also be mediated by calpains and caspases, which are families of cysteine proteases. Their proteolytic activity increases during cellular necrosis or apoptosis, causing overall suspension of cell function by inhibition signal transduction (*176*). Their relevance during muscle atrophy remains however unclear.

Forkhead box proteins (FoxOs) as upstream regulator of atrogenes

FoxO1,3 and 4 are transcription factors downstream of the IGF-1/Insulin-Akt pathway and the inhibition of their activity can fully prevent loss of muscle mass and strength resulting from fasting,

denervation, diabetes, or glucocorticoids (*177, 178*). The expression of FoxO3 is sufficient and required for lysosomal-dependent muscle protein breakdown both in cells and *in vivo* (*179*).

FoxOs are regulated at several levels. FoxO expression can be transcriptionally upregulated in catabolic conditions through glucocorticoid/REDD1/KLF15 signaling that inhibits mTOR pathway (*180*). Furthermore, multiple post-translational modifications regulate the activity of FoxOs, including phosphorylation, acetylation, ubiquitination, and methylation. Consequently, FoxO activity changes according to the stimulus under the action of different kinases (such as Akt, AMPK, MAPK, ERK). For example, p300/CBP-driven acetylation inactivates FoxO3 (*181*), and deacetylation by histone deacetylase activates FoxOs (*182*). In addition to post-translational modifications, FoxO activity can also be inhibited by other transcription factors, such as the master regulator of mitochondrial biogenesis PGC1-α (*183, 184*), or synergize with β−catenin to worsen muscle atrophy (*185*).

Cytokines-driven control of muscle mass

Cancer-induced muscle wasting is primarily mediated by excessive inflammation. Early studies first found that TNF-α, initially known as cachectin, triggers anorexia and muscle atrophy through NF-κB signaling (*186, 187*). Other pro-inflammatory cytokines including IFN-γ, IL-1, and IL-6 a have been successively identified as inducers of atrophy. Several signaling pathways involve and integrate their mass-modulating effects (**Fig. 5**), notably:

1. Ligands of TGF-β superfamily and signaling

The transforming growth factor β (TGF-β) superfamily comprises over 30 ligands, among which myostatin (also known as GDF8), activin, and TGF-β are well-known inhibitors of muscle hypertrophy (*188-190*), while bone morphogenic proteins (BMP7,13 or 14) have been identified as pro-hypertrophic (*122*). These ligands share common receptors that are activin type II receptors (ActRIIA/B) but activate distinct transcription factors that have opposite effects on muscle growth.

The binding of myostatin, activins or TGF-β to ActRIIA/B or TGF-βRII recruits ALK4/5/7 to phosphorylate and induce complex formation of Smad2/3 with Smad4, resulting in their translocation into the nucleus. The complex then activates the transcription of atrogenes promoting muscle atrophy. Importantly, Smad2 or Smad3 inhibition is sufficient to induce muscle growth (*191, 192*). Pharmacological antagonism of ActRIIB rescued muscle and cardiac wasting in tumor-bearing mice,

leading to prolonged survival (*193*). Similarly, myostatin blockade promotes hypertrophy, which can be reversed upon rapamycin treatment, indicating that myostatin hampers muscle growth by interfering with mTOR pathway (*191, 192*).

BMP ligands (BMP7,13 or 14) bind additionally to BMP type II receptors (BMPRII), activating ALK2/3/6 which triggers the complex formation of Smad 1/5/8 with Smad4. Nuclear translocation of this complex results in increased protein synthesis, possibly through mTOR pathway. Of note, BMP and TGF-β/myostatin/activins signaling can be negatively regulated by extracellular cytokines, such as noggin and follistatin (*122, 194*).

2. TNF-α family/ NF-κB pathway

NF-κB is a key transcription factor mediating the inflammatory effects of cytokines, particularly TNF-α, IL-1 and IL-6. TNF Receptor Associated Factors (TRAFs) are intracellular adaptors that interact with the surface receptors of TNF-α family ligands, such as TNFR-1 and -2, Toll-like receptor 4 (TLR4), and IL-1R to integrate their inflammatory signals through NF-κB and MAPK pathways (*158*). Inactive NF-κB is held by IκB in the cytoplasm. TNF-α binding to its receptor TNFR stimulates the TRAF2/TRADD complex, which activates the IκB kinase (IKK). The phosphorylation of IκB triggers its ubiquitination and proteasomal degradation, releasing NF-κB that translocates into the nucleus where it activates atrogene expression (notably MuRF1) (*195*). Indeed, transgenic mice with muscle-specific overexpression of IKK-β developped severe muscle atrophy (*195*), whereas blockade of NF-κB attenuated muscle wasting in mouse models of pulmonary inflammation (*196*), cancer cachexia and denervation (*195, 197*).

Besides TNF-α, tumor necrosis factor-like weak inducer of apoptosis (TWEAK or TNFSF12, which is another member of the TNF superfamily ligands) also induces muscle atrophy through NF-κB (*198*). Notably, TWEAK binds to fibroblast growth factor-inducible 14 (Fn14 or TNFRSF12A), which is upregulated in the skeletal muscle following denervation (but not with glucocorticoid treatment) and recruits TRAF6 to activate NF-κB signaling (*198*). TRAF6 was found to increase in LLC-tumor bearing mice, and its muscle-specific depletion protected from atrophy (*199*).

In addition to proteolysis induction, inflammatory cytokines also impair myogenesis during muscle regeneration through NF-κB signaling (*200-202*), highlighting the importance of NF-κB in mediating inflammation-driven muscle atrophy.

3. MAPK signaling

The MAPK family consists of four types of kinases: Extracellular signal-regulated kinases 1/2 (ERK1/2), p38 MAPK, c-Jun NH2-terminal kinases (JNK), and ERK5 (*203*), which have been associated with muscle wasting. Along with NF−κB, p38 MAPK also mediates the induction of MuRF1 and Atrogin-1 by TNF-α and IL-1 (*204-206*), and also increase energy expenditure through CCAAT/enhancer binding protein (C/EBPβ) activation in tumor-bearing mice (*207*). JNK controls cell proliferation and differentiation through Activator Protein-1, cyclins, and matrix metalloprotease 2 (MMP2) that are activated in muscle atrophy (*208, 209*). Coherently, increased phosphorylation of ERK correlates with impaired myogenesis and muscle atrophy in C26 tumor-bearing mice, which can be alleviated by ERK inhibition (*159*).

4. JAK/STAT3 signaling

Pro-inflammatory cytokines IFN-α/β/γ, TNF-α, IL-1, and IL-6 also activate the Signal Transducer and Activator of Transcription (STAT3) (*210*). Circulating IL-6 levels correlate with p-STAT3 and Atrogin-1 mRNA levels in the skeletal muscle of tumor-bearing mice (in C26 and APC models) (*211, 212*). The binding of IL-1 to its receptor activates the tyrosine kinase JAK that in turn phosphorylates STAT3 through homo or heterodimerization, enabling its nuclear translocation (*213*). STAT then stimulates C/EBP, thereby upregulating myostatin, Atrogin-1, MuRF1, and caspase-3 expression (*214-216*). Blockade of IL-6R with neutralizing antibody, or pharmacological STAT3 inhibition attenuated muscle loss in C26-bearing mice (*211, 217*). Conversely, IL-6 upregulation is sufficient to induce muscle atrophy, as observed in transgenic mice with human IL-6 overexpression (*218*), as well as rats receiving intra-peritoneal (*219*) or intra-muscular (*214*) injections of IL-6. *In vitro* data have furthermore shown that besides atrogene transcription, IL-6 also suppresses mTOR-dependent protein synthesis through STAT3 (*220*).

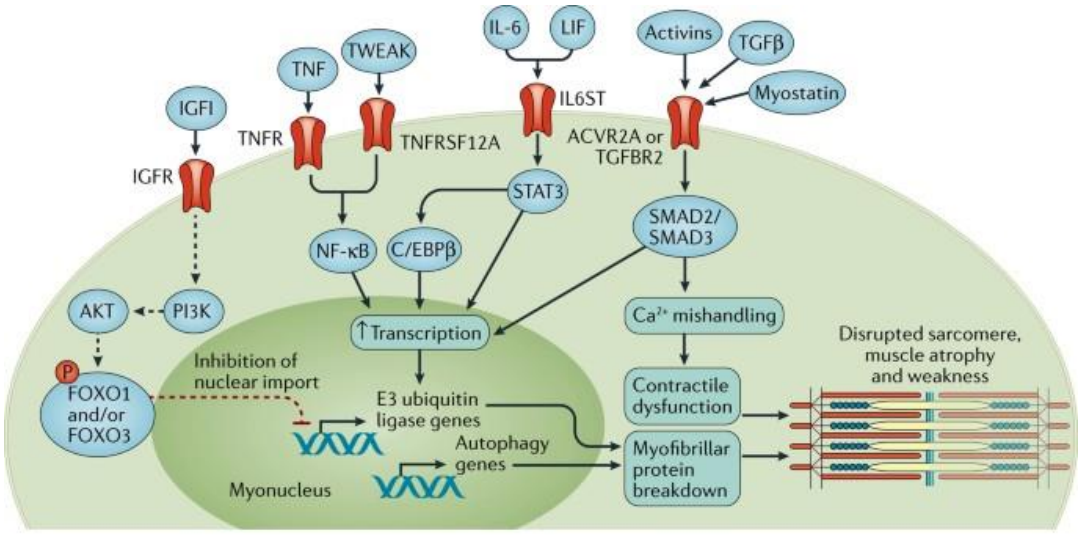

<u>Figure 5. Muscle mass modulation by extracellular (pro-inflammatory) ligands</u> (*62*)
Muscle mass is controlled by extracellular ligands, which include endocrine factors or hormones (IGF-1, insulin, glucocorticoids, activins), cytokines (TNF, TWEAK, IL-6, TGF, *etc*) and paracrine/autocrine factors (BMPs, myostatin). Their signals are integrated by transcription factors (FoxOs, NF-κB, STAT3, SMADs) which induce catabolic program while inhibiting synthesis by the PI3K/Akt/mTOR axis.

Mitochondrial control of muscle homeostasis

Energy production by mitochondrial metabolism is essential to sustain anabolism, as protein synthesis consumes considerable amount of energy. For instance, mitochondrial calcium uniporter (MCU), which is responsible for mitochondrial calcium uptake, also controls glucose oxidation and maintains myofiber size in physiological conditions. Consistently, MCU overexpression prevents atrophy following denervation, likely through PGC1-α upregulation (*221*).

PGC1-α is a key regulator of mitochondrial biogenesis, downstream of AMPK, that allows metabolic adaptions to endurance exercise, and its overexpression attenuates fasting, denervation, and cancer-induced atrophy via inhibition of FoxO (*183*, *222*). This explains at least partly why exercise-trained muscles or oxidative muscle fibers are less susceptible to undergo atrophy. However, PGC1-α overexpression does not increase protein synthesis nor muscle hypertrophy in healthy mice (*229*).

Mitochondrial dysfunction, caused by aberrant mitochondrial dynamics (increased fission and decreased fusion), impaired mitochondrial biogenesis, and/or mitochondrial metabolism, has been associated with catabolic conditions and muscle wasting (**Fig. 6**) (*223*, *224*). Notably, increased

expression of BNIP3 (marker of mitophagy) along with decreased mitochondrial content and oxidative capacity precede muscle atrophy in tumor-bearing mice (*225*). Akin to these observations, silencing of the fusion protein OPA1 (Optic Atrophy 1) or the fission component DRP1 (Dynamin Related Protein 1) lead to muscle wasting in mice (*223*, *226*). Moreover, acute OPA1 inhibition leads to oxidative stress, systemic inflammation and premature senescence *in vivo* (*223*), while DRP1 ablation disrupts calcium homeostasis and mitochondria–ER tethering, causing muscle degeneration without impacting lifespan in mice (*226*). Nevertheless, impaired mitochondrial respiration (decreased oxidative metabolism) is a common feature linking different types of mitochondrial defects and muscle atrophy.

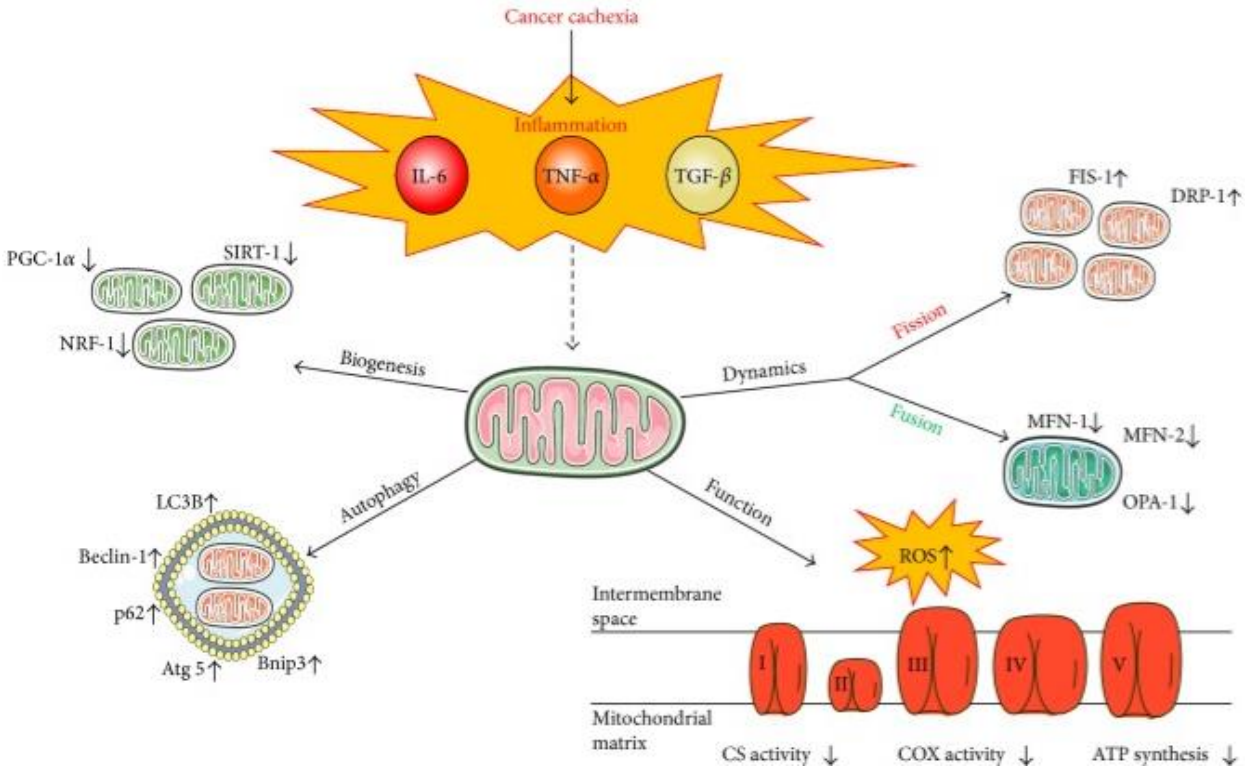

Figure 6. Mitochondrial features in cancer-induced muscle wasting (*224*)
Altered mitochondrial dynamics (fission and fusion), mitophagy, biogenesis, and metabolism have been linked to several wasting diseases, notably cancer cachexia.

Chemotherapy-induced cardiac and skeletal muscle wasting

As noted above, anticancer therapies can significantly alter body composition, causing fat, cardiac, and skeletal muscle wasting as well as decreased bone mass in cancer patients (*227*). In addition, cachexia reduces tolerance and response to treatment, thereby impacting further the quality of life and survival. Current chemotherapies work as double-edged swords: The anticancer effects lead to decreased tumor-induced inflammation, but meanwhile other off-target tissues can be affected by drug toxicity, inducing inflammatory signaling that worsens cachexia. For instance, cisplatin and mitomycin stimulate TNF-α production by macrophages (*228*). Moreover, cisplatin, cyclophosphamide, and anthracyclines (*e.g.* doxorubicin) have been shown to directly activate proteasome- and autophagy-mediated protein degradation (*88, 229, 230*). Similarly, most chemotherapeutic agents can induce oxidative stress that cause mitochondrial dysfunction and oxidation of myofibrillar proteins (*231-233*), which increases their degradation (*234, 235*). In addition, doxorubicin also inhibits muscle protein synthesis by mTOR signaling (*236*). Interestingly, although the skeletal muscle and heart show similar degree of mass loss upon doxorubicin exposure, changes in protein synthesis, protein ubiquitination, and atrogene levels were less evident in the heart (*237*).

Altered iron metabolism as a feature of cancer

All forms of life require iron as a cofactor to sustain vital biological processes such as DNA replication and energy production (*238-240*). Recent bioinformatic data estimated that 2% of the human genome encodes iron-containing proteins, and 6.5% of enzymes depend on iron for catalysis (*241*). In addition to its natural abundance, the versatile feature of iron is largely attributable to its electro-chemical properties as a transition metal that can fluctuate between a broad range of redox states, with Fe^{2+} (ferrous) and Fe^{3+} (ferric) being the most common (*242*). While a trace amount of iron is essential for cell survival, excessive iron promotes reactive oxygen species generation (ROS) (*243, 244*). Hence, iron levels are finely tuned by regulatory mechanisms within cells and between organs in the body. Iron is an essential constituent of hemoproteins (which include hemoglobin, myoglobin, and cytochromes), and iron-sulfur proteins that are responsible for a plethora of systemic functions ranging from oxygen transport to cell metabolism and DNA synthesis (*245*). Systemic iron deficiency ultimately leads to anemia and represents one of the most common health conditions in humans. Conversely, iron overload is also a frequent disorder typically due to genetic diseases such as hereditary hemochromatosis (*246*). Research in the field of iron metabolism has been focused on hematology, while accumulating studies highlight the importance of an adequate iron supply in non-erythroid cells. Besides blood disorders, disrupted iron homeostasis has been linked to pathogenesis of metabolic diseases, including diabetes and cancer (*247, 248*). In particular, cancer cells have to adapt to this double-edged sword as they require unphysiological amount of iron to sustain cell proliferation which meanwhile contributes to increasing oxidative stress. The latter promotes deleterious protein, lipid, and DNA modifications and further metabolic changes, thereby selecting cells with most aggressive phenotype for tumor growth.

Epidemiology linking iron to cancer

Iron is an essential trace metal acquired from dietary sources that can be classified into plant-based, inorganic iron and animal-derived heme iron. Results from large epidemiological studies have concluded that red meat intake is positively associated with liver, lung, pancreatic, breast, esophageal, and colorectal cancers (*249-254*). The latter has been given particular attention in epidemiology, and high heme content in red meat was found to underlie the positive association between meat consumption and colorectal cancer (*255, 256*). Notably, meat-derived heme catalyzes the formation of lipid peroxides (*257*) and nitroso-compounds (notably nitrosyl-heme and nitrosothiols, (*258*)), giving rise to reactive species and carcinogenic DNA adducts (*259*).

Besides dietary iron intake, accumulating clinical studies have shown a positive correlation between systemic iron levels and different types of cancer in humans (reviewed by Torti et al (*248*)). Notably, high transferrin saturation (above 40%) has been associated with increased risk of cancer in both genders (*260*). Patients suffering from iron overload due to hemochromatosis or homozygous β-thalassemia, were also reported to present a higher risk of liver cancer (*261-263*). In contrast, iron reduction by regular blood donations, or by phlebotomy in peripheral arterial disease patients, has been associated with a lower risk for cancer (*264, 265*).

Systemic iron metabolism

Total body iron depends on the age, gender, diet, and health condition, but ranges between 3 and 4 grams in healthy adults, of which about two-third is contained by hemoglobin in red blood cells, which is continuously recycled by the reticulo-endothelial system (*266, 267*). Dietary iron absorption is relatively poor and generally yields negligible 1-2mg of bioavailable iron (*266*). Non-heme iron absorption via the duodenal apical membrane is influenced by factors including intraluminal pH, the presence of reducing substances, such as ascorbic acid, and the redox state. Ferrous (II) iron is absorbed with greater efficiency, while ferric (III) iron is reduced to the ferrous state to be absorbed through divalent metal transporter 1 (DMT1). Heme iron absorption is not influenced by such factors and is taken up by enterocytes via a low-affinity heme carrier protein 1 (HCP1), then degraded by heme-oxygenase 1 (HO1) to yield iron (*268*). After absorption, iron is exported from enterocytes to the blood system through the basolateral membrane transporter ferroportin (FPN), the only known exporter of iron (*269*). Iron (II) is oxidized by hephaestin and ceruloplasmin (HEPH/CP) to ferric state (III) prior to its binding to transferrin which allows its circulation in the bloodstream (*266, 270*). Of note, transferrin is the predominant iron-binding protein in the circulation, other homologues include melanotransferrin that is lowly expressed on cell membranes (*271, 272*), and lactoferrin, a glycoprotein secreted by exocrine glands and immune cells with iron-sequestrating properties (*273*). Nevertheless, both melanotransferrin and lactoferrin have much lower affinity for TFR1 and have a minor role in iron metabolism (*274-276*).

Indeed, all cells require iron, but most is used by the bone marrow for erythropoiesis (*246*). Unused iron from peripheral tissues is then stored by the liver, that plays a major role in the maintenance of systemic iron homeostasis by secreting hepcidin (**Fig. 7**). Hepcidin binds to FPN and induces its internalization and lysosomal degradation leading to reduced circulating iron levels (*277-280*).

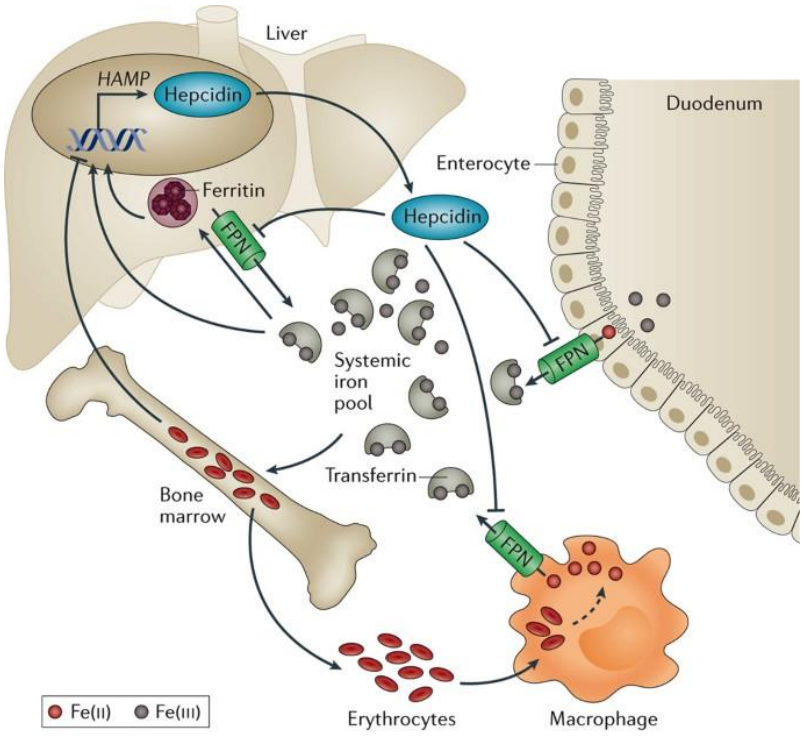

Figure 7. Main regulators of systemic iron homeostasis (*238*)
Iron comes from dietary absorption by the duodenum. Enterocytes exports iron to the bloodstream, where it is transported by transferrin. Circulating iron is mainly taken up by the bone marrow for erythropoiesis, while the reticuloendothelial system recycles iron from senescent erythrocytes. The liver fine-tunes iron levels by secreting hepcidin, which inhibits the membrane expression of ferroportin in peripheral tissues.

When anemia occurs suddenly, *e.g.* after hemorrhage, erythroblasts also secrete a hormone termed erythroferrone (ERFE), which inhibits hepatic hepcidin production thus resulting in higher iron levels to fuel erythropoiesis (*281*). A muscle-derived hormone termed myonectin was later found identical to ERFE but has been described primarily as a regulator of systemic lipid metabolism, and its relevance in iron metabolism remains elusive (*282*).

Cellular iron metabolism

Since iron is both essential and toxic, iron uptake, trafficking, and storage are tightly controlled cellular processes to maintain homeostasis (**Fig. 8**). In non-erythroid peripheral tissues, transferrin-bound iron (TBI) binds to its receptor (TFR1) and enters into the cells through endocytosis, is reduced to Fe (II) by STEAP (six-transmembrane epithelial antigen of prostate) reductases and released from the endosome by dimetal transporter 1 (DMT1) (*283, 284*). Unlike TFR1, TFR2 shows low affinity to Tf and is mainly expressed in the liver where it acts as an iron sensor regulating hepcidin production (*285*).

For heme, several proteins (mostly non-selective) are involved in the uptake, including heme carrier protein 1 (HCP1), FLVCR2, clusters of differentiation 91 and 163, whose expression and role depend on the cell type. Circulating heme can also be imported via endocytosis, requiring heme-responsive gene 1 (HRG1) to release heme in the intracellular space which can then be degraded by heme oxygenase 1 (HO1) to yield iron (*286*). Iron can remain free in the cytosol (labile iron pool) while a major amount enters mitochondria through mitoferrin (MFRN) 1/2 in erythroid and non-erythroid cells, respectively (*287, 288*). Excessive iron in the cytosol is sequestrated by its storage protein ferritin (FT), composed of heavy and light subunits (*238*). Ferritin degradation by a process similar to autophagy (process termed ferritinophagy) requiring a cargo receptor NCOA4 (nuclear receptor coactivator 4) releases bioavailable iron back to the cytosol (*289*). How iron is reduced back to the ferrous state remains to be elucidated.

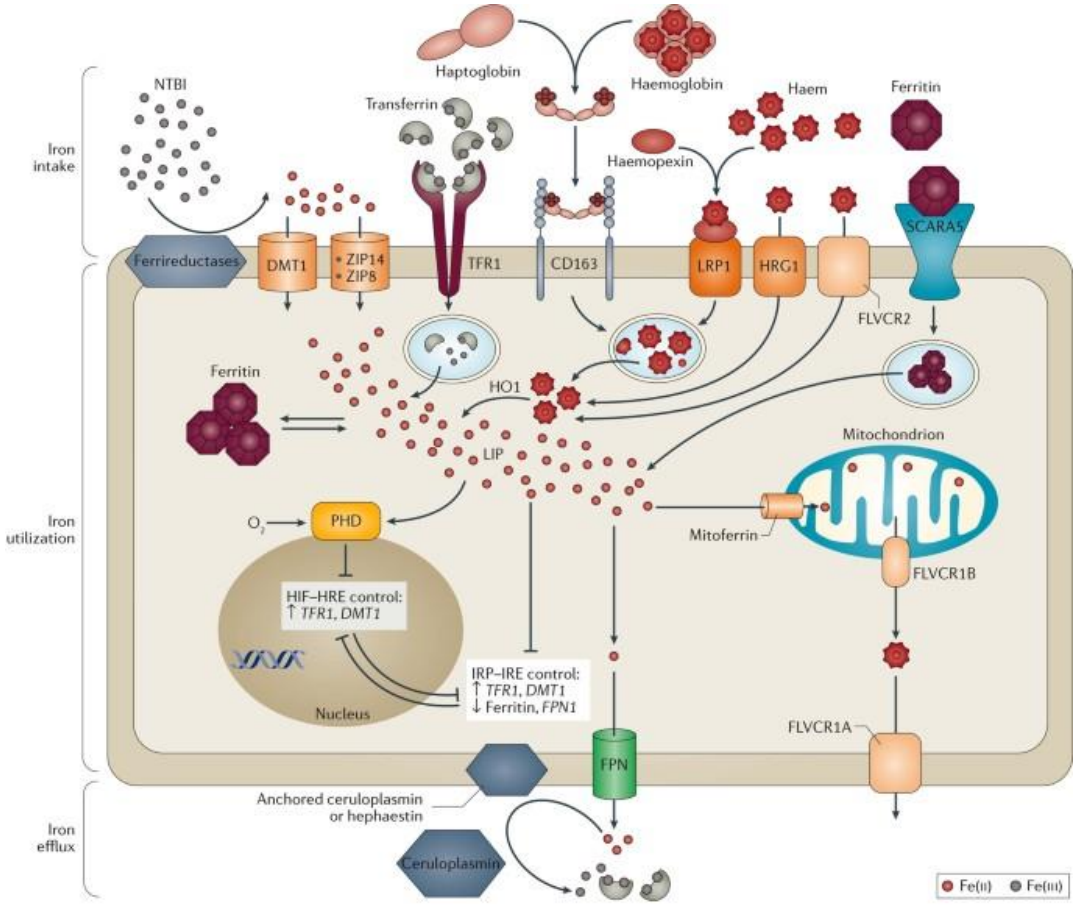

Figure 8. Cellular iron metabolism (*238*)

In normal cells under physiological conditions, iron is mainly taken up by TFR1, and sequestrated by ferritin in the cytosol, enters mitochondria through mitoferrin for ISC and heme synthesis, and exported through ferroportin. In cancer cells, the expression of these and other regulators of intracellular iron

trafficking (less relevant in physiological conditions) can be significantly altered. Noteworthy, many proteins mediate the uptake of iron (DMT1, ZIP14/8) or heme (CD163, LRP1, HRG1, FLVCR2), but only one exporter has been identified for each (FPN and FLVCR1a).

Intracellular iron homeostasis is primarily maintained by iron-regulatory proteins (IRP) 1/2, which regulate iron uptake, storage, and excretion by post-transcriptional modifications of major proteins involved in iron trafficking (*290*). During iron deficiency, IRPs bind to iron-responsive elements (IREs) located in the 5' or 3' untranslated regions (UTR) of target transcripts. Binding of IRPs to 5'UTR IRE results in translation repression of the mRNA (for ferritin and ferroportin), while binding to 3'UTR IRE stabilizes the mRNA to increase translation (such as for transferrin receptor 1) (*290*).

Despite the same role in iron metabolism regulation, the two IRPs function with distinct iron-sensing mechanisms. In iron-replete conditions, IRP1 is an cytosolic iron-sulfur enzyme known as aconitase, which converts citrate to isocitrate (*291*), whereas IRP2 is degraded by the ubiquitin-proteasome system after recognition by FBXL5 (F-Box And Leucine Rich Repeat Protein 15) (*292*). The lack of iron-sulfur cluster due to iron deficiency triggers the functional switch of IRP1 while stabilizing IRP2 (**Fig. 9**).

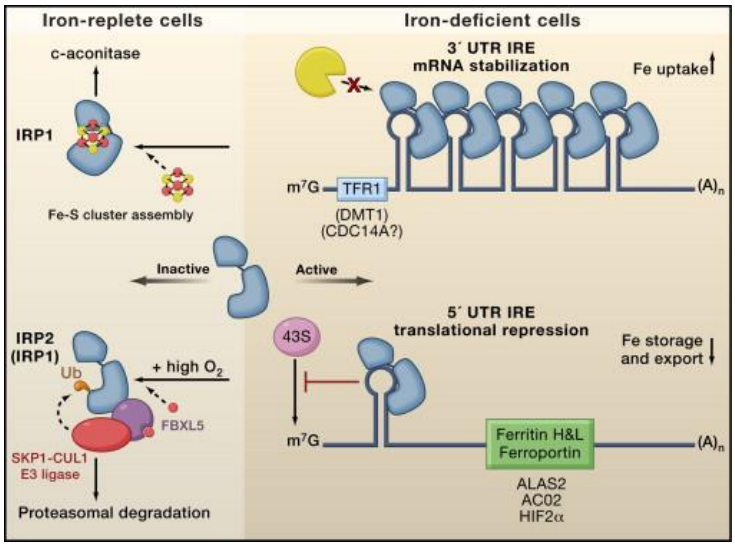

Figure 9. Cellular iron homeostasis control by iron regulatory proteins (*293*)

In iron replete cells, IRP1 exerts its activity as an enzyme while IRP2 is ubiquitinylated by an iron-dependent ligase (SKP-CUL1 E3) and degraded. In iron deficient cells, IRP1 loses its activity, and IRP2 is stabilized. IRPs bind to iron-responsive elements (IREs) that are located in the untranslated regions (UTR) of mRNAs encoding proteins involved in iron trafficking. The binding of IRPs to IREs in the 5′ UTR of target mRNAs inhibits their translation (*e.g.* ferritin, ferroportin), whereas the binding in the 3′ UTR IREs increases mRNA stability (*e.g.* TFR1, DMT1).

Mitochondrial iron and oxidative metabolism

Mitochondria import iron through mitoferrin 1/2 (*287, 288*). Most of the imported iron is used for heme and iron sulfur-clusters synthesis that mainly take place in the mitochondria. These cofactors are highly versatile and essential to cellular metabolism. The biosynthesis pathways of both heme and iron-sulfur clusters have been extensively described previously and will be briefly outlined herein (*268, 294, 295*).

Heme metabolism and hemoproteins

Substantial increase in heme biosynthesis as well as accumulation of protoporphyrin IX have been linked to different cancers (*286*). Heme is a prosthetic group that consists of iron complexed with a protoporphyrin IX ring found in various proteins involved in oxygen binding, metabolism, detoxification, and even signaling. Heme synthesis starts with the generation of 5-aminolevulinic acid (ALA) from glycine and succinyl-coenzyme A by aminolevulinate synthase (ALAS). ALA is sequentially converted to protoporphyrin IX, into which iron is incorporated by ferrochelatase (FECH). Besides the use by mitochondrial proteins, a substantial amount of heme is also exported from the mitochondria to the cytosol through Receptor of feline leukemia virus subgroup C 1- isoform b (FLVCR1b) (*268*). Noteworthy, the isoform a (FLVCR1a) exports cytoplasmic heme and is required on developing erythroid cells by conferring protection against heme toxicity. Inhibition of FLVCR in human leukemic cells decreases heme export, impairs erythroid maturation and leads to apoptosis (*296*). In line with these observations, full body FLVCR knockout in mice leads to lethality due to impaired erythropoiesis and severe anemia, indicating that the survival of erythroid precursors requires heme export. Moreover, FLVCR also mediates heme export from macrophages that ingest senescent red cells and recycle iron. Therefore, the trafficking of heme (in addition to the one of elemental iron) is required for erythropoiesis and systemic iron balance (*297*).

Heme plays a major role in both pro-oxidant and antioxidant reactions. Most catalases (anti-oxidant enzymes that break down hydrogen peroxide to water and oxygen) are heme-containing enzymes that have a ferric protoporphyrin IX (or heme b) in their active sites (*298*). Increased catalase expression has been reported in several cancer cell types (*299*), and recent meta-analyses revealed a correlation between a specific polymorphism of catalase and prostate cancer (*300, 301*). Besides antioxidant defense, heme also participates in oxidative stress and inflammation. For instance, nitric oxide synthase (NOS) requires heme as a cofactor to produce NO from L-arginine. Particularly, inducible NOS (iNOS or NOS2) isoform has been commonly found upregulated in tumors, where NO is viewed as an

oncogenic molecule that promotes a wide range of pro-tumoral effects including genome instability, cell invasion and angiogenesis (*302, 303*).

Similar to the effects exerted by NO, prostanoids (prostaglandins and thromboxane) are arachidonic acid-derived lipophilic signaling molecules that mediate inflammation and vasodilation. Their syntheses are catalyzed by cyclooxygenases COX1 and COX2, which require a heme prosthetic group (*304*). COX2 is an inducible form that has been associated with excessive inflammation and carcinogenesis along with increased angiogenesis, tissue invasion, resistance to apoptosis and immune defense (*305, 306*).

Iron sulfur proteins

Iron sulfur clusters (ISC) are inorganic complexes formed by two or more atoms of iron and sulfur from cysteine residues in proteins. As both iron and sulfur can donate or accept electrons, the resulting coordination presents a wide range of oxidation states (*307, 308*). All forms of life require iron sulfur clusters for cellular homeostasis, and the proteins involved in their synthesis have been highly conserved throughout evolution (*308*).

Mammalian iron sulfur-clusters synthesis starts in the mitochondrial matrix with the transfer of free iron and sulfur from cysteine to the scaffold protein ISCU (Iron-sulfur cluster assembly enzyme) by a protein complex composed of dimerized NFS1 (cysteine disulfurase) and ISD11 (LYR Motif-Containing Protein 4). Frataxin (FTX) binds to the core complex inducing a conformational change that fosters the formation of ISC (*309-311*). Iron-binding proteins glutathione, glutaredoxin, and frataxin have been suggested to provide iron to the nascent ISC (*312-314*). The ISC is then transferred from the scaffold protein to apoproteins to finally form iron-sulfur proteins. ISC can be also exported from the mitochondria to the cytosol by ABCB7 (ATP-binding cassette sub-family B member 7) (*315*). Several components of its biosynthetic pathway, including cysteine disulfurase (NFS1), frataxin (FTX), and glutathione have been shown to foster tumor progression and resistance to therapies (*316-318*).

A recently characterized class of iron-sulfur proteins named NEET has also gained interest in the field of cancer. Notably, MitoNEET is anchored in the outer membrane of mitochondria (*319, 320*), and NAF1 (another member of the NEET family) is expressed in both mitochondria and endoplasmic reticulum (*321*). In non-malignant cells, NEET proteins are involved in remarkably broad processes including autophagy, fatty acid metabolism and insulin secretion (*322-324*). Both mitoNEET and

NAF1 have been reported to predict negative prognosis in breast, liver, pancreatic and cervical cancers (*325-327*). Notably, the overexpression of NEET proteins promoted breast tumor growth by enhancing mitochondrial oxidative metabolism and resistance to autophagy (*328-330*).

Interestingly, iron availability regulates directly mitochondrial biogenesis and oxidative metabolism (*331*). Indeed, both heme and ISC are essential to mitochondrial function as they enable several steps of the tricarboxylic acid (TCA) cycle and electron transport chain (ETC). The TCA cycle is a metabolic pathway through which acetyl-CoA derived from carbohydrates, lipid, or amino-acid catabolism is oxidized, yielding energy in the form of ATP and reduced cofactors. In humans, two reactions of the TCA cycle require ISC: Succinate dehydrogenase (SDH, also complex II of the ETC) and cconitase (ACO) (*332*). Deficient expression or activity of these enzymes typically denotes mitochondrial dysfunction that has long been linked to tumorigenesis. Aconitase catalyzes the second step of the TCA cycle that consists in the isomerization of citrate to iso-citrate via cis-aconitate formation. The conformation of aconitase changes according to the ISC and determines its enzymatic activity: Liaison with a [3Fe-4S] cluster is found in the inactive form, while the addition of an iron atom forming [4Fe-4S] activates the enzyme (*333, 334*). This labile iron is susceptible to oxidation and removal by various oxidizing molecules including ROS and NOS, which inactivate the enzyme (*335-337*).

Decreased mitochondrial aconitase ACO2 predicted poor prognosis in gastric and breast cancers (*338*). Conversely, induction of ACO2 promoted ROS production, hampering cancer cell proliferation (*338*). A cytosolic isoform more commonly termed Iron-Regulatory Protein 1 (IRP1) or iron-responsive element binding protein (IRE-BP) exerts the same catalytic function but serves as an iron-sensing, mRNA binding protein as discussed above (*339*).

Succinate dehydrogenase (SDH) catalyzes the oxidation of succinate to fumarate that is then hydrated by fumarate hydratase into malate. X-ray crystallography of SDH revealed two hydrophilic subunits (SdhA, SdhB) and two hydrophobic, membrane anchoring subunits (SdhC and SdhD). SdhB contains three ISC, while SdhC and SdhD coordinate a heme prosthetic group necessary for the stability of the complex (*340, 341*). Mutations inducing SdhB loss of function or deficiency have been shown to cause the development of paragangliomas, pheochromocytomas, gastrointestinal and renal cancers (*342-346*). Furthermore, SdhB silencing was sufficient to induce ROS generation and metabolic switch that increased cancer cell proliferation and tumor growth *in vivo* (*347, 348*). Indeed, excessive levels of succinate (known as oncometabolite) stabilize HIF1-α and initiate tumorigenesis (*349*).

Catabolic pathways including glycolysis, tricarboxylic acid cycle and fatty acid oxidation generate reduced cofactors NADH and FADH2 which are oxidized by the ETC. The successive transfer of electrons creates a proton gradient across the inner mitochondrial membrane that drives the synthesis of ATP by oxidative phosphorylation of ADP. Indeed, iron is a step-limiting factor of the ETC as all four complexes require at least one ISC, heme or both to support the electron-transferring activity (*350, 351*). Consequently, a functional ETC is essential for efficient ATP generation to sustain cell proliferation. Impaired ETC is widely known to cause mitochondrial ROS that activate signaling pathways and metabolic rewiring fostering tumorigenesis (*352, 353*). Nevertheless, excessive ROS also triggers apoptosis, hence inhibitors of ETC have emerged as anti-cancer strategy (*354*).

Finally, many enzymes involved in DNA replication and repair carry at least one ISC that is essential for the enzymatic activity. The presence of ISC is required for functional activity of DNA polymerases, glycosylases, helicases as well as exonucleases (*355-358*). Recent findings show that lack of ISC in eukaryotic DNA polymerase leads to poor fidelity of replication and severe genome defects (*355, 359, 360*). Furthermore, iron chelation inhibits ribonucleotide reductase (RNR) that catalyzes the reduction of ribonucleotide to deoxynucleotides, as well as a class of histone lysine demethylases, which enable gene transcription of several oncogenes (*361-364*). Similarly, iron is also essential for nucleotide catabolism. ISC is required for the activity of xanthine oxidoreductases (XOR) that catalyze the oxidation of hypoxanthine to xanthine and ultimately to uric acid, along with the production of superoxide and hydrogen peroxide. The latter contributes directly to oxidative stress by producing ROS and RNS, while uric acid can further trigger inflammation (*365*). In summary, iron availability controls cell proliferation by regulating DNA synthesis, repair, transcription, and catabolism.

Free iron as an enzymatic cofactor

Although catalytic iron is mostly complexed within heme or ISC, free iron can also directly act as a cofactor. A notable example is the family of prolyl/asparagyl hydroxylases, that catalyzes post-translational hydroxylation of hypoxia-inducible factor 1α (HIF1-α), resulting in its ubiquitination and subsequent proteasomal degradation. Besides oxygen, this modification is in fact dependent on the presence of 2 oxo-glutarate as the substrate and ferrous iron (Fe^{2+}) as the cofactor. The requirement of iron in the degradation of HIF1-α was first evidenced by the normoxic stabilization of HIF1-α upon deferoxamine treatment *in vitro* (*366, 367*). Once stabilized, HIF1-α translocates into the nucleus where it interacts with HIF1β (also known as ARNT) to bind HRE (hypoxia-response element), which then

initiates the transcription of multiple genes to modulate glycolysis, angiogenesis, cell proliferation, and migration (*368*). Similarly, deoxyhypusine hydroxylase (DOHH) is the enzyme catalyzing the last step of hypusine synthesis which relies on iron (*369, 370*). Hypusine is a highly conserved amino acid found solely in the eukaryotic translational initiation factor 5A (eIF5A). Functional DOHH is therefore essential to cellular viability as mature eIF5A regulates eukaryotic cell proliferation (*371*).

Systemic iron alterations in cancer

Anemia is commonly found in cancer patients, and mostly arises from chronic inflammation characterized by iron restriction and decreased erythropoiesis, known as the anemia of chronic disease or of inflammation (*372*). For instance, interleukin 6 (IL-6) mediates hepcidin upregulation through JAK-STAT pathway (*373-376*), while tumor necrosis factor-α (TNF-α) inhibits erythropoiesis (*377*). *In vitro* studies have further shown that other cytokines, such as interleukin 1-β (IL-1β), also promote hepcidin synthesis (*378, 379*). Importantly, immune cells including macrophages and neutrophils also secrete hepcidin through TLR-4 induction as innate immune response (*380-382*). Moreover, bone morphogenic proteins (BMPs), a class of transforming growth factor β ligands whose upregulation has been reported in various cancers including breast, prostate and bladder cancers, can induce hepcidin secretion by cancer cells (*383*). Consistently, circulating plasma hepcidin is typically high and correlates with disease stage in breast, non-small lung, urothelial, and renal cancers (*384-388*). Elevated serum ferritin has also been reported in many types of cancers including neuroblastoma, lymphomas, colorectal, cervical and breast cancers, and used both as a diagnostic tool and prognostic factor (*389-394*). Interestingly, excessive circulating ferritin, which modulates cancer cell metabolism and stimulates their proliferation, originates largely from tumor-associated-macrophages (TAM) (*395*).

Cellular iron dysregulation in cancer

An overall increased iron turnover with enhanced avidity is a salient feature of several cancers (*396*). TFR1 overexpression has been commonly observed in both cancer cells *in vitro* and tumor tissues, including glioma, leukemia, breast, ovarian, prostate, colorectal and liver cancers (*397*). Consequently, high TFR1 levels are typically associated with poor prognosis. Similarly, melanotransferrin is upregulated notably in melanoma tissues, and to a lesser degree in liposarcoma, breast, and lung cancers (*398*). Moreover, melanotransferrin overexpression is associated with high tumor grade and metastases in human colorectal cancer (*399*). In contrast to its homologues, lactoferrin (Lf) has been shown to possess anti-tumoral activity with abnormally low levels found in several cancers (*400*), and

higher levels of Lf predicted better prognosis in breast carcinoma patients (*401*). Lf supplementation decreased colon cancer progression in humans (*402*) and significantly improved clinical prognosis in colorectal cancer patients receiving chemotherapy and in breast carcinoma patients (*403*). Although it is unclear whether such tumor suppressive effects are mediated by its iron-binding role, Lf has emerged as a promising prognostic factor and adjuvant therapy.

Unlike TFR1, TFR2 is mostly expressed in the liver with low affinity to Tf and is not regulated by IRPs in physiological conditions (*285*). TFR2 is commonly upregulated in human cancer cell lines as well (*404, 405*), and was shown to act as a signaling protein activating mitogen-activated protein kinase (MAPK) pathway in human leukemia cells (*406*). Other proteins involved in the uptake of iron that show abnormally high expression in cancers include DMT1, as well as heme importers HCP1, HRG1, CD91, and CD163, which are indicators of dismal prognosis (*286, 407-414*). Finally, a scarcely investigated yet noteworthy iron importer is ZIP14, whose main substrate is zinc but can also mediate the uptake of NTBI and intracellular release of TBI from endosomes (*415*).

Lipocalin 2 (LCN2 or NGAL), is a soluble iron-binding glycoprotein expressed mainly by neutrophils (*416*). Data about its role in cancer remains controversial and varies depending on iron saturation and on the cancer type. Interestingly, LCN2 can either import or export iron, and consequently promotes proliferation or apoptosis (*417-419*). A clear correlation between LCN2 levels and tumor grade was found in in breast and thyroid cancers), whereas the opposite was suggested in ovarian and pancreatic cancers (*420*). Nevertheless, these results collectively indicate that LCN2 is also involved in angiogenesis and inflammation within the tumor.

Since iron uptake is strongly enhanced, cancer cells expectedly present aberrant intracellular iron storage and trafficking to cope with the increased risk of iron-related oxidative stress. Reduction of ferric to bioactive ferrous iron by STEAP reductases is required to release endosomal TBI to the cytosol. Particularly, STEAP 1 and 2 are overexpressed in various human cancers and were shown to drive cancer cell proliferation and resistance to apoptosis (*421-423*). In addition to the abnormally high levels of circulating ferritin, some cancers exhibit alterations in both ferritin expression and intracellular localization. For example, glioblastoma and breast cancer cells exhibited nuclear expression of FTL and FTH, respectively (*424, 425*). Of note, FTH overexpression has been linked to chemotherapy (doxorubicin and cisplatin) resistance in breast and ovarian cancers (*425, 426*). Interestingly, p53 activation induced both FTH and FTL expression in human lung cancer cells (*427*).

Similarly, heme levels have also been shown to influence cancer progression. In leukemia and lung cancer cells, increased heme synthesis and availability fostered cell proliferation by fueling oxidative metabolism (*428-430*). Other studies have demonstrated that heme inhibit p53 (*431*), and induces c-Myc (*432*). Interestingly, heme was shown to interfere directly with p53 gene expression while triggering the proteosomal degradation of p53 protein (*431*). Nevertheless, the effect of heme degradation by HO1 in cancer cells has been controversial; some found that HO1 deficiency led to defective DNA, carcinogenesis, and resistance to ferroptosis (discussed hereafter), other data indicated that HO1 promotes antioxidant potential and cancer growth (*433, 434*).

Despite sharing almost identical roles, IRPs show rather distinct patterns in tumors. Downregulation of IRP1 was found in hepatocellular carcinoma and predicted tumor stage and prognosis (*407*), and IRP1 overexpression in human non-small cell lung carcinoma cells suppressed tumor growth in mice (*435*). In contrast, colorectal tumors showed IRP2 overexpression that is associated with BRAF mutations and MAPK activation (*436*). In prostate cancer, apoptosis induction was observed after knockdown of IRP2, but not IRP1, in prostate cancer cell lines (*437*). Although both IRPs are increased expression in breast cancer cells compared to non-malignant mammary epithelial cells, only IRP2 knockdown led to decreased tumor growth *in vivo*. Moreover, IRP2 expression correlated with histological grade and molecular subtype of human breast cancer. (*438*).

In cancer cells, other notable regulators of cellular iron metabolism include hypoxia-inducible factor 1α (HIF1-α), the proto-oncogene c-Myc and nuclear factor erythroid 2-related factor 2 (NRF2). In oxidative stress or iron overload conditions, NRF2 induces FTH, FTL, ferroportin, and heme oxygenase transcription to prevent excessive ROS formation promoted by iron availability (*439*). Constitutive activation of NRF2 has been consistently found in various cancer types and linked to poor prognosis (*440, 441*). However, due to its pleiotropic effects, whether cancer progression promoted by NRF2 is iron-dependent or not has not been clear. In B-cell lymphoma cells, c-Myc activates the transcription of TFR1 and DMT1 and repress the one of FTH and FTL to increase the labile iron pool (*442*). Similarly, hypoxia induces TFR1, DMT1 and hepcidin transcription through stabilization HIF1-α, leading to increased intracellular iron content (*375, 443, 444*). In line with elevated hepcidin levels, decreased iron export is also a feature of several cancers (*445-448*). In breast and pancreatic cancers, low FPN expression is associated with worse prognosis, while higher FPN expression in breast cancer patients corresponded to a cohort of patients presenting very high progression-free survival (*448*).

Likewise, FPN was downregulated in multiple myeloma cells isolated from patients compared to plasma cells from healthy donors and correlated with negative clinical outcomes (*449*). In several cell lines of prostate cancer, low FPN expression resulting from hepcidin upregulation was shown to promote proliferation, migration, and resistance to apoptosis (*450*). Interestingly, human colorectal tumors were reported to upregulate FPN, but histological analysis revealed aberrant cytoplasmic localization of the transporter, hence non-functional FPN (*451*). In summary, cancer cells commonly display increased iron import and decreased export, while how they cope with the increased labile iron depends on the stage and type of cancer.

Iron-induced oxidative stress and ferroptosis

Ferroptosis is an iron-dependent form of regulated cell death that results from excessive lipid peroxidation (*452*). The process depends essentially on labile iron which participates directly to radical generating reactions, notably Fenton's reaction, in which ferrous iron reacts with hydrogen peroxide to yield the hydroxyl radical ($Fe^{2+} + H_2O_2 \rightarrow Fe^{3+} + OH^{\cdot} + OH^{-}$). ROS then trigger sequential peroxidation of unsaturated fatty acids particularly in the cell membrane. The build-up of oxidized lipids ultimately leads to cell death (*453*). Indeed, cells are equipped with anti-oxidant enzymes that neutralize lipid ROS to prevent further oxidative damage, notably glutathione peroxidase 4 (GPX4) (*454*). Beside iron chelators, lipophilic antioxidants including vitamin E (*455*), Ferrostatin-1 (*456*), and coenzyme Q10 (CoQ10, also known as ubiquinone) (*457*) have also been shown to prevent ferroptosis. In contrast, ferroptosis is inducible *in vitro* by inhibiting GPX4 or by raising intracellular iron levels and ROS. Consequently, the expression levels of iron-regulating proteins such as TFR1, FPN or FT determine the sensitivity of cancer cells to ferroptosis (*458, 459*). Recent studies have found that cancer cells in a mesenchymal state are more sensitive to GPX4 inhibitors, hence prone to ferroptosis (*460, 461*). The efficacy of ferroptosis induction in reducing cell proliferation and tumor growth *in vivo* either alone or in association with standard chemotherapy has been validated recently (*462, 463*). Although the role of ferroptosis in physiological conditions remains largely unknown, these studies underscore the promising clinical prospect of ferroptosis inducers as anticancer therapies.

Iron in the tumor environment

A hallmark of malignant cells is the ability to reshape the environment where they reside, especially by inducing angiogenesis, remodeling the extracellular matrix, and evading host–to sustain their growth (*464*). Notably, polarization of tumor-associated macrophages (TAM) determines their iron metabolism

(*465*): Pro-inflammatory, anti-tumoral M1-like TAM upregulate FT levels while downregulating FPN, leading to an iron-sequestering phenotype (*466*). Interestingly, iron loading in macrophages correlated with improved survival in lung cancer patients (*467*). In contrast, anti-inflammatory, pro-tumoral M2-like TAM release iron to support tumor growth (*468*). Noteworthy, besides FPN, M2-TAM can also secrete iron-containing LCN2 in the tumor microenvironment (*469*). Moreover, TAM can directly contribute to tumor growth by feeding iron to cancer cells, or indirectly by fostering angiogenesis. For instance, LCN2 expression in TAM promoted lymphangiogenesis and metastasis in a murine breast cancer model (*470*). However, the effect of iron on angiogenesis seems different according to the dose. While iron supplementation inhibited VEGF (Vascular endothelial growth factor) signaling in endothelial cells and reduced lung carcinoma vascularization (*471*), LCN2 supplementation resulted in ROS accumulation and increased brain endothelial cell migration which was reversible upon iron chelation (*472*). Hence, it appears that low dose of iron inhibits angiogenesis whereas high dose promotes oxidative stress that is widely recognized as pro-angiogenic (*473*).

Direct effects of iron on multistep tumorigenesis

Accumulating studies have identified iron as a relevant promoter of tumorigenesis in different aspects, including genetic and epigenetic changes, tumor initiation, cell motility and invasiveness. Repeated administration of iron in rats led to high incidence of renal cell carcinoma associated with large-scale genomic modifications (*474*). Similarly, iron supplementation induced hypomethylation of oncogenes involved in PI3K/AKT, MAPK/ERK and RAP1/RAS pathways in colonocytes (*475*). *In vitro,* treatment with iron triggered increased migration and invasion via ROS production in human lung carcinoma and melanoma cells (*476*). Treatment of colon cancer cells with ferric chloride induced an aggressive, mesenchymal phenotype with loss of intercellular adhesion by E-cadherin (*477*). Moreover, DFO reduced histone demethylases in human breast cancer cells and raised their sensitivity to chemotherapies *in vitro* (*478*). In line with these findings, iron deprivation *in vitro* by iron chelators led to cell cycle inhibition and apoptosis of human colon, liver, breast cancers, and neuroblastoma, notably though activation of p53 and cyclin-dependent kinases (*431, 479, 480*). High-throughput screening further identified iron chelators DFO, deferasirox and ciclopirox as inhibitors of Wnt/β-catenin signaling, which is pivotal to cancer initiation and maintenance (*481*). However, DFO-induced iron deficiency also led to normoxic stabilization of HIF1-α and epithelial-to-mesenchymal transition (EMT) in colorectal cancer cells (*482*). These findings highlight the multiple facets of iron as a peculiar metabolic cofactor, signaling element, as well as catalyst of oxidative stress.

Background and aims of the study

Iron deficiency and anemia are very common comorbidities in cancer patients. Especially in pancreatic, colorectal and lung cancer patients, roughly half present iron deficiency and/or anemia (**Fig. 10**), which has been linked to asthenia (fatigue and weakness). Noteworthy, these cancer types are also the most associated with cachexia (**Fig. 2**). However, whether one condition influences the other remains unclear. In this study, we mainly aim at understanding whether and how:

1. Cancer affects iron metabolism in the skeletal muscle
2. Iron availability regulates muscle mass and function
3. Iron metabolism in the muscle can influence tumor progression

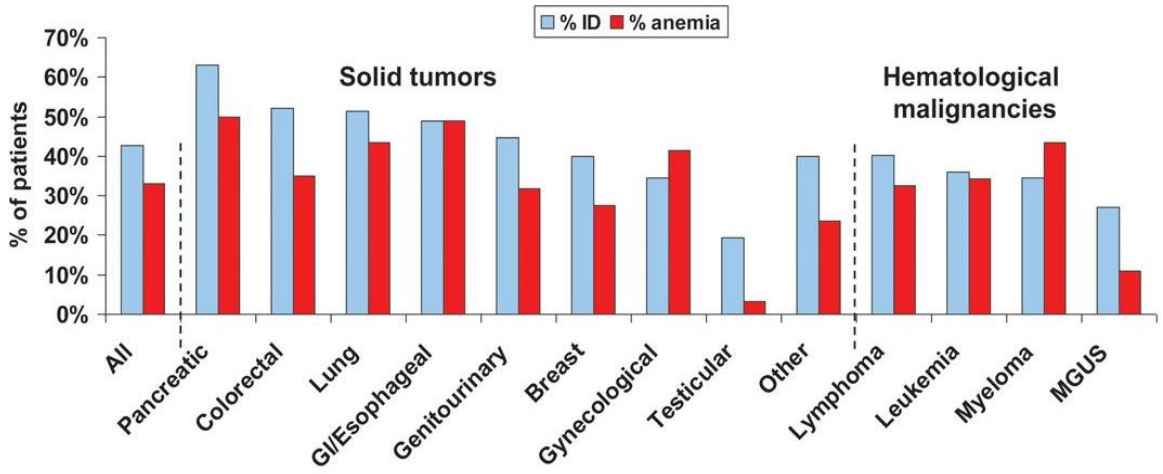

Figure 10. Prevalence of iron deficiency and anemia in patients according to the cancer type (*483*)
Up to 60% patients diagnosed with pancreatic, colorectal, and lung cancers also present iron deficiency and/or anemia. These are also the cancer types with the highest prevalence of cachexia.

Results

Cancer induces altered iron metabolism in the skeletal muscle

Although iron deficiency is highly prevalent in cancer patients and has been associated with advanced stage and poor prognosis (*483*), iron metabolism in the skeletal muscle during cancer cachexia has not been investigated. First, we modeled cancer cachexia in mice by inoculating C26-colon cancer cells in Balb/C mice, which led to significant reduction in hematocrit, total body weight and muscle weight within two weeks (**Fig. 11A-C**). During iron deficiency, cells normally increase iron import through TFR1 to maintain homeostasis (*484*). Strikingly, cachectic mice showed a drastic reduction of TFR1 levels in both transcript and protein levels in the skeletal muscle (**Fig. 11D-E**). We furthermore found an upregulation of ferritin (FT) (**Fig. 11F-G)**, which serves as a cytosolic storage protein for iron, while ferroportin (FPN) protein expression is downregulated despite the upregulated mRNA levels (**Fig. 11H-I**). However, in other organs such as the liver, we observed no change in TFR1 or FPN (**Fig. 11J-K)**. These data indicate that iron metabolism is strongly perturbed in the skeletal muscle during cancer progression.

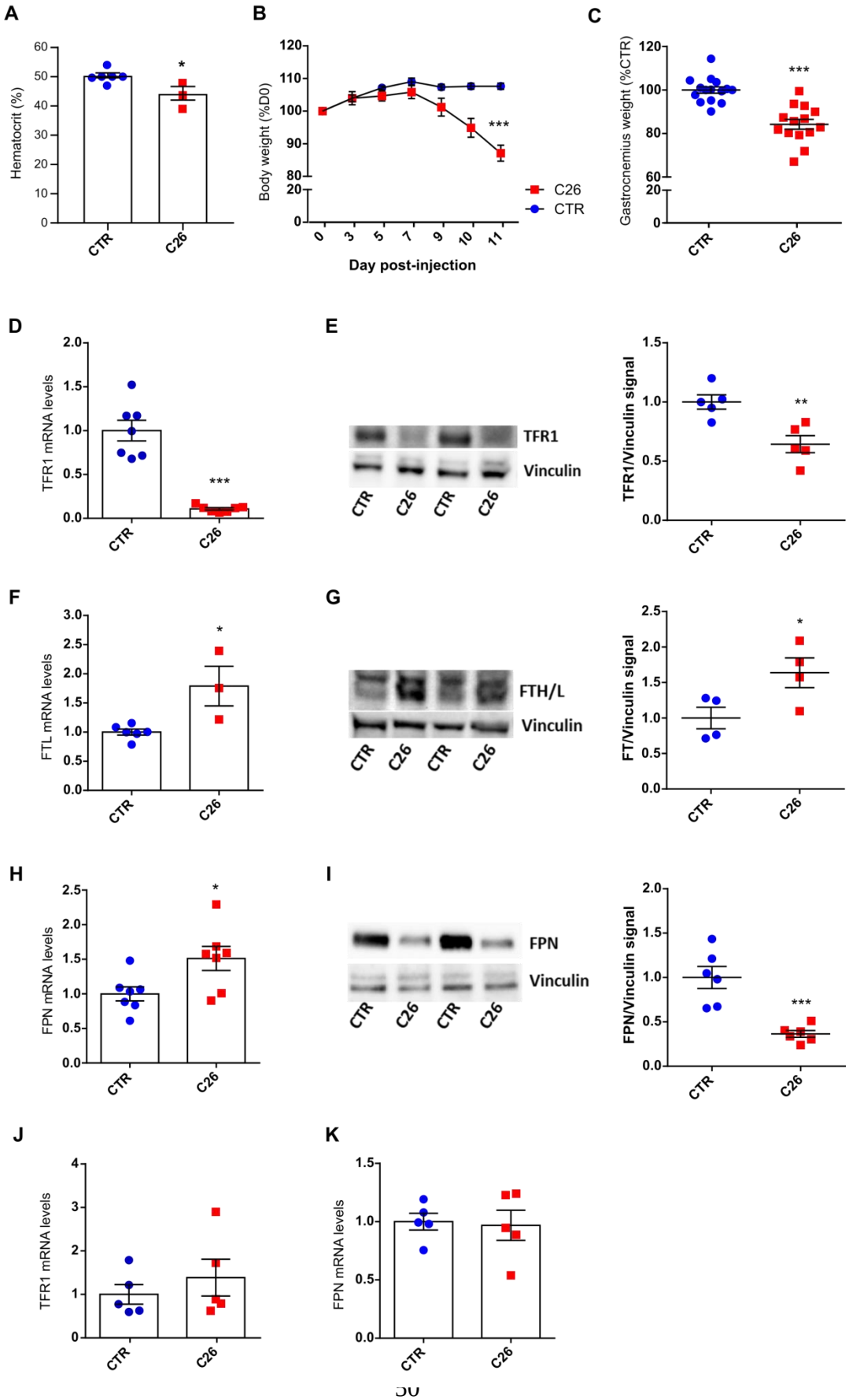
A
Hematocrit (%)
CTR
C26
B
Body weight (%D0)
Day post-injection
C26
CTR
C
Gastrocnemius weight (%CTR)
D
TFR1 mRNA levels
E
TFR1
Vinculin
TFR1/Vinculin signal
F
FTL mRNA levels
G
FTH/L
Vinculin
FT/Vinculin signal
H
FPN mRNA levels
I
FPN
Vinculin
FPN/Vinculin signal
J
TFR1 mRNA levels
K
FPN mRNA levels

Figure 11. Altered iron metabolism in the skeletal muscle is a feature of cancer-induced cachexia

(A) Hematocrit of mice 12 days after C26-injection (n=3-6)

(B) Body weight evolution in percentage of initial weight (n=6-7)

(C) Gastrocnemius weight normalized to tibial length in mice 12 days post C26-injection (n=14-15).

(D-E) Transferrin receptor 1 (TFR1) mRNA levels normalized to 18s (D) and representative immunoblot depicting TFR1 protein expression with corresponding densitometric quantification (E) in mouse gastrocnemius (n=6-7).

(F-G) Ferritin light (FTL) mRNA levels normalized to 18s (F), representative immunoblot depicting FTH/L protein expression with corresponding densitometric quantification (G) in mouse gastrocnemius (n=4).

(H-I) Ferroportin (FPN) mRNA levels normalized to 18s (H), representative immunoblot depicting FPN protein expression with corresponding densitometric quantification (I) in mouse gastrocnemius (n=4).

(J-K) TFR1 (J) or FPN (K) mRNA levels normalized to 18s in the liver of C26-tumor bearing mice (n=5)

Statistical significance was calculated by two-way Anova (B) or unpaired, two-tailed Student's T-test. Significance was defined as *:$p<0.05$, **:$p<0.01$ and ***:$p<0.001$ compared to control.

Cachectic muscles show impaired iron regulation and abnormal compartmentalization

Next, we assessed the activity of cytosolic aconitase (which reflects inversely the fraction of IRP1) in the skeletal muscle of tumor-bearing mice and found a strong decrease (**Fig. 12A**). Consistently, IRP2 was overexpressed (**Fig. 12B**), indicating altogether an intracellular iron deficiency. These findings raised a conundrum as IRP activity should upregulate TFR and downregulate FT through post-transcriptional regulation. To elucidate such discrepancy, we checked the oxidative status in the skeletal muscle of tumor bearing mice since it has been reported that oxidative stress can repress IRP function (*485*). We found that tumor-bearing mice display higher levels of protein carbonylation, indicative of oxidative stress (**Fig. 12C**). Furthermore, through RNA electrophoretic mobility shift assay (REMSA), we observed a lower RNA-binding activity to the IRE site of ferritin in cachectic muscle in native conditions without EDTA/DTT (**Fig. 12D**). Intriguingly, the opposite pattern was evidenced by performing the assay in reducing condition, suggesting an oxidative damage of IRP function (**Fig. 12D-E**). In line with the loss of IRP function and increased ferritin, intracellular protein-bound iron is strongly increased despite no change in total iron content in the skeletal muscle of tumor bearing mice (**Fig. 12F-G**). Finally, given that mitochondria are the main consumers of iron, we specifically measured the iron content in mitochondrial extracts and found a significant decrease in C26 tumor-bearing mice (**Fig. 12H**). This observation was coupled to upregulated transcripts of mitoferrin 2 (MFRN2, mitochondrial iron importer) and aminolevulinate synthase 2 (ALAS2, which catalyzes the first step of heme synthesis in the mitochondria) (**Fig. 12I-J**).

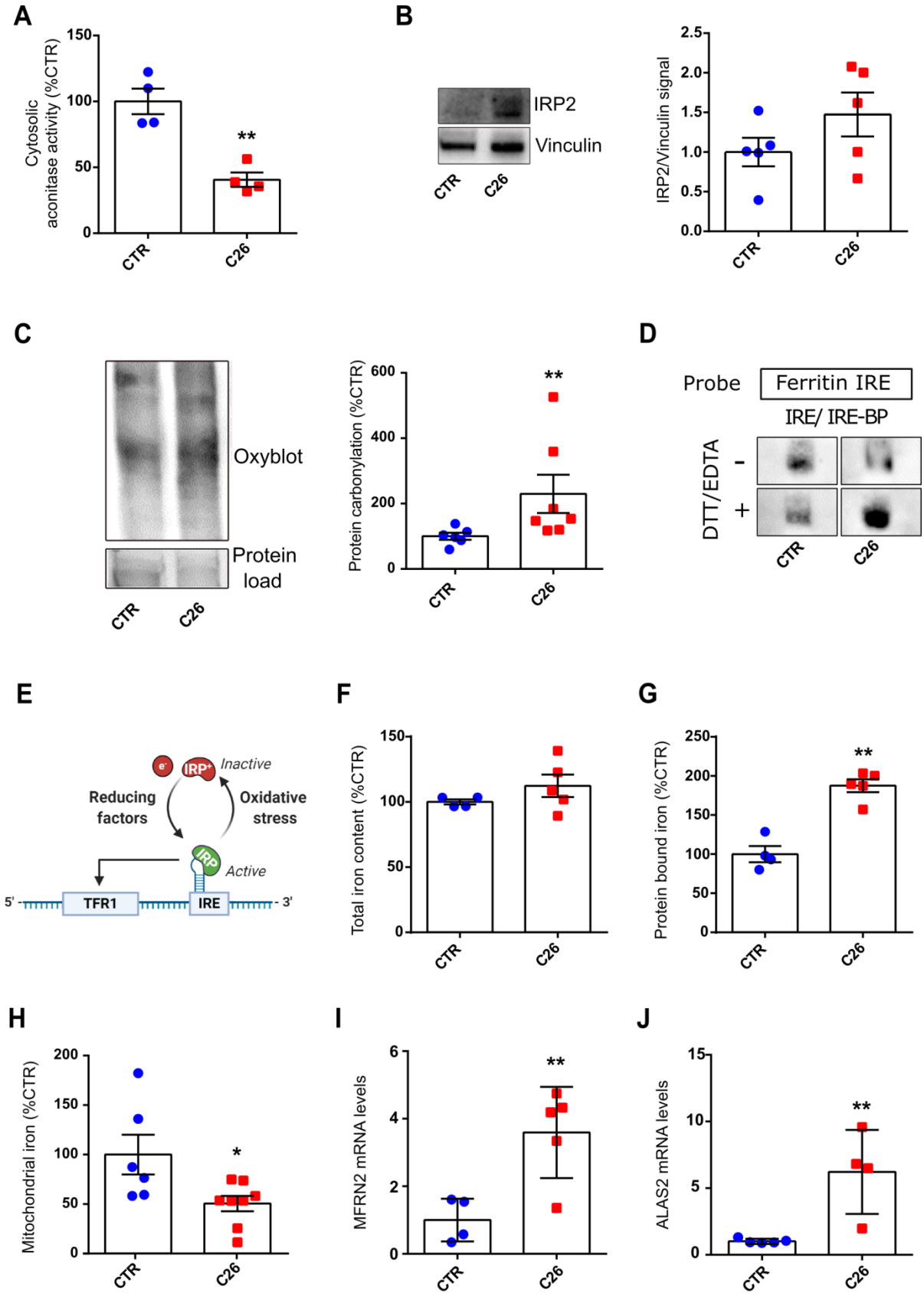
A
Cytosolic aconitase activity (%CTR)
150
100
50
0
**
CTR
C26
B
IRP2
Vinculin
CTR
C26
IRP2/Vinculin signal
2.5
2.0
1.5
1.0
0.5
0.0
CTR
C26
C
Oxyblot
Protein load
CTR
C26
Protein carbonylation (%CTR)
600
400
200
0
**
CTR
C26
D
Probe
Ferritin IRE
IRE/ IRE-BP
DTT/EDTA
-
+
CTR
C26
E
Inactive
IRP
Reducing factors
Oxidative stress
Active
5'
TFR1
IRE
3'
F
Total iron content (%CTR)
150
100
50
0
CTR
C26
G
Protein bound iron (%CTR)
250
200
150
100
50
0
**
CTR
C26
H
Mitochondrial iron (%CTR)
200
150
100
50
0
*
CTR
C26
I
MFRN2 mRNA levels
6
4
2
0
**
CTR
C26
J
ALAS2 mRNA levels
15
10
5
0
**
CTR
C26

Fig 12. Impaired iron sensing underlies aberrant iron compartmentalization characterized by decreased loading in the mitochondria

(A) Cytosolic aconitase activity in the gastrocnemius of C26-tumor bearing mice (n=4)

(B) Representative immunoblot showing IRP2 expression in mouse gastrocnemius and respective densitometric quantification (n=5).

(C) Representative oxyblot depicting protein carbonylation in mouse quadriceps and respective densitometric quantification (n=5-7)

(D) Binding activity of IRPs to the ferritin iron-regulatory element (IRE) in the cytosolic gastrocnemius extracts from mice, under native or reducing conditions (n=3).

(E) Simplified schematic representation of the working hypothesis on IRP-dependent iron regulation.

(F-H) Relative iron content quantified by ICP-MS of total (I), protein-bound (J) or mitochondrial iron normalized to protein content of the sample in mouse quadriceps (n=4-8).

(I-J) Mitoferrin 2 (H) or aminolevulinic acid synthase 2 (J) mRNA levels normalized to 18s in the gastrocnemius of C26-tumor bearing mice (n=4-5).

Statistical significance was calculated by unpaired, two-tailed Student's T-test. Significance was defined as *:$p<0.05$ and **:$p<0.01$ compared to control.

Iron deficiency causes skeletal muscle atrophy

To induce the phenotype of low intracellular iron availability observed *in vivo* without other cofounding systemic factors, we silenced TFR1 in C2C12 myotube with interfering RNAs, which led to significant myotube atrophy (**Fig. 13A**). Similarly**,** blocking intracellular iron mobilization by silencing NCOA4 (a cytoplasmic protein that mediates autophagic degradation of ferritin (*486*)), also induced myotube atrophy (**Fig 13B**). The same effect could be obtained by treatment with iron chelators, such as deferoxamine (DFO), bathophenanthroline disulfonic acid (BPS, a cell membrane-impermeable chelator), or apo-transferrin (apo-Tf, which reduces TFR1-mediated iron uptake) (**Fig. 13C**). All these treatments expectedly reduced labile iron pool *in vitro* (**Fig. 13D**). Notably, iron deprivation in C2C12 myotubes by DFO significantly increased REDD1 transcript levels and reduced S6 phosphorylation, suggesting an overall inhibited protein synthesis (**Fig. 13E-F**).

To confirm these findings *in vivo*, we also checked whether iron deficiency impacts muscle mass in mice by several means. In line with our *in vitro* data, electroporation of tibialis anterior with TFR1-silencing plasmid (shTFR-pGFP) in healthy mice led to significant reduction of cross-sectional area of the positive myofibers (**Fig. 13G**). Furthermore, iron-deficiency (ID) anemia resulted from phlebotomy and iron-deficient diet also led to significant muscle weight loss associated with TFR1 downregulation (**Fig. 13H-J**), whereas the hepatic TFR1 was induced (**Fig. 13K**). These findings corroborate with the observations made in cancer-induced cachexia models and indicate altogether that iron deficiency is sufficient to induce muscle wasting.

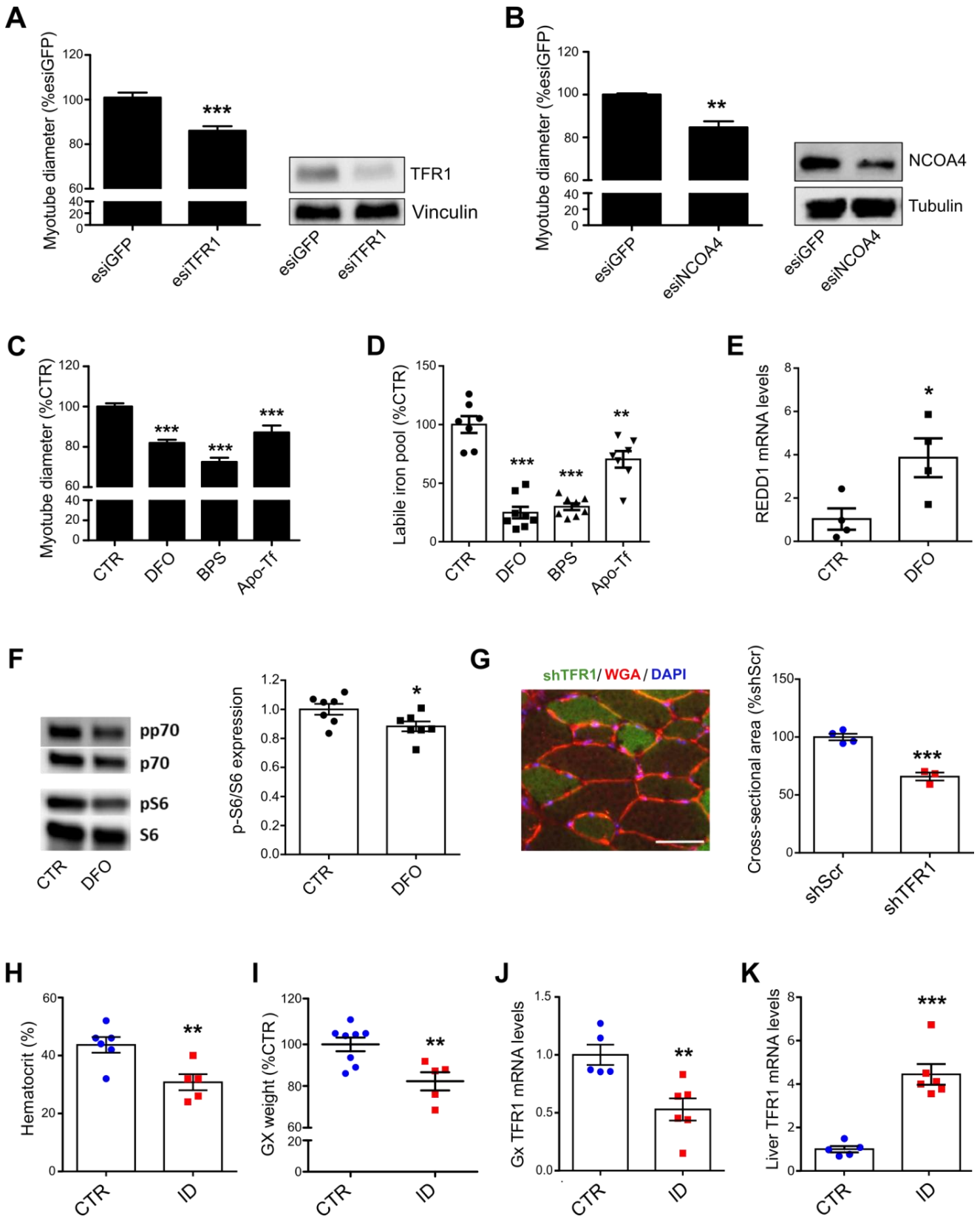
A
Myotube diameter (%esiGFP)
120
100
80
60
40
20
0
***
esiGFP
esiTFR1
TFR1
Vinculin
B
Myotube diameter (%esiGFP)
**
esiGFP
esiNCOA4
NCOA4
Tubulin
C
Myotube diameter (%CTR)
***
***
***
CTR
DFO
BPS
Apo-Tf
D
Labile iron pool (%CTR)
150
100
50
0
***
***
**
CTR
DFO
BPS
Apo-Tf
E
REDD1 mRNA levels
8
6
4
2
0
*
CTR
DFO
F
pp70
p70
pS6
S6
CTR
DFO
p-S6/S6 expression
1.2
1.0
0.8
0.6
0.4
0.2
0.0
*
CTR
DFO
G
shTFR1/ WGA / DAPI
Cross-sectional area (%shScr)
150
100
50
0
***
shScr
shTFR1
H
Hematocrit (%)
60
40
20
0
**
CTR
ID
I
GX weight (%CTR)
120
100
80
60
20
0
**
CTR
ID
J
Gx TFR1 mRNA levels
1.5
1.0
0.5
0.0
**
CTR
ID
K
Liver TFR1 mRNA levels
8
6
4
2
0
***
CTR
ID

Figure 13. Iron deprivation triggers atrophy both *in vitro* and *in vivo*

(A-B) Myotube diameter measured 72h after knockdown of TFR1 (H) or NCOA4 (I) with immunoblot depicting the corresponding expression (n=7 and n=3 respectively).

(C-D) Myotube diameter (C) and labile iron pool (D) of C2C12 myotubes after 48h treatment with Deferoxamine 100µM (DFO), bathophenanthroline disulfonate 100µM (BPS), or apo-transferrin (Apo-Tf)

(E) REDD1 mRNA levels in C2C12 myotubes treated with DFO for 24h (n=4).

(F) Representative immunoblot of p70, S6, the respective phosphorylation (left) and quantitative analysis of p-S6 normalized to total S6 (right) in C2C12 myotubes treated with DFO for one hour (n=7).

(G) Representative picture of a tibialis anterior electroporated with shTFR1-pGFP (left, scale bar =50µm) and average cross-sectional area of myofibers (right) transfected with shSCR (scramble) or shTFR1 (n=3-4).

(H-K) Hematocrit (H), gastrocnemius weight (I), TFR1 transcript levels in the gastrocnemius (J) and liver (K) of mice following iron deprivation (ID) induced by phlebotomy and iron deficient diet (n=5-8).

Statistical significance was calculated by unpaired, two-tailed Student's T-test (A-B and E-K) or one-way Anova with Bonferroni's correction (C-D). Significance was defined as *:$p<0.05$, **:$p<0.01$ and ***:$p<0.001$ compared to control.

Iron promotes hypertrophy

We next speculated that increasing iron availability can positively regulate muscle mass. Intriguingly, electroporation of tibialis anterior with TFR1-overexpressing plasmid (TFR-pHuji) in healthy mice induced myofiber hypertrophy (**Fig. 14A**). Likewise, iron ionophore hinokitiol (HNK, that mediates transmembrane iron uptake independently of TFR1 expression) completely reverted atrophy induced by TFR1 silencing *in vitro* without affecting its levels (**Fig. 14B**). We then asked whether normalization of iron levels could counteract conditioned medium-induced atrophy. While C26-conditioned medium (CM) induced significant myotube diameter reduction as expected, co-treatment of conditioned medium with hinokitiol prevented atrophy (**Fig. 14C**). To confirm that iron directly mediates myotube size modulation, we supplemented CM-treated myotube with low dose of iron citrate (250nM). Consistently, iron supplementation also prevented atrophy as observed with hinokitiol (**Fig. 14D**).

Furthermore, LLC-conditioned medium (LLC-CM) or activin A (ActA)-induced atrophy was also prevented by iron citrate (**Fig. 14E-F**), suggesting that iron metabolism might be altered also in other cancer models of cachexia. Noteworthy, to clarify the potential effects on myogenesis, myotube size was monitored before and after treatments. While untreated myotubes showed a steady increase in size over time, C26-CM reduced myotube size that could be remarkably counteracted by iron supplementation (**Fig. 14G**). In addition, we found that C26-CM and iron did not affect myonuclear turnover (**Fig. 14H**), demonstrating altogether that normalizing iron levels prevents or even rescue atrophy without influencing myogenesis at least *in vitro*.

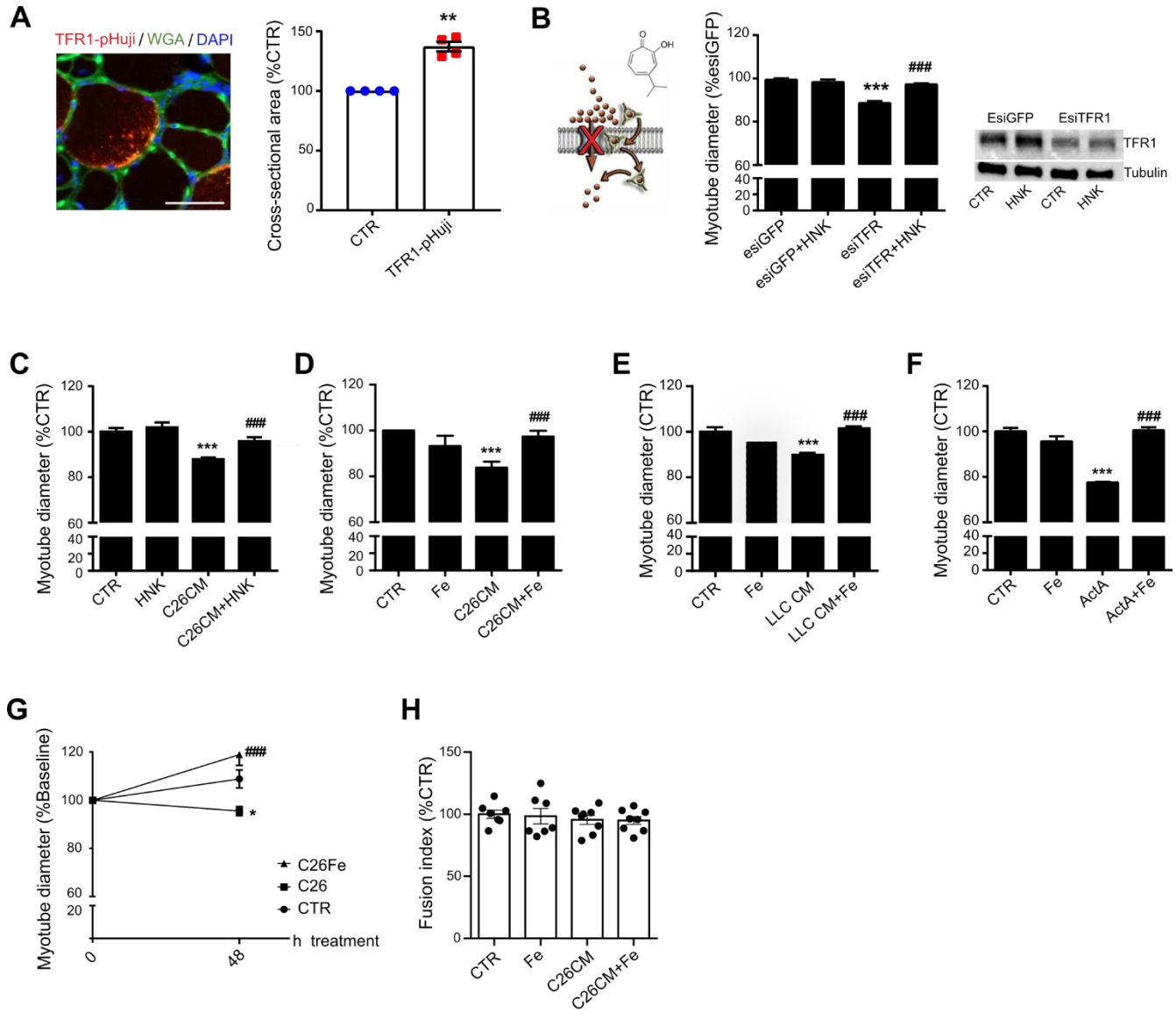

Figure 14. Increased iron availability favors hypertrophy *in vitro* and *in vivo*

(A) Representative picture (left, scale bar =50µm) and cross-sectional area (right) of tibialis anterior fibers transfected with TFR1-pHuji (n=4).

(B) Simplified scheme of hinokitiol-mediated iron uptake (left, from Grillo et al., Science 2017). Myotube diameter and TFR1 expression levels (right) after 24h 5µM hinokitiol (HNK, 5µM) treatment following TFR1 silencing (n=5-8).

(C-D) Myotube diameter following 10% C26-CM and 5µM hinokitiol (C) or 250nM iron citrate (D) treatment for 48h (n=4-7).

(E-F) Myotube diameter following co-treatment of iron citrate with 10% LLC-CM (E) or 1nM activin A (ActA, F) (n=4).

(G) Myotube diameter following 48h treatment of C26-CM and iron citrate, normalized to day 0 values (n=5-6).

(H) Fusion index of C2C12 myotubes after 48h treatment with C26-CM and iron citrate (n=7-8).

Statistical significance was calculated by unpaired, two-tailed Student's T-test (A), or one-way Anova with Bonferroni's correction (B-H). Significance was defined as *:p<0.05, ***:p<0.001 compared to control and ###:p<0.001 compared to treated (esiTFR or CM) condition.

Iron supplementation refuels mitochondrial iron and restores energy metabolism

In most cells, the mitochondria take up a considerable amount of iron to produce ISCs and heme that serve as cofactors for several enzymes involved in mitochondrial oxidative metabolism, which is typically impaired in skeletal muscle atrophy (*487*). Therefore, we postulated that iron supplementation could enhance mitochondrial function. Using the Seahorse analyzer, we assessed mitochondrial oxidative metabolism in C2C12 myotubes treated with C26-CM. Co-treatment with ferric citrate considerably prevented the drop in mitochondrial oxidative metabolism induced by C26-CM, notably basal and ATP-linked oxygen consumption rates (OCR) (**Fig. 15A-D**). We further found that iron fails to rescue myotube atrophy induced by low dose rotenone, an inhibitor of complex 1 of the electron transport chain (**Fig. 15E**). These findings indicate altogether that the protective effects of iron are mediated by increased mitochondrial function *in vitro*.

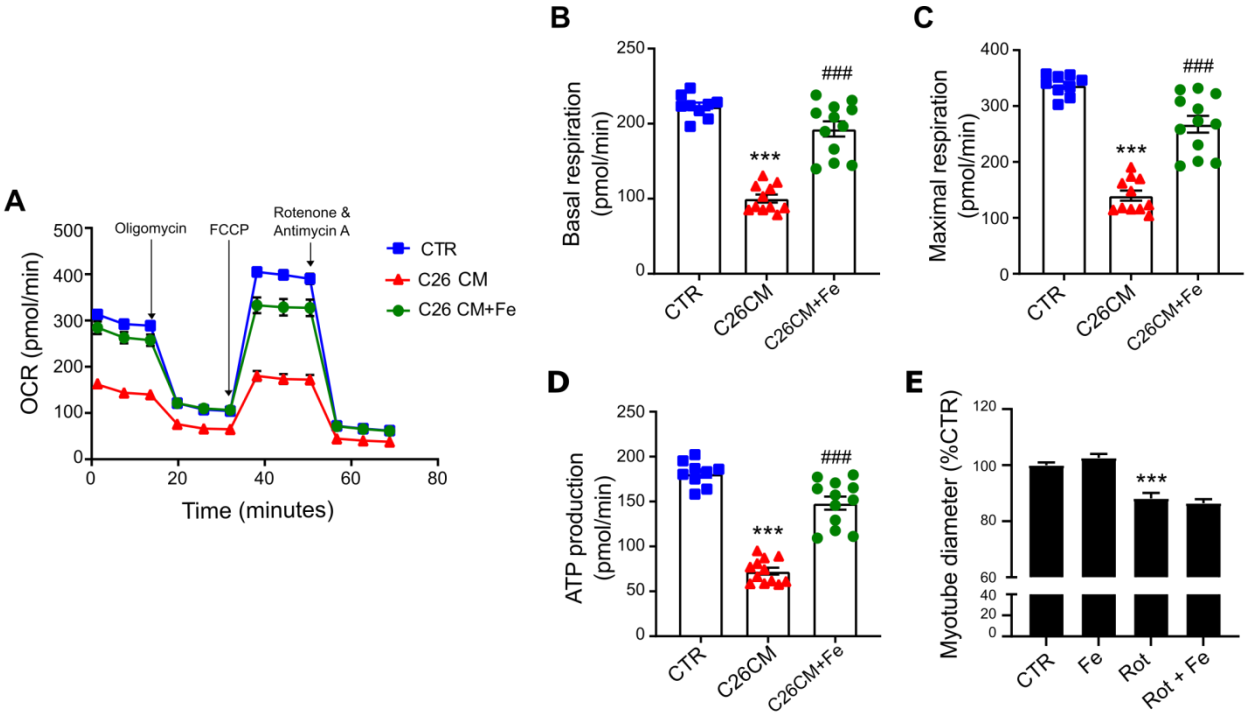

Figure 15. Iron enhances mitochondrial function in cancer-induced myotube atrophy

(A-D) Profile of oxygen consumption rate OCR (A) which summarizes the basal OCR (B), maximal OCR capacity (C) and OCR resulting from mitochondrial ATP production (D) in C2C12-myotubes after 48h treatment with C26 CM and iron citrate (Fe). Data normalized to protein content (n=4-5).

(E) Myotube diameter following 20nM rotenone (Rot) and iron citrate treatment (Fe) (n=3). Statistical significance was calculated by one-way Anova with Bonferroni's correction. Significance was defined as ***:p<0.001 compared to control and ###:p<0.001 compared to treated (C26CM or Rot) condition.

Iron supplementation prevents cancer-induced muscle wasting *in vivo*

Since we saw that iron levels significantly affect myotube size *in vitro* and muscle mass *in vivo* prompted us to ascertain whether iron supplementation is beneficial in cancer cachexia. C26-tumor-bearing mice were treated intravenously with ferric carboxymaltose (FeCM) every 5 days post-C26 injection. Remarkably, repeated intravenous injection of iron resulted in healthier (smooth fur, no orbital discharge, no humpback) and more physically active mice that survived far beyond the usually fatal two weeks (**Fig. 16A-B**). For the sake of consistency, experimental comparison between treated and untreated tumor-bearing mice were performed on samples obtained on day 12 post-C26 injection.

Consistently, iron supplementation conferred significant protection against the loss of strength in tumor-bearing mice (**Fig. 16C**), that finally preserved total body and muscle weight (**Fig. 16D-E**). Coherently, histological analysis of cross-sectional area (CSA) distribution showed a shift towards higher frequency in larger myofiber CSA in FeCM-treated compared to untreated mice, especially for fast-twitch fibers (**Fig. 16F-G**). These findings were further validated by mitigated induction of Atrogin-1, MuRF1, and REDD1 mRNA levels, which encode for ubiquitin ligases and a mTOR-inhibiting protein, respectively (**Fig. 16H-J**).

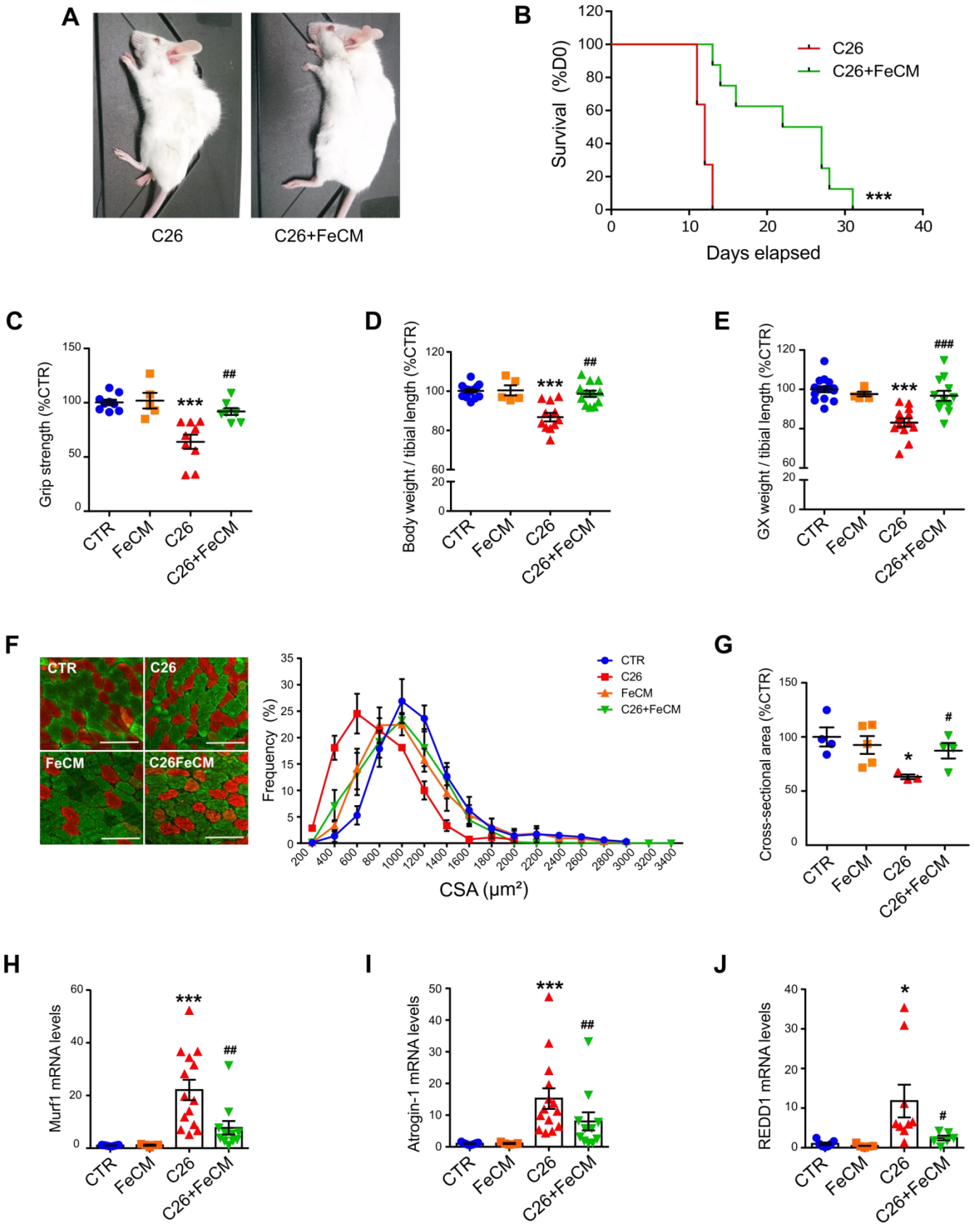
A
C26
C26+FeCM
B
Survival (%D0)
Days elapsed
C26
C26+FeCM
***
C
Grip strength (%CTR)
D
Body weight / tibial length (%CTR)
E
GX weight / tibial length (%CTR)
CTR
FeCM
C26
C26+FeCM
F
CTR
C26
FeCM
C26FeCM
Frequency (%)
CSA (µm²)
G
Cross-sectional area (%CTR)
H
Murf1 mRNA levels
I
Atrogin-1 mRNA levels
J
REDD1 mRNA levels

Figure 16. Iron supplementation prevents cancer-induced cachexia in tumor-bearing mice

(A) Representative images of C26-tumor bearing mice receiving saline solution (left, C26) or iron carboxymaltose 15mg/kg I.V. injection (right, C26 + FeCM) taken at day 12 after C26 injection.

(B) Kaplan-Meier survival curve of C26-tumor bearing mice after I.V. injection of saline or iron every 5 days post C26-injection (3-month-old Balb/C, n=8-11).

(C) Grip strength of mice measured at day 12 post C26 injection. Healthy mice were treated with vehicle (CTR) or iron carboxymaltose (FeCM). Data normalized to average strength of the control group (n=5-9).

(D) Final body weight of C26-tumor bearing mice after iron supplementation at day 12 post C26 injection (n=5-12).

(E) Gastrocnemius weight normalized to tibial length of C26-tumor bearing mice after iron supplementation at day 12 post C26 injection (n=5-12).

(F-G) Immunofluorescent staining of myosin heavy chain fast (green) and slow (red) of transversal sections of gastrocnemius (midbelly) with corresponding frequency distribution (F) and average cross-sectional areas (G) (n=3-5).

(H-J) mRNA levels of Murf 1 (H), Atrogin 1 (I), and REDD1 (J) normalized to GAPDH in gastrocnemius (n=5-14).

Statistical significance was calculated by one-way Anova with Bonferroni's correction, or chi-square test for the survival curves (B). Significance was defined as *:$p<0.05$, ***:$p<0.001$ compared to control and #:$p<0.05$, ##:$p<0.01$ and ###:$p<0.001$ compared to C26 group.

Iron supplementation does not modulate tumor growth in C26-tumor bearing mice

Importantly, C26 tumor growth was unchanged following FeCM injection in mice (**Fig. 17A**), ruling out that the improvement of muscle function and mass following FeCM injection in C26-tumor bearing mice could be due to reduced tumor burden. Indeed, despite increased iron content (**Fig. 17B**), tumors extracted from iron-treated mice showed decreased TFR1, increased FPN and FT expression, indicating a normal physiological response to increased iron levels (**Fig. 17C**).

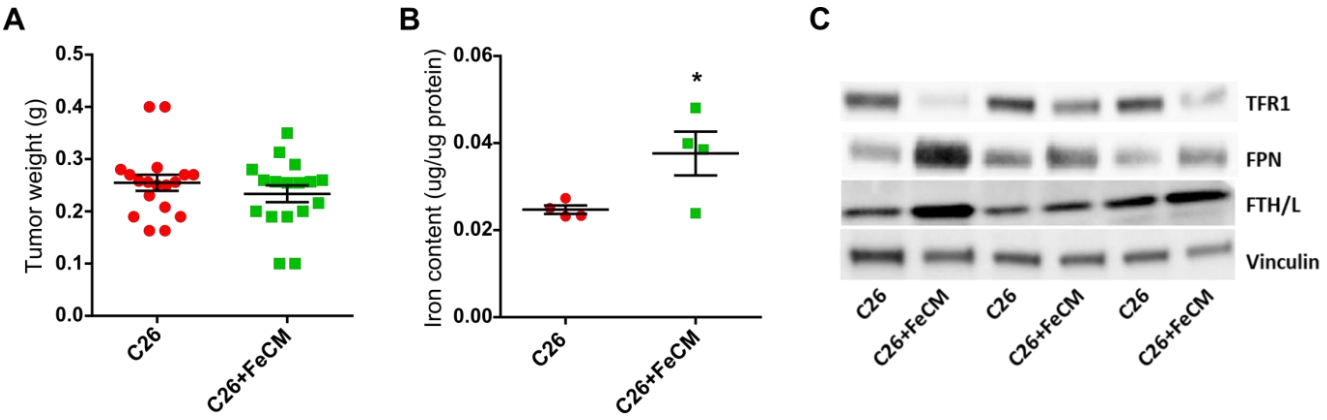

Figure 17. Iron supplementation does not alter tumor growth in mice

(A) Final weight of total tumor mass extracted from mice after sacrifice (12 days after C26-injection, n= 17).
(B) Total iron content in C26-tumors quantified by ICP-MS and normalized to protein content (n=4).
(C) Representative immunoblots showing the expression of iron trafficking proteins (TFR1, FPN, and FT) in C26-tumors (n=4).
Statistical significance was calculated by unpaired, two-tailed Student's T-test. Significance was defined as *:$p<0.05$ compared to C26 group.

Iron supplementation does not affect inflammation nor anemia in cachexia

Since cancer-induced cachexia is largely driven by inflammation, we checked how iron supplementation affects the inflammatory state of cachexia. In the skeletal muscle, we found no significant difference in IL-6 or IL-1β levels after iron treatment in tumor-bearing mice (**Fig. 18A-B**). Indeed, systemic inflammation can also lead to anemia through several mechanisms, and anemia has been associated with muscle weakness. Consistent with the unchanged inflammation, we found that iron supplementation does not rescue anemia in tumor-bearing mice (**Fig. 18C**). Therefore, the improved strength and overall health in mice receiving iron treatment does not result from changes in inflammation or hematocrit.

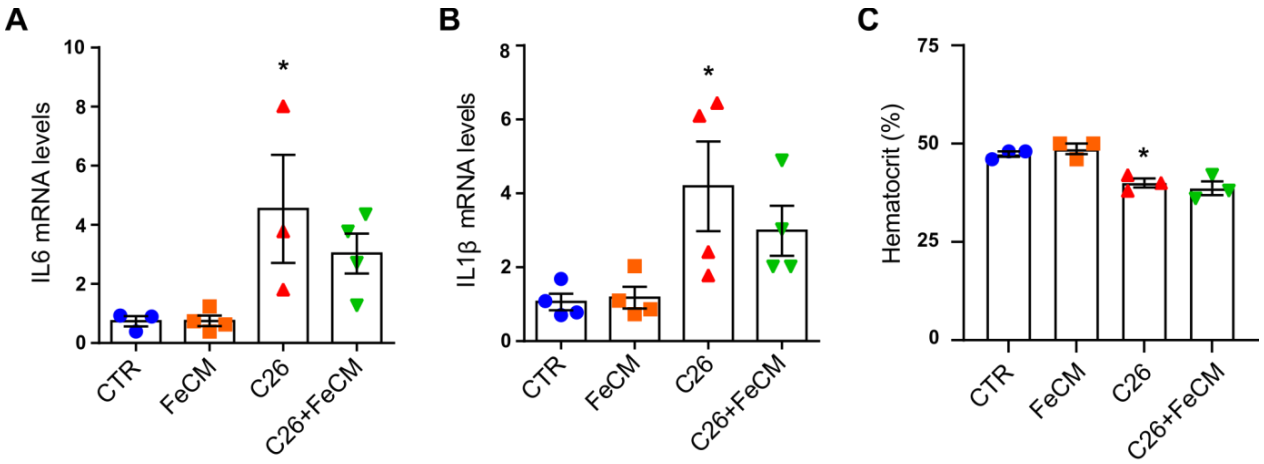

Figure 18. Inflammation and anemia remain in tumor bearing mice after iron supplementation
(A-B) Interleukin 6 (A) and interleukin 1 beta (B) mRNA levels in mouse gastrocnemius (n=3-4).
(C) Hematocrit in healthy or tumor-bearing mice, treated with vehicle or iron carboxymaltose 12 days after C26-injection (n=3).
Statistical significance was calculated by one-way Anova with Bonferroni's correction. Significance was defined as *:$p<0.05$ compared to control.

Mitochondrial iron repletion refuels oxidative metabolism *in vivo*

Since we previously evidenced a decrease in mitochondrial iron levels *in vivo* and enhanced oxidative metabolism upon iron supplementation *in vitro*, we postulated that mitochondrial iron levels specifically control muscle mass *in vivo*.

First, we verified that mitochondrial iron stores are replete in tumor-bearing mice that received iron injections (**Fig. 19A**). Given that iron is required for the activity of several enzymes involved in the TCA cycle and mitochondrial oxidative metabolism (OXPHOS) (*351*), we assessed the enzymatic activity of two iron-sulfur proteins, aconitase (ACO) and succinate dehydrogenase (SDH). Coherent with the mitochondrial iron levels, we observed a drop in the activity of both enzymes in the skeletal muscle of tumor-bearing mice, which could be counteracted by iron supplementation (**Fig. 19B-C**). Along with these alterations, we observed a drop in mitochondrial ATP (**Fig. 19D**) and increased AMPK phosphorylation, denoting energy shortage in cachectic muscles (*488*) (**Fig. 19E**), that were also reverted upon iron supplementation. Indeed, AMPK activation can cause fatty acid oxidation (FAO), which has been shown to promote muscle wasting (*489*). Consistently, iron supplementation abrogated the induction of FAO genes by cancer cachexia, namely ACOT1 (Acyl-CoA Thioesterase 1), MCD (Malonyl-CoA decarboxylase), and CPT1b (Carnitine Palmitoyltransferase 1b) (**Fig. 19F-H**).

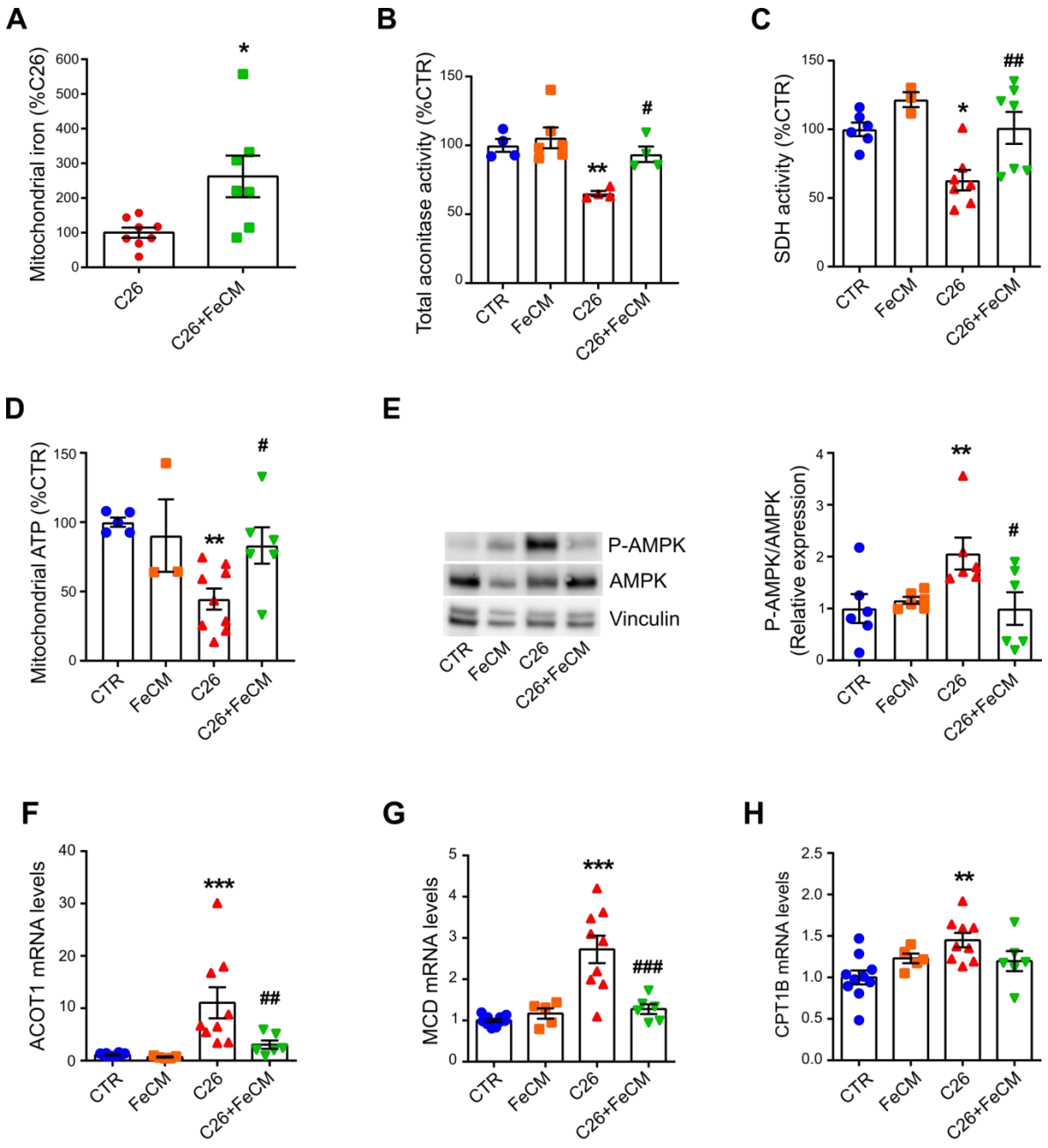

Figure 19. Mitochondrial iron repletion enhances oxidative metabolism

(A) Mitochondrial iron quantified by ICP-MS in quadriceps of C26-tumor bearing mice treated with vehicle or iron carboxymaltose supplementation (n=7-8).

(B) Aconitase activity of quadriceps lysates normalized to protein content (n=4-6).

(C) Succinate Dehydrogenase activity staining of gastrocnemius transversal sections and resulting intensity quantification (n=3-7).

(D) Mitochondrial ATP content determined by luminescence assay in the quadriceps (n=3-9).

(E) Representative immunoblot and densitometric quantification of phospho-AMPK and total AMPK in the gastrocnemius (n=6).

(F-H) mRNA levels of ACOT 1 (F), MCD (G), and CPT1B (H) normalized to GAPDH in the gastrocnemius (n=5-10). Statistical significance was calculated by unpaired, two-tailed Student's T-test (A) or one-way Anova with Bonferroni's correction (B-H). Significance was defined as *:$p<0.05$, **:$p<0.01$ and ***:$p<0.001$ compared to control and #:$p<0.05$, ##:$p<0.01$ and ###:$p<0.001$ compared to C26 group.

Cancer patients show increased strength following iron treatment

Based on the promising outcome obtained from our *in vivo* model of cachexia, we further assessed TFR1 transcript levels in the skeletal muscle (precisely rectus abdominis) of colorectal or pancreatic cancer patients presenting anemia and significant body weight loss (**Fig. 20A-B**). In line with our murine models, biopsies from cachectic patients showed considerably lower TFR1 levels (**Fig. 20C**). Next, we measured the grip force of a small cohort of anemic cancer patients who reported muscle weakness, before and after FeCM injection. Improved strength was found in most patients in the dominant hand (**Fig. 20D-F**) within as short as three days. Altogether, these findings indicate that altered iron metabolism contributes to muscle weakness in cachectic patients and highlight a promising therapeutic strategy to counteract skeletal muscle wasting using a clinically available drug.

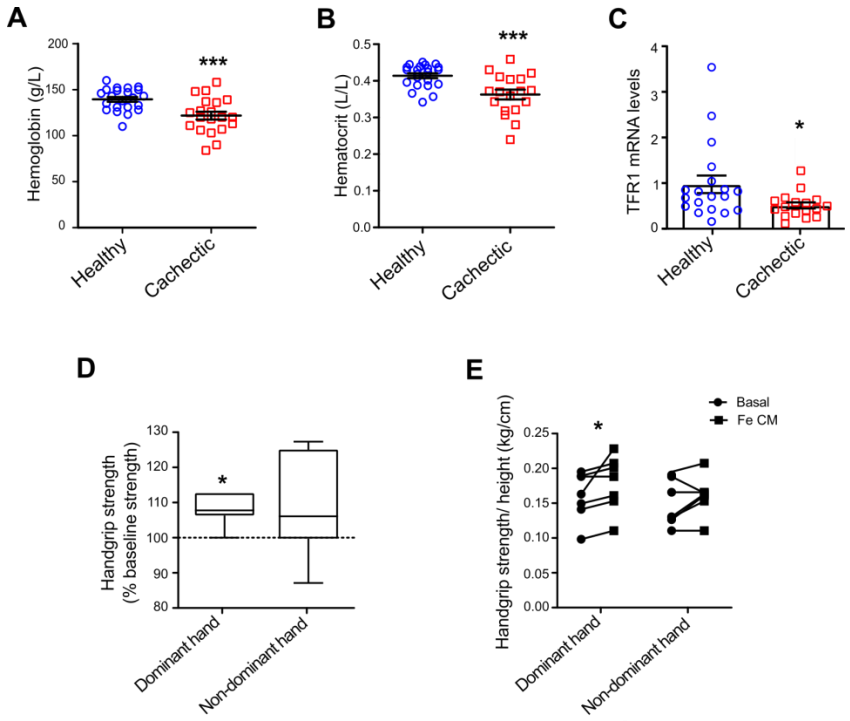

Figure 20. Iron supplementation increases force in cancer patients

(A-B) Hemoglobin (A) and hematocrit (B) levels of healthy subjects and cachectic cancer patients presenting a body weight loss superior to 10% of initial body weight (19 healthy subjects, 17 cachectic patients).

(C) TFR1 mRNA levels in muscle biopsies from cancer-patients of late stage cachexia (19 healthy subjects, 17 cachectic patients with at least 10% total body weight loss)

(D-E) Grip force of dominant or non-dominant arm in iron-deficient cancer patients expressed in percentage of baseline force (D) and absolute values normalized to height (E) before and after single dose of iron carboxymaltose (15mg/kg, 7 subjects).

Statistical significance was calculated by Mann-Whitney U-test. Significance was defined as *:$p<0.05$ compared to healthy patients (A-C) or basal conditions (D-E).

Cancer reduces heme content of the skeletal muscle

We next asked whether the skeletal muscle could mobilize iron towards the circulation through other mechanism than ferroportin during cancer progression. In particular, the skeletal muscle is highly enriched in heme due to the expression of myoglobin, which is responsible for the intracellular storage and transport of oxygen. Intriguingly, we found a significant decrease in heme levels in the skeletal muscle of C26 tumor-bearing mice (**Fig. 21A**). Furthermore, the cytoplasmic heme exporter FLVCR1a is significantly upregulated in the skeletal muscle of C26-tumor bearing mice (**Fig. 21B**), indicating altogether a mobilization of heme from the skeletal muscle to the systemic route. Notably, this phenotype was also observed to a lesser degree in LLC-tumor bearing mice (**Fig. 21C-D**).

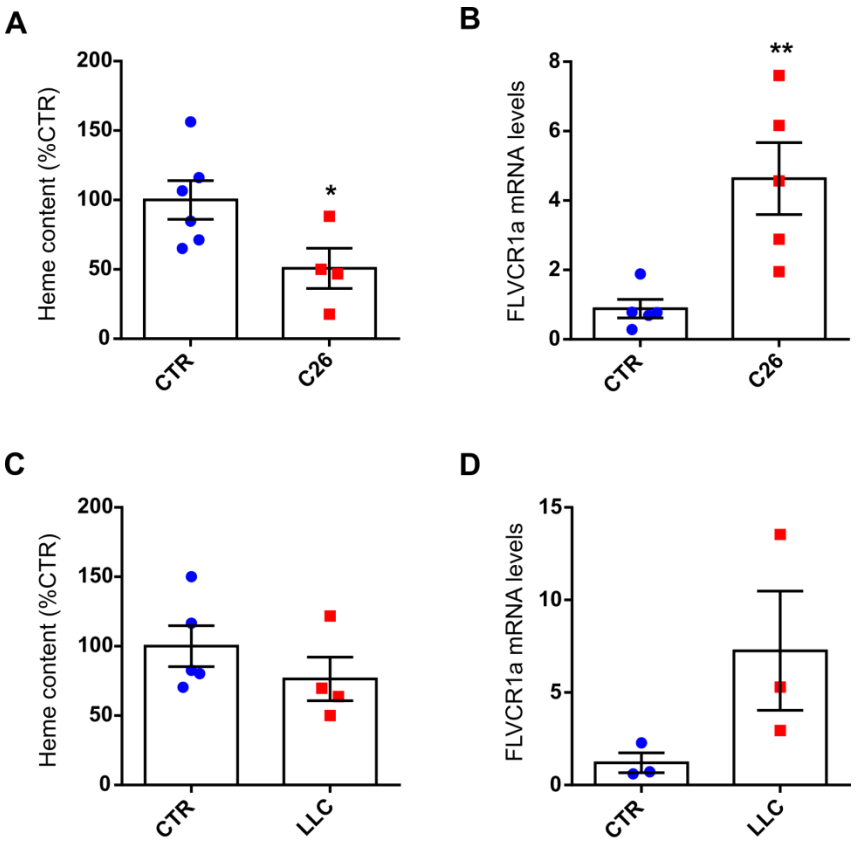

Figure 21. Heme is potentially released from the skeletal muscle during cancer progression

(A-B) Heme content (A) and FLVCR1a mRNA levels normalized to 18s (B) in the gastrocnemius of C26 tumor-bearing mice (n=4-6).

(C-D) Heme content (C) and FLVCR1a mRNA levels normalized to 18s (D) in the gastrocnemius of LLC tumor-bearing mice (n=3-5).

Statistical significance was calculated by unpaired, two-tailed Student's T-test. Significance was defined as *:$p<0.05$ and **:$p<0.01$ compared to control group.

Muscle-specific FLVCR1a knockout mice do not display overt anomaly

To understand the relevance of increased heme export through FLVCR1a from the skeletal muscle during cancer progression, *myoD-Cre* with *FLVCR1a* $^{fl/fl}$ mice were crossed to generate constitutive, skeletal muscle-specific FLVCR1a knockout C57 BL/6 mice (**Fig. 22A**). Interestingly, the knockout did not affect intracellular heme levels, suggesting the presence of a buffering mechanism (**Fig. 22B**). Although FLVCR1a-null mice are associated with defective erythropoiesis and embryonic lethality (*297*), muscle-specific KO mice are viable and do not show altered hematocrit in adulthood (**Fig. 22C**). Similarly, no macroscopic difference in body weight, grip strength or muscle weight was detected (**Fig. 22D-F**).

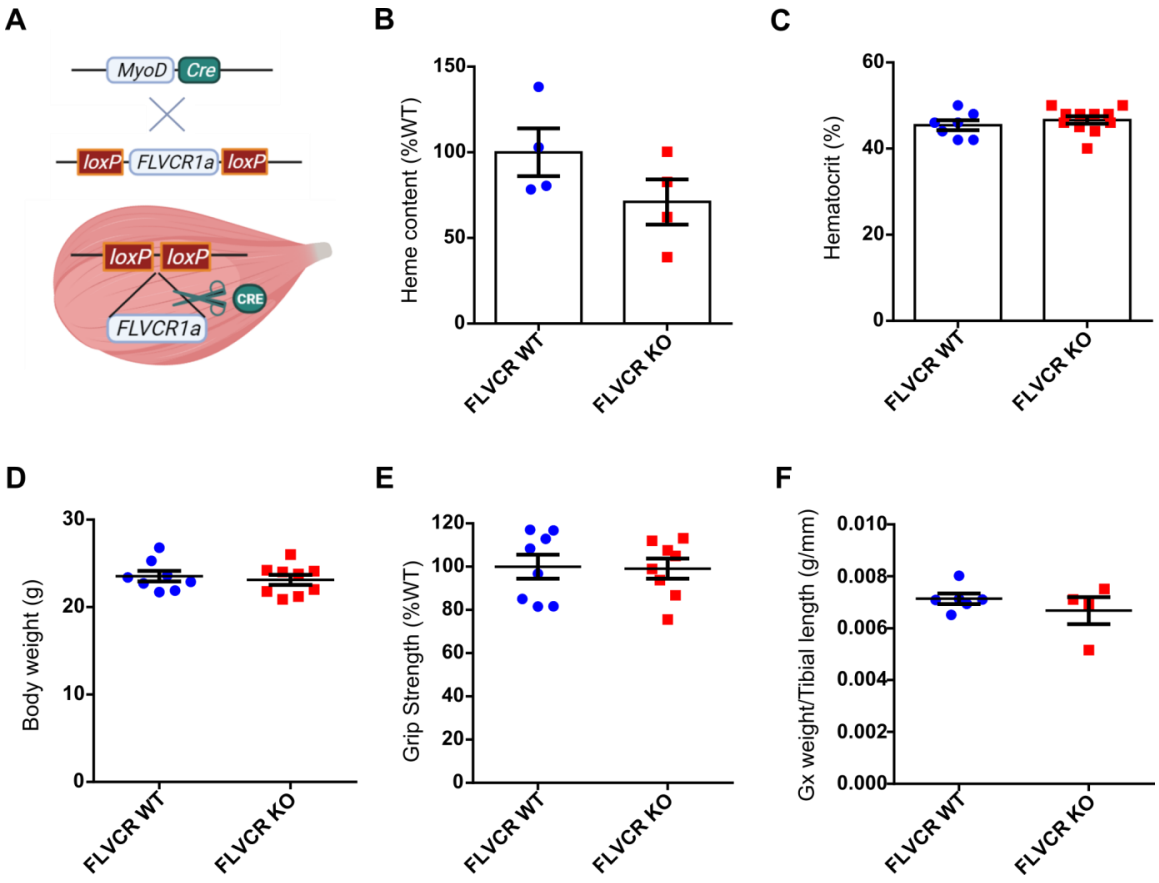

Figure 22. Phenotypic characterization of mice with muscle FLVCR1a silencing
(A) Schematic representation of the genetic breeding of muscle specific FLVCR1a silencing
(B) Heme content in the quadriceps of 10-week-old mice (n=4).
(C) Hematocrit in FLVCR1a MyoD Cre^{+} mice (n=6-12).
(D-F) Body weight (D), grip strength (E), and gastrocnemius weight normalized to tibial length (F) of FLVCR1a MyoD Cre^{+} mice (n=4-9). Statistical significance was calculated by unpaired, two-tailed Student's T-test.

Muscle-specific FLVCR1a knockout hinders tumor metastasis

Next, to assess the impact of muscle FLVCR1a knockout on tumor progression, we used the model of LLC (subcutaneous injection) that has a slower kinetic in tumor growth to allow accurate monitoring, in addition to its metastatic potential which can provide a valuable insight into another aspect of tumor progression. At the end of the experiment (day 25 post-injection), we did not observe significant change in the evolution of body weight and tumor growth between wildtype and muscle-FLVCR1a knockout mice (**Fig. 23A-B**). As for non-tumor bearing mice, we found no difference in muscle strength (**Fig. 23C**), muscle and organ weights (**Fig. 23D-H**). Nevertheless, lung metastasis was substantially reduced, notably in terms of size in FLVCR1a knock-out mice despite consistent tumor growth (**Fig**. **23I**).

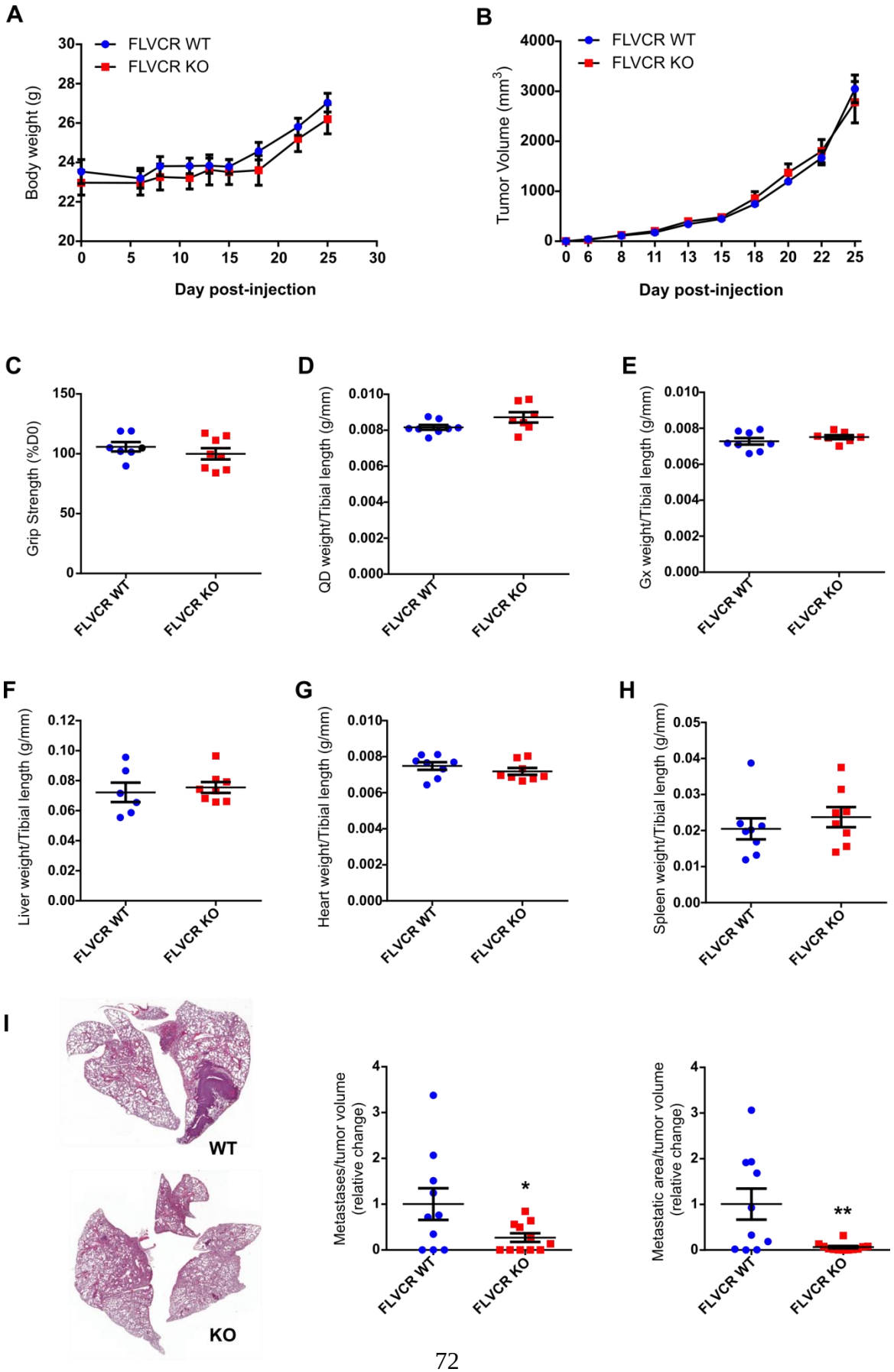
A
FLVCR WT
FLVCR KO
Body weight (g)
Day post-injection
B
FLVCR WT
FLVCR KO
Tumor Volume (mm3)
Day post-injection
C
Grip Strength (%D0)
FLVCR WT
FLVCR KO
D
QD weight/Tibial length (g/mm)
FLVCR WT
FLVCR KO
E
Gx weight/Tibial length (g/mm)
FLVCR WT
FLVCR KO
F
Liver weight/Tibial length (g/mm)
FLVCR WT
FLVCR KO
G
Heart weight/Tibial length (g/mm)
FLVCR WT
FLVCR KO
H
Spleen weight/Tibial length (g/mm)
FLVCR WT
FLVCR KO
I
WT
KO
Metastases/tumor volume (relative change)
*
FLVCR WT
FLVCR KO
Metastatic area/tumor volume (relative change)
**
FLVCR WT
FLVCR KO

Figure 23. Muscle-FLVCR1a silencing reduces tumor metastasis without affecting tumor growth

(A) Evolution of body weight of LLC-tumor bearing mice (n=7-8).

(B) Evolution of tumor growth in volume of LLC-tumor bearing mice (n=7-8).

(C-H) Grip strength (C), quadriceps (D), gastrocnemius (E), liver (F), heart (G), and heart (H) weights normalized to tibial length of LLC-tumor bearing mice (n=7-8).

(I) Representative pictures of hematoxylin/eosin-stained lungs (left), number of metastasis (middle) or metastatic area (right) normalized to primary tumor volume of LLC-tumor bearing mice (n=10-12).

Statistical significance was calculated by ordinary two-way Anova (A-B) or unpaired, two-tailed Student's T-test (C-I). Significance was defined as *:$p<0.05$ and **:$p<0.01$ compared to wildtype group.

Muscle FLVCR1a modulates the immune landscape

Considering that heme has been shown to activate immune cells (notably macrophages) and endothelial cell migration (*490*). We hypothesized that muscle FLVCR1a expression influences tumor angiogenesis or immune profile of the primary tumor, thereby promoting metastasis. Therefore, we performed FACS analysis of LLC primary tumors to analyze cellular composition and found no significant changes in myeloid-derived suppressor cells, endothelial cells, T-cells, or macrophages (**Fig. 24A-D**), but a strong and consistent decrease in neutrophil count in muscle-FLVCR1a knockout mice (**Fig. 24E**). These findings require further validation but indicate that heme derived from the skeletal muscle can potentially fuel tumor progression through modulation of the immune system.

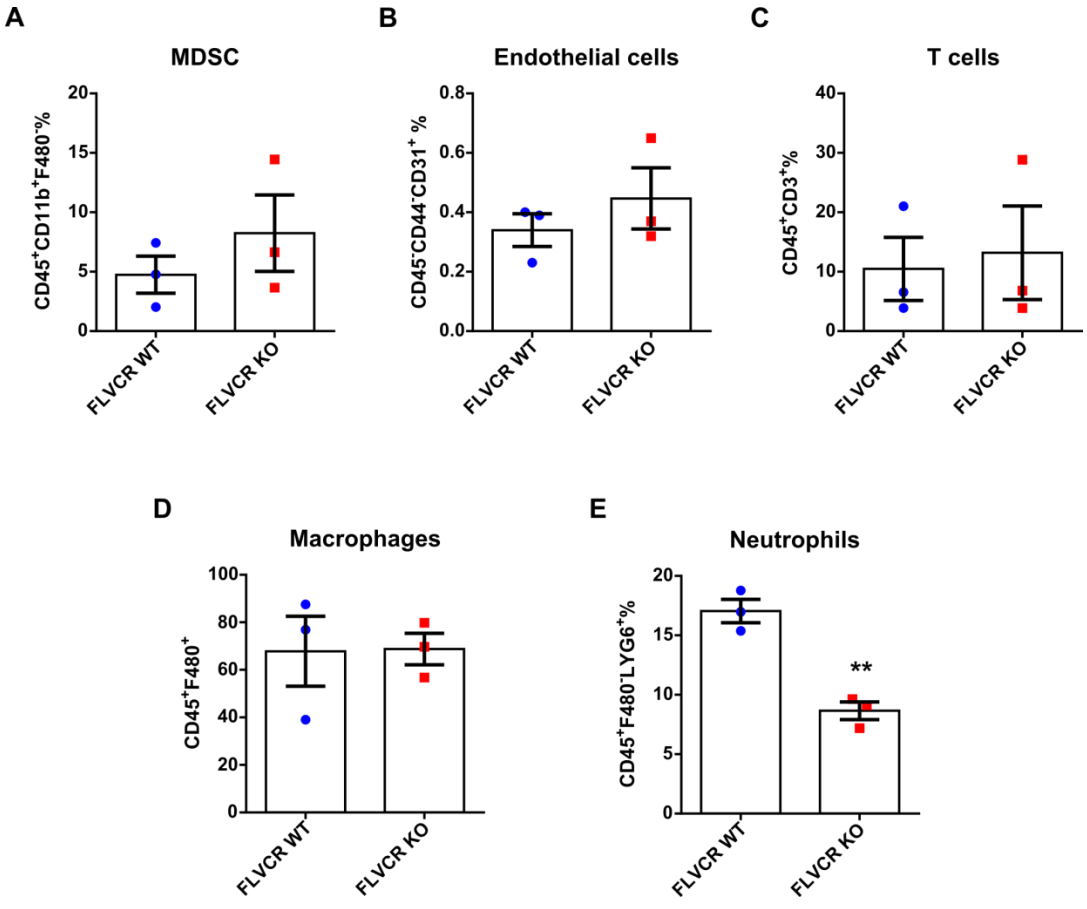

Figure 24. Muscle-FLVCR1a decreases neutrophil infiltration in the primary tumor

(A-E) Percentage of myeloid-derived suppressor cells (**A**), endothelial cells (**B**), T-lymphocytes (**C**), macrophages (**D**), and neutrophils (**E**) in the primary tumor measured by FACS and normalized to total cell count or myeloid cell count (n=3). Statistical significance was calculated by unpaired, two-tailed Student's T-test. Significance was defined as **:$p<0.01$ compared to wildtype group.

Discussion

This work provides evidence of an iron-mediated control of muscle mass in the context of cancer cachexia. We show that cancer induces striking alterations of iron metabolism in the skeletal muscle, characterized by aberrant expression of iron-trafficking proteins that likely results from impaired iron-regulation. Consequently, insufficient mitochondrial iron leads to metabolic dysfunction and energy imbalance, driving skeletal muscle wasting. We further demonstrate that muscle force and mass can be maintained, or even rescued by iron supplementation.

Despite being the biggest tissue in human body, the involvement of skeletal muscle in systemic iron homeostasis has been overlooked. However, the skeletal muscle holds a substantial pool of iron that can be mobilized for instance to support erythropoiesis in healthy humans, as an adaption mechanism to high-altitude hypoxia (*491*). Since iron-deficiency and anemia are both common in cancer patients (*483*) and are associated with impaired physical function, weakness, and fatigue, we hypothesized a link between altered iron metabolism and muscle wasting. Surprisingly, we found that in both mice and humans, TFR1 is paradoxically downregulated in the skeletal muscle despite iron deficiency or anemia, highlighting the role of skeletal muscle as an expendable body compartment.

Intriguingly, C26 tumor-bearing mice displayed normal total iron content, but elevated protein-bound iron as reflected by increased ferritin expression. We further found that tumor-bearing mice display IRP dysfunction due to oxidative stress, consequently leading to sequestration of cytosolic iron and downregulation of iron import despite iron deficiency. This phenotype matches the observations reported in several IRP2 knockout models (*492-494*). In the other hand, the discrepancy between the elevated FPN mRNA levels but its reduced protein expression could result from the complex regulation of FPN at different levels. Despite the supposedly increased translation due to IRP dysfunction, massive inflammation as seen in our C26-cachexia model can eventually suppress FPN protein levels through hepcidin overload.

Based on the consistent findings of TFR1 downregulation in several murine models and cancer patients, we first silenced TFR1 in myotubes and in the skeletal muscle of healthy mice, which was sufficient to cause atrophy. This demonstrates an important role of iron metabolism in muscle mass homeostasis, and was confirmed by iron chelation through apotransferrin, DFO, or BPS treatment *in vitro,* or by subjecting mice to phlebotomy and iron-deficient diet (causing severe iron deficiency and anemia).

Conversely, TFR1 overexpression in the skeletal muscle resulted in hypertrophic myofibers, and iron replenishment proved to be protective against conditioned medium-induced atrophy. These observations are in line with the severe systemic metabolic dysfunction reported in muscle specific TFR1 knockout mice (*495*). To validate the beneficial effects of iron in cancer-cachexia *in vivo*, we used ferric carboxymaltose (FeCM), a clinically approved supplement (*496*) which can enter in cells independently of TFR1 expression (*497*). Promisingly, intravenous administrations of FeCM rescued body mass, muscle mass and function, and even increased the viability of tumor-bearing mice. From the mechanistic standpoint, our work shows that iron supplementation refuels mitochondrial function. Noteworthy, the upregulation of MFRN2 and ALAS2 in the skeletal muscle of tumor-bearing mice could be interpreted as a compensatory response to mitochondrial iron deficiency. Interestingly, ALAS2 overexpression has been previously linked to muscle weakness and atrophy in a transgenic mouse model (*498*).

Indeed, iron is essential for mitochondrial function (*499*) as it catalyzes a myriad of bioenergetic processes and its deprivation impairs mitochondrial biogenesis, enhances mitophagy and leads to metabolic dysfunction (*500-502*). In other studies, mitochondrial dysfunction has been functionally linked to wasting in both pathological conditions and aging (*223, 503, 504*). In particular, cancer-induced muscle atrophy typically features reduction of mitochondrial content and DNA copy (*225, 505*). Therefore, reduced mitochondrial iron availability expectedly arises from diminished organelle number. However, our findings of mitochondrial iron loading and aconitase activity decrease were normalized to mitochondrial protein content, hence independently of mitochondrial mass or number.

Notably, this observation is associated with decreased mitochondrial activity and increased AMPK phosphorylation, hence an overall increased catabolism in cachectic mice. The oxidative stress generated by dysfunctional mitochondria might exacerbate the abnormal iron metabolism via IRP inhibition, creating a vicious cycle. We found especially a drop of enzymatic activity of two major ISC proteins of the TCA cycle and electron transport chain: Aconitase and SDH, corroborating with the declined oxidative capacities and energetic inefficiency found in cachexia (*506, 507*). Our work confirms and extends studies showing that iron deficiency decreases ISC proteins, cytochrome content, and/or total oxidative capacity in the skeletal muscle (*508-511*). Furthermore, mitochondrial dysfunction is known to trigger catabolic pathways, notably FAO (*512*) that has been widely associated with skeletal muscle wasting (*225, 513*). While the induction of fatty acid catabolism genes we found is

in line with the findings of Fukawa et al. on human kidney cancer-induced cachexia (*489*), other models of cancer-cachexia and iron deficiency have been linked to suppressed FAO (*514, 515*). Given the dysfunctional mitochondria in the skeletal muscle of tumor bearing mice, it is possible that the upregulation of FAO genes rather reflects an attempt of the skeletal muscle to buffering the energetic failure.

Coherently with previous reports on cancer patients, our data supports the correlation between ferritin levels and muscle atrophy (*516*). Furthermore, we provide evidence of an altered intracellular distribution of the element rather than a general overload. Although our findings suggest that this alteration primarily results from oxidative stress-induced impairment of iron-regulatory proteins, antioxidant therapy (catechins, quercetin and vitamin C) has been previously reported to accelerate muscle wasting and death in C26-tumor bearing mice (*517*). Moreover, iron repletion led to increased muscle mass in tumor-bearing mice without counteracting the altered expression of iron-trafficking proteins (data not shown), implying the persistence of impaired iron-sensing, and indicates that iron availability directly controls muscle mass despite sustained oxidative status. Nonetheless, given the multifaceted roles of iron, it is not surprising that iron overload can also lead to defective autophagy causing muscle atrophy (*518*).

Recent studies have shown that iron levels influence myogenesis (satellite cell activation and fusion) (*519, 520*). However, we found that the effect of iron on myogenesis is negligible at least *in vitro*, while it mainly modulates myotube mass through the regulation of protein turnover and metabolic function. This is congruent with previous work showing that iron chelation attenuates protein synthesis *in vitro* characterized by AMPK activation (*521*) and mTORC1 inhibition via REDD1 (*522, 523*). Coherently, the rapid rescue of muscle strength (occurring within 24h or few days) detected in tumor-bearing mice and cancer patients following iron injection is unlikely due to increased stem cell differentiation or myogenesis. Similarly, this short timeframe would not allow enough time for erythropoiesis, and anemia consistently remained after iron supplementation in C26-tumor bearing mice.

Of note, myofiber-specific TFR1 silencing is sufficient to cause atrophy in healthy mice, and cytokine expression within the skeletal muscle remains unchanged following iron supplementation (despite increased mass) in tumor-bearing mice. These data suggest altogether that the regulation of muscle mass by iron is unrelated to inflammation. Nevertheless, we do not exclude other systemic effects upon

iron repletion. For instance, iron could regulate endocrine (*524*), hepatic (*525*) and adipose tissue function (*526*), or even immune response (*465*), which might contribute to the increased survival. For example, early investigation has reported that iron deficiency attenuates hepatic gluconeogenesis in rats (*525*). Moreover, we could also conjecture that iron increases immunity as iron loading in macrophage was shown to improve survival in lung cancer patients (*467*)

Coherently with the *in vivo* data, we observed an improvement of handgrip strength within few days after iron treatment in iron-deficient patients (hence excluding the potential involvement of erythropoiesis or muscle generation), while previous data on cardiac failure patients reported beneficial effects after long term treatment (*527*). Further studies will be essential to better define the impact of short-term iron treatment on patients, especially on blood parameters and endocrine regulation. Importantly, together with the fact that iron levels directly regulate muscle strength and mass, one can postulate that iron supplementation is potentially beneficial also in other muscle atrophy diseases besides cancer cachexia.

Although iron addiction has become a general paradigm of cancer, we surprisingly observed a physiological response from C26-tumors characterized by reduced TFR1, increased FPN and FT levels. Indeed, low dose of iron treatment considerably fostered C26 cancer cell proliferation *in vitro* (data not shown), tumor growth *in vivo* was however unaffected despite the increased iron levels. Consistently, this finding was confirmed in LLC and KPC (K-ras$^{LSL.G12D/+}$; p53$^{R172H/+}$; PdxCre) cancer models after 3-4 weeks of repeated iron treatment (data not shown). Several possibilities may underlie these unexpected observations: A significant amount of iron could be taken up by non-cancer cells of the tumor niche, *e.g.* fibroblasts, adipocytes, immune cells (especially macrophages which could then polarize to pro-inflammatory phenotype). Second, the doubled iron loading within the tumor could possibly promote ferroptosis if most iron is taken up by malignant cells. Indeed, ferritin and ferroportin upregulation by the tumor can indicate excessive iron but also oxidative stress. Histological studies of the tumor or iron quantification following cell-sorting should elucidate better the fate of iron within the tumor. Our data corroborates with the longer survival observed in C26-tumor bearing mice upon prevention of muscle atrophy but not tumor growth by ActRIIB antagonism (*193*). Altogether, these findings highlight that cancer and cachexia are two dissociable conditions, and further supports iron supplementation as a therapeutic option in the treatment of cancer-induced cachexia. Yet, this strategy should be validated in other cancer models as some cancer types feature more addiction for iron than others.

Noteworthy, our *in vitro* data from myotubes do not fully recapitulate the ones *in vivo.* The relevance of TFR1 in CM-induced atrophy is less clear *in vitro* as we did not observe changes in TFR1 levels upon treatment with conditioned medium at the time of analysis (48h, data not shown). Since we expect that the drop in TFR1 expression in cancer cachexia results mainly from oxidative-stress induced IRP impairment, we could speculate that 48h of CM treatment induces only mild oxidative stress *in vitro*. Consequently, the levels of iron trafficking proteins are maintained at homeostasis. Further investigation should unravel the mechanism through which C26-CM eventually causes lower intracellular availability *in vitro.*

Besides the metabolic alteration of iron in the skeletal muscle, this work further demonstrates its crosstalk with the tumor through the release of heme. The trigger of heme export from the skeletal muscle and the potential causative relationship in muscle wasting warrant further investigation. Interestingly, circulating heme was previously found to compromise host tolerance to infection by accelerating severe sepsis irrespective of pathogen load in mice (*528*). Elevated plasma heme levels were also found in prostate cancer patients (*432*). However, the contribution of skeletal muscle to systemic heme homeostasis has not been studied up to date.

Unexpectedly, we did not observe heme accumulation in FLVCR1a-silenced skeletal muscle. This observation suggests the presence of a compensatory mechanism to maintain intracellular heme levels, *e.g.* decreased heme synthesis and/or increased degradation. In the latter case, pro-inflammatory heme is broken down to carbon monoxide and biliverdin, two signaling molecules with potent anti-inflammatory properties (*268*). Moreover, FLVCR1a has been shown to regulate cellular oxidative metabolism (*529*). Its alteration can hence result in substantial metabolic changes. Metabolomic analysis of the skeletal muscle and serum will clarify whether the effects observed are directly caused by the inhibition of heme export (hence reduced circulating heme levels), or eventually by other metabolites resulting from metabolic rewiring of the skeletal muscle.

As for iron, heme avidity has been largely acknowledged as a feature of cancers. Nevertheless, heme can also activate innate immune cells and promote inflammation by increasing vascular permeability, leukocyte migration and acute-phase protein secretion (*530, 531*). Notably, heme can directly induce neutrophils migration as a chemotactic molecule, or through leukotriene B4 secretion by macrophages (*532, 533*). Therefore, the effects of heme are highly variable according to the context. Unrelated to heme, several lines of evidence support the role of neutrophils in the multistep metastatic process of

cancer cell, including migration, invasion, and intra/extravasation (*534*). Importantly, neutrophils were found to infiltrate lungs before metastatic spread in a murine model of breast cancer, and neutrophil-derived leukotrienes promoted the expansion of cancer cells with high tumorigenic potential (*535*). The same study showed that mice with neutropenia have specifically lower metastatic burden, although the tumor growth was not affected (*535*). Similarly, our muscle specific FLVCR1a knockout mice have no difference in tumor growth despite the significantly reduced neutrophil count, which however impacted metastasis. Noteworthy, in light of the strongly decreased size (more than the number) of metastasis, one can expect a stronger immune modulation in the metastatic niche, hence in the lungs. Future work is however required to yield deeper mechanistic explanation.

In conclusion, our findings establish a direct role of iron availability in the control of skeletal muscle mass, and evidence a new line of crosstalk between skeletal muscle and tumors. Our data suggests two main mechanisms mediating increased muscle mass after iron-repletion: First, iron rapidly boosts the activity and/or abundance of iron-dependent enzymes, improving primarily mitochondrial function. Second, through the regulation of REDD1-mTOR signaling, iron favors overall protein synthesis. Altogether, iron supplementation restores skeletal muscle homeostasis notably *via* mitochondrial metabolism normalization, paving the way for a new therapeutic strategy to prevent or even rescue muscle atrophy in cancer-induced cachexia, but also in non-cancer conditions presenting iron deficiency as co-morbidity, such as COPD and chronic cardiac failure. Furthermore, we show that skeletal muscle can influence cancer progression through to immune modulation, providing an important insight into tumor-host crosstalk that can potentially be targeted.

Materials and Methods

Human skeletal muscle biopsies

The study enrolled patients (age > 18 years) with pancreatic cancer surgically treated at the 3rd Surgical Clinic of Padova University Hospital. Cancer patients were classified as severely cachectic in cases of >10% weight loss in the 6 months preceding surgery. The study also enrolled control, healthy donors undergoing elective surgery for non-neoplastic and non-inflammatory diseases. Patients with signs of infection were excluded. All patients joined the protocol according to the guidelines of the Declaration of Helsinki and the research project has been approved by Ethical Committee for Clinical Experimentation of Provincia di Padova (protocol number 3674/AO/15). Written informed consent was obtained from participants. The biopsies were performed during elective surgery within 30 min of the start of the surgery by cold section of a rectus abdominal fragment of about 0.5-1 cm. The fragment was immediately frozen and conserved in liquid nitrogen for gene expression analysis.

Human handgrip strength

Participants with either an absolute iron deficiency (AID) or a functional iron deficiency (FID) were included in the clinical study. AID is defined by an iron-saturation of transferrin (TSAT) <20% and serum ferritin level < 30 ng/ml. FID is defined by a TSAT <20% and serum ferritin levels above 30ng/ml. Patients were treated with a single intravenous infusion of 1000 mg of iron (ferric carboxymaltose). Participants were asked to perform two handgrip tests to measure their strength using a hand dynamometer. The first handgrip test (HG1) was conducted prior to iron administration. The second handgrip test (HG2) was conducted within 2-12 days after iron administration.

The hand dynamometer was calibrated and the measurements have an accuracy of +/- 5%. The test-retest reliability is good ($r > 0.80$) and the inter-rater reliability is excellent ($r = 0.98$). The handgrip test required the participants to be seated, positioning their forearm of their hand in a 90° angle with their body. The arm should not be pressed to the body or supported by an armrest and the shoulders should be relaxed. The grip of the hand dynamometer was adjusted to the hand size of the participant. The hand dynamometer was placed in the dominant hand and the participant was asked to squeeze the hand dynamometer as hard as possible until the strength indicator was stabilized (this took approximately 3-5 seconds). This was repeated three times, in between each measurement the participant was given 30 seconds to relax the arm and hand muscles. All participants gave written informed consent to participate in the study and the study was approved by the Antwerp University Hospital ethical

committee in accordance with the ethical standards established by the 1964 Declaration of Helsinki.

Animal experimentation

All animal experiments were authorized by the Italian Ministry of Health and carried out according to the European Community guiding principles in the care and use of animals. Cancer cell lines (C26 colon murine adenocarcinoma or LLC Lewis lung carcinoma, $1x10^6$ cells/mouse) were injected subcutaneously in the flank of 8 weeks old female mice (BALB/C for C26, C57 BL/6 for LLC). LLC (Lewis Lung Carcinoma) tumor-bearing mice were necropsied on day 25 post injection. For C26, all mice were sacrificed at day 12 except for the survival experiment.

Ferric carboxymaltose (Ferrinject 15mg/kg, Vifor Pharma) or saline solution (NaCl 0.9%) was injected in the tail vein every 5 days starting from day 5 post-C26 inoculation. Blood was collected by cardiac puncture, and perfusion with PBS after anesthesia was performed to obtain samples for iron quantification.

Electroporation experiments were performed as previously described (*536*) on tibialis anterior with TFR1-pHuji plasmid (Addgene 61505) or shTFR1-pGFP plasmid using BlockIT miRNA expression kit (Thermo Fisher K493600). All mice were sacrificed two weeks after electroporation.

For the iron deprivation experiment, 8 weeks old female C57BL/6 mice were subjected retroorbital bleeding (400µl blood) under anesthesia, and then fed with iron-deprived diet (Mucedola) for 11 days before sacrifice.

To measure strength, mice were held by the middle part of the tail and allowed to grab the metal grid of a dynamometer (2Biol) in a parallel position before being gently pulled backwards. The maximal force generated by the grip was recorded, and the measure was repeated six times. In all experiments were freshly isolated, weighted, and normalized to the respective tibial length.

Cell culture and *in vitro* treatments

C2C12 myoblasts were purchased from ATCC and cultured in DMEM with 10% fetal bovine serum (FBS). After reaching full confluency, differentiation was induced by switching to 2% horse serum (HS) DMEM for 4 days. Conditioned medium (CM) was prepared as previously described (*537*). Briefly, cancer cells were grown to high confluency, then conditioned in serum-free DMEM for 24h, medium was harvested and centrifuged at 500g for 10min. Supernatant was collected and used as conditioned medium at 10% final concentration. Deferoxamine (DFO, Sigma D9533) and bathophenanthroline

disulphonic acid (BPS, Sigma 146617) were used at 100µM. Apo-transferrin (Sigma T0178), hinokitiol (HNK, Sigma 469521) and ferric citrate (Sigma F3388) were used at 400µg/ml, 5µM and 250nM, respectively. Activin A (RnD Sytem 338-AC), Dexamethasone (DEXA, Sigma D4902) were used at 1nM and 1µM, respectively. Rotenone was used at 20 nM. Except where noted otherwise, myotubes were treated for 48h for all compounds. For cell transfection, C2C12 myoblasts were differentiated for 3 days prior to transfection with esiTFR1, esiNCOA4, or esiGFP using Lipofectamine 2000 (Invitrogen 11668019). Myotubes were photographed and lysed at 72h post-transfection. For myotube diameter quantification, pictures of myotubes were taken with phase contrast microscopy (Zeiss) at 200x magnification, and myotube diameter was measured using the software JMicroVision as previously described (*538*). For the fusion index, C2C12 cells were fixed in 4% PFA , permeabilized and stained for Myosin Heavy Chain (Sigma M4276) and nuclei were stained with DAPI. The fusion index was determined as the ratio of nuclei number per myotube on the total number of nuclei in the field.

Western blotting

Frozen gastrocnemii were lysed in RIPA lysis buffer (150mM NaCl, 50mM Tris-HCl, 0.5% sodium deoxycholate, 1.0% Triton X-100, 0.1% SDS, and 1mM EDTA) supplemented with protease and phosphatase inhibitor cocktail (Roche). Protein concentration was determined using BCA assay (Thermo Fisher Scientific). 15 or 30µg of protein from cell or gastrocnemius lysates, respectively, were loaded per well for SDS-PAGE then transferred onto PVDF membranes prior to immunoblotting analysis. Blots were probed with the following primary antibodies: P-Thr172-AMPK (Cell Signaling 2535), Total-AMPK (Cell Signaling 2532), Ferritin (Sigma F5012), IRP2(PA-116544), Transferrin Receptor 1 (Santa Cruz sc65882), Ferroportin (Novus NBP1-21502). NCOA4 (Santa Cruz C-4), Vinculin (Cell Signaling 4650). Protein carbonylation was assessed by measuring the levels of carbonyl groups using the OxyBlot protein oxidation detection kit (Sigma-Aldrich S7150). Quantification analysis of blots was performed with Image Lab software (BioRad).

Iron quantification and heme assay

Iron content in skeletal muscle was quantified by ICP-MS (Element-2; Thermo-Finnigan, Rodano, Italy) using medium mass resolution ($M/\Delta M \sim 4{,}000$). 50 to 100mg of freshly excised and snap-frozen quadriceps were submitted to overnight dialysis. Samples were collected before and after dialysis to assess total and protein-bound iron, respectively. Additionally, iron content was also measured in isolated mitochondria from quadriceps extracted by fractionation. All samples were digested overnight

in 0.5mL of concentrated HNO_3 (70%) and mineralized by microwave heating for 6min at 150°C (Milestone, Ethos Up Microwave Digestion System). A natural abundance iron standard solution was analyzed in parallel to check for changes in the systematic bias. The calibration curve was obtained using four iron standard solutions (Sigma-Aldrich) in the range of 0.2–0.005 μg/mL. For liver and spleen iron, samples were heated at 180°C overnight and mineralized in 10mL HCl 3M/ 10% trichloroacetic acid per gram of dry tissue overnight at 65°C with gentle shaking. 10μL of supernatants were mixed with a solution of 1.7% of thioglycolic acid (TGA), 84.7% of sodium acetate acetic acid pH 4.5, 13.6% of bathophenanthroline disulfonic acid (Sigma 146617). After 1 hour of incubation at 37°C, absorbance was measured at 535nm. Iron content was determined using a standard curve of ferrous ammonium sulfate. Heme concentration was determined by fluorescence assay as previously described (*539*). Saturated oxalic acid solution was added to 40ug proteins from gastrocnemius lysates prior to heating at 95°C for 30min. Samples were loaded in triplicates and fluorescence was measured at 400nm excitation and 662nm emission wavelengths. For labile iron pool measurement, C2C12 cells were treated with 500nM Calcein AM (Sigma 56496) for 15 min and fluorescence intensity was measured using a microplate reader (ex/em: 475/520nm) . Cells were then incubated for 15 min with 100μm of 2',2'-Bipyridyl (BIP) prior to the second measurement of fluorescence. The LIP was calculated as the difference between two values and normalized to DAPI fluorescence intensity.

Mitochondria isolation and metabolic assays

Mitochondria were isolated from snap-frozen quadriceps by Mitocheck Mitochondrial Isolation kit (Cayman chemical 701010). ATP content was quantified in 20 μg of fresh isolated mitochondria by CellTiter-Glo® Luminescent Cell Viability Assay (Promega G7570). Aconitase activity was measured in quadriceps homogenates by enzymatic assay (Cayman Chemical 705502). Oxygen Consumption Rate (OCR) measurements were conducted using a Seahorse XFe96 analyzer according to manufacturer's protocol. C2C12 myotubes were treated with C26 CM and iron for 48h and incubated in 5% CO_2 at 37°C. One hour prior to analysis, growth medium was replaced with assay medium (DMEM without phenol red and sodium bicarbonate (Corning 90-013-PB) that was supplemented with 1mM pyruvate, 2mM L-glutamine, and 10 mM glucose, pH 7.4) and incubated in a non-CO_2 incubator. During the assay, 1μM oligomycin (Sigma 495455), 1μM FCCP (Sigma C2920), and 0.5μM rotenone/antimycin A (Sigma R8875 and A8674) were sequentially injected into each well in accordance with standard protocols. Absolute rates (p moles/min) were normalized to respective protein concentration determined by Bradford Assay (BioRad 5000006).

Histology

Extracted gastrocnemii were immediately frozen in isopentane cooled in liquid nitrogen and stored at -80°C. Transversal sections of 5µm thickness were cut at the midbelly with a cryostat. Sections were fixed for 10 minutes in PFA 4%, then blocked with 0.1% triton x-100, 1% BSA in PBS before incubating with primary antibodies against fast/slow isoforms of myosin heavy chain and laminin (Abcam 91506, Abcam M8421, Santa Cruz 59854), followed by incubation with the corresponding secondary antibodies (Alexa-488, Alexa-568). For the electroporation of tibialis anterior with reporter plasmids, 8µm sections were stained with AlexaFluor 555-conjugated Wheat Germ Agglutinin (WGA, Thermo Fisher Scientific W32464) and DAPI.

Pictures were captured with a fluorescent microscope (Zeiss/Olympus) and fiber areas were measured with ImageJ software (more than 500 fibers were analyzed per animal). The enzymatic activity of succinate dehydrogenase (SDH) was measured by Succinate Dehydrogenase Activity Colorimetric Assay Kit (BioVision K660-100).

RNA isolation and quantitative PCR

Total RNA was isolated from snap-frozen tissue samples using TRIzol reagent (Invitrogen 15596026) according to the manufacturer's guidelines. 1µg of total RNA was reverse transcribed using the High Capacity cDNA Reverse Transcriptase kit (Applied Biosystems 4374966). cDNA was analyzed by Real Time Quantitative PCR (ABI PRISM 7900HT FAST Real-Time PCR system, Applied Biosystems) using the Luna Universal Probe qPCR master mix (NEB M3004) and the Universal Probe Library system (Roche Applied Science), or with SYBR Green master mix (Applied Biosystems A25741). Relative mRNA levels were calculated using the 2-ΔΔCT method and normalized to GAPDH or 18s mRNA (Eukaryotic 18s rRNA Endogenous Control, Thermo Fisher 4310893E), respectively. For human skeletal muscle biopsies, 500 ng of RNA was reverse transcribed using SuperScript IV Reverse Transcriptase (Thermo Fisher 18090010). Human data were all normalized to Actb gene expression. For *FLVCR1a* transcripts, specific primers and probe were designed using Primer Express Software Version 3.0 (Applied Biosystems). The following primers were used for the remaining genes:

Gene	Forward sequence (5'-3')	Reverse sequence (5'-3')

Human TFR1	aggaaccgagtctccagtga	atcaactatgatcaccgagt
mTFR1	tccttttccttgcatattctgg	ccaaataaggatagtctgcatcc
mFPN	acccatccccatagtctctgt	ccgattctagcagcaatgact
mMFRN2	tgtgtggcgacattacttcat	gcatcctctgcttgacgact
mALAS2	ctcaccgtctttggttcgtc	ggacaggaccgtagcaacat
mAtrogin-1	agtgaggaccggctactgtg	gatcaaacgcttgcgaatct
mMuRF1	tgacatctacaagcaggagtgc	tcgtcttcgtgttccttgc
mREDD1	ccagagaagagggccttga	ccatccaggtatgaggagtctt
mCPT1B	aagagaccccgtagccatcat	gacccaaaacagtatcccaatca
mACOT1	caactacgatgacctcccca	gagccattgatgaccacagc
mMCD	gcacgtccgggaaatgaac	gcctcacactcgctgatctt
mGAPDH	aggtcggtgtgaacggatttg	tgtagaccatgtagttgaggtca

RNA Electrophoretic Mobility Shift Assay (REMSA)

The fractionation method described by Rothermel *et al.* (*540*) was adopted with minor modification to extract the cytosolic protein fractions from the gastrocnemius muscle. Briefly, after removal of connective tissues, muscle was homogenized for 1 minute in ice-cold lysis buffer (25mM Hepes pH 8, 5mM KCl, 0.5mM $MgCl_2$, 1% NP-40, 1x protease inhibitors) using a tight-fitting Teflon pestle attached to a Potter S homogenizer (Sartorius Stedium) at 1,000 rpm. Following centrifugation at 800 *g* for 15 min at 4°C to pellet the nuclei and cell debris, supernatants were collected, subjected to further centrifugation three times at 500 *g* for 15 min at 4°C to remove residual nuclei and used for the REMSA as nuclei-free total cytosolic protein fractions. IRP-IRE interactions were revealed using LightShift Chemiluminescent RNA Electrophoretic mobility shift assay kit (REMSA, Thermo Fisher 20148). Briefly, 20µL of reaction containing nuclease-free water, 5×REMSA Binding Buffer (50mM Tris-HCl pH 8.0, 750mM KCl, 0.5% Triton-X 100, 62.5% glycerol), tRNA (Thermo Fisher 20158), 6 µg of muscle cytosolic extracts, biotinylated and unlabeled ferritin probe 5′ – UCCUGCUUCAACAGUGCUUGGACGGAAC – 3', plus 0.5 mM EDTA and 1 mM DTT for reducing conditions, were incubated for 30 min at room temperature. Afterwards, samples were carefully mixed with 5µL of 5×REMSA Loading Buffer and resolved on 6% polyacrylamide gel and transferred on to nylon membrane (Roche Diagnostics, Indianapolis, IN). IRP-IRE complexes were visualized by the chemiluminescent nucleic acid detection module (Thermo Fisher 20158).

Quantification and statistical Analysis

All graphs show mean ± SEM and n represents the total number of independent biological replicates. Statistical significance was determined as indicated in figure legends with GraphPad Prism (version 6.0, GraphPad Software), comparing selected groups according to the hypothesis postulated (*e.g.* CTR vs C26, and C26 vs C26+Fe). Except indicated otherwise, parametric analysis was performed as data are assumed to follow a normal distribution. Significance was defined as *:$p<0.05$, **:$p<0.01$ and ***:$p<0.001$ compared to control and #:$p<0.05$, ##:$p<0.01$ and ###:$p<0.001$ compared to the respective vehicle- treated condition.

References

1. D. Hanahan, R. A. Weinberg, The hallmarks of cancer. *Cell* **100**, 57-70 (2000).
2. M. Egeblad, E. S. Nakasone, Z. Werb, Tumors as organs: complex tissues that interface with the entire organism. *Dev Cell* **18**, 884-901 (2010).
3. C. A. Lyssiotis, A. C. Kimmelman, Metabolic Interactions in the Tumor Microenvironment. *Trends Cell Biol* **27**, 863-875 (2017).
4. T. Bertero *et al.*, Tumor-Stroma Mechanics Coordinate Amino Acid Availability to Sustain Tumor Growth and Malignancy. *Cell Metab* **29**, 124-140 e110 (2019).
5. A. Menga *et al.*, N-acetylaspartate release by glutaminolytic ovarian cancer cells sustains protumoral macrophages. *EMBO Rep* **22**, e51981 (2021).
6. A. I. Minchinton, I. F. Tannock, Drug penetration in solid tumours. *Nat Rev Cancer* **6**, 583-592 (2006).
7. A. Tsuyada *et al.*, CCL2 mediates cross-talk between cancer cells and stromal fibroblasts that regulates breast cancer stem cells. *Cancer Res* **72**, 2768-2779 (2012).
8. T. S. Zhu *et al.*, Endothelial cells create a stem cell niche in glioblastoma by providing NOTCH ligands that nurture self-renewal of cancer stem-like cells. *Cancer Res* **71**, 6061-6072 (2011).
9. C. Engblom *et al.*, Osteoblasts remotely supply lung tumors with cancer-promoting SiglecF(high) neutrophils. *Science* **358**, (2017).
10. A. Orimo *et al.*, Stromal fibroblasts present in invasive human breast carcinomas promote tumor growth and angiogenesis through elevated SDF-1/CXCL12 secretion. *Cell* **121**, 335-348 (2005).
11. P. Mauffrey *et al.*, Progenitors from the central nervous system drive neurogenesis in cancer. *Nature* **569**, 672-678 (2019).
12. J. L. Ambrus, C. M. Ambrus, I. B. Mink, J. W. Pickren, Causes of death in cancer patients. *J Med* **6**, 61-64 (1975).
13. S. S. McAllister, R. A. Weinberg, Tumor-host interactions: a far-reaching relationship. *J Clin Oncol* **28**, 4022-4028 (2010).
14. S. I. Grivennikov, F. R. Greten, M. Karin, Immunity, inflammation, and cancer. *Cell* **140**, 883-899 (2010).
15. H. Knupfer, R. Preiss, Serum interleukin-6 levels in colorectal cancer patients--a summary of published results. *Int J Colorectal Dis* **25**, 135-140 (2010).
16. M. Terlizzi, V. Casolaro, A. Pinto, R. Sorrentino, Inflammasome: cancer's friend or foe? *Pharmacol Ther* **143**, 24-33 (2014).
17. L. Tao, G. Huang, H. Song, Y. Chen, L. Chen, Cancer associated fibroblasts: An essential role in the tumor microenvironment. *Oncol Lett* **14**, 2611-2620 (2017).
18. J. L. Guerriero, Macrophages: The Road Less Traveled, Changing Anticancer Therapy. *Trends Mol Med* **24**, 472-489 (2018).
19. T. Nagasaki *et al.*, Interleukin-6 released by colon cancer-associated fibroblasts is critical for tumour angiogenesis: anti-interleukin-6 receptor antibody suppressed angiogenesis and inhibited tumour-stroma interaction. *Br J Cancer* **110**, 469-478 (2014).
20. S. Jain, V. Gautam, S. Naseem, Acute-phase proteins: As diagnostic tool. *J Pharm Bioallied Sci* **3**, 118-127 (2011).
21. G. A. Nieuwenhuijzen *et al.*, Macrophage elimination increases bacterial translocation and gut-origin septicemia but attenuates symptoms and mortality rate in a model of systemic inflammation. *Ann Surg* **218**, 791-799 (1993).
22. N. Iida *et al.*, Commensal bacteria control cancer response to therapy by modulating the tumor microenvironment. *Science* **342**, 967-970 (2013).
23. S. Viaud *et al.*, The intestinal microbiota modulates the anticancer immune effects of cyclophosphamide. *Science* **342**, 971-976 (2013).
24. D. J. Brown, R. Milroy, T. Preston, D. C. McMillan, The relationship between an inflammation-based prognostic score (Glasgow Prognostic Score) and changes in serum biochemical variables in patients with advanced lung and gastrointestinal cancer. *J Clin Pathol* **60**, 705-708 (2007).
25. K. Nakamura, M. J. Smyth, Targeting cancer-related inflammation in the era of immunotherapy. *Immunol Cell Biol* **95**, 325-332 (2017).
26. D. I. Gabrilovich, S. Nagaraj, Myeloid-derived suppressor cells as regulators of the immune system. *Nat Rev Immunol* **9**, 162-174 (2009).
27. K. E. de Visser, A. Eichten, L. M. Coussens, Paradoxical roles of the immune system during cancer development. *Nat Rev Cancer* **6**, 24-37 (2006).
28. G. Chen *et al.*, Exosomal PD-L1 contributes to immunosuppression and is associated with anti-PD-1 response. *Nature* **560**, 382-386 (2018).

29. M. Zhou *et al.*, Pancreatic cancer derived exosomes regulate the expression of TLR4 in dendritic cells via miR-203. *Cell Immunol* **292**, 65-69 (2014).
30. S. Shalapour, M. Karin, Immunity, inflammation, and cancer: an eternal fight between good and evil. *J Clin Invest* **125**, 3347-3355 (2015).
31. T. P. Braun *et al.*, Central nervous system inflammation induces muscle atrophy via activation of the hypothalamic-pituitary-adrenal axis. *J Exp Med* **208**, 2449-2463 (2011).
32. K. G. Burfeind *et al.*, TRIF is a key inflammatory mediator of acute sickness behavior and cancer cachexia. *Brain Behav Immun* **73**, 364-374 (2018).
33. G. Strassmann, M. Fong, J. S. Kenney, C. O. Jacob, Evidence for the involvement of interleukin 6 in experimental cancer cachexia. *J Clin Invest* **89**, 1681-1684 (1992).
34. H. Soygur *et al.*, Interleukin-6 levels and HPA axis activation in breast cancer patients with major depressive disorder. *Prog Neuropsychopharmacol Biol Psychiatry* **31**, 1242-1247 (2007).
35. T. R. Flint *et al.*, Tumor-Induced IL-6 Reprograms Host Metabolism to Suppress Anti-tumor Immunity. *Cell Metab* **24**, 672-684 (2016).
36. K. Fearon, J. Arends, V. Baracos, Understanding the mechanisms and treatment options in cancer cachexia. *Nat Rev Clin Oncol* **10**, 90-99 (2013).
37. F. S. Dhabhar, Effects of stress on immune function: the good, the bad, and the beautiful. *Immunol Res* **58**, 193-210 (2014).
38. L. Cao *et al.*, Environmental and genetic activation of a brain-adipocyte BDNF/leptin axis causes cancer remission and inhibition. *Cell* **142**, 52-64 (2010).
39. H. H. Grytli, M. W. Fagerland, S. D. Fossa, K. A. Tasken, L. L. Haheim, Use of beta-blockers is associated with prostate cancer-specific survival in prostate cancer patients on androgen deprivation therapy. *Prostate* **73**, 250-260 (2013).
40. S. Lemeshow *et al.*, beta-Blockers and survival among Danish patients with malignant melanoma: a population-based cohort study. *Cancer Epidemiol Biomarkers Prev* **20**, 2273-2279 (2011).
41. A. Melhem-Bertrandt *et al.*, Beta-blocker use is associated with improved relapse-free survival in patients with triple-negative breast cancer. *J Clin Oncol* **29**, 2645-2652 (2011).
42. E. V. Yang *et al.*, Norepinephrine up-regulates the expression of vascular endothelial growth factor, matrix metalloproteinase (MMP)-2, and MMP-9 in nasopharyngeal carcinoma tumor cells. *Cancer Res* **66**, 10357-10364 (2006).
43. E. V. Yang *et al.*, Norepinephrine upregulates VEGF, IL-8, and IL-6 expression in human melanoma tumor cell lines: implications for stress-related enhancement of tumor progression. *Brain Behav Immun* **23**, 267-275 (2009).
44. T. Fujii *et al.*, Expression and Function of the Cholinergic System in Immune Cells. *Front Immunol* **8**, 1085 (2017).
45. C. M. Zhao *et al.*, Denervation suppresses gastric tumorigenesis. *Sci Transl Med* **6**, 250ra115 (2014).
46. C. Magnon *et al.*, Autonomic nerve development contributes to prostate cancer progression. *Science* **341**, 1236361 (2013).
47. P. Jobling *et al.*, Nerve-Cancer Cell Cross-talk: A Novel Promoter of Tumor Progression. *Cancer Res* **75**, 1777-1781 (2015).
48. A. Falanga, M. Marchetti, A. Vignoli, Coagulation and cancer: biological and clinical aspects. *J Thromb Haemost* **11**, 223-233 (2013).
49. S. Zucker *et al.*, Vascular endothelial growth factor induces tissue factor and matrix metalloproteinase production in endothelial cells: conversion of prothrombin to thrombin results in progelatinase A activation and cell proliferation. *Int J Cancer* **75**, 780-786 (1998).
50. K. Stark, S. Massberg, Interplay between inflammation and thrombosis in cardiovascular pathology. *Nat Rev Cardiol* **18**, 666-682 (2021).
51. K. Aksu, A. Donmez, G. Keser, Inflammation-induced thrombosis: mechanisms, disease associations and management. *Curr Pharm Des* **18**, 1478-1493 (2012).
52. P. E. Porporato, Understanding cachexia as a cancer metabolism syndrome. *Oncogenesis* **5**, e200 (2016).
53. K. Fearon *et al.*, Definition and classification of cancer cachexia: an international consensus. *Lancet Oncol* **12**, 489-495 (2011).
54. N. Nakajima, Differential Diagnosis of Cachexia and Refractory Cachexia and the Impact of Appropriate Nutritional Intervention for Cachexia on Survival in Terminal Cancer Patients. *Nutrients* **13**, (2021).
55. S. M. Kazemi-Bajestani, H. Becher, K. Fassbender, Q. Chu, V. E. Baracos, Concurrent evolution of cancer cachexia and heart failure: bilateral effects exist. *J Cachexia Sarcopenia Muscle* **5**, 95-104 (2014).
56. S. Antoun *et al.*, Association of skeletal muscle wasting with treatment with sorafenib in patients with advanced renal cell carcinoma: results from a placebo-controlled study. *J Clin Oncol* **28**, 1054-1060 (2010).

57. L. Martin *et al.*, Diagnostic criteria for the classification of cancer-associated weight loss. *J Clin Oncol* **33**, 90-99 (2015).
58. L. Martin *et al.*, Cancer cachexia in the age of obesity: skeletal muscle depletion is a powerful prognostic factor, independent of body mass index. *J Clin Oncol* **31**, 1539-1547 (2013).
59. J. Arends *et al.*, ESPEN guidelines on nutrition in cancer patients. *Clin Nutr* **36**, 11-48 (2017).
60. C. M. Prado *et al.*, Central tenet of cancer cachexia therapy: do patients with advanced cancer have exploitable anabolic potential? *Am J Clin Nutr* **98**, 1012-1019 (2013).
61. Y. C. Tseng *et al.*, Preclinical Investigation of the Novel Histone Deacetylase Inhibitor AR-42 in the Treatment of Cancer-Induced Cachexia. *J Natl Cancer Inst* **107**, djv274 (2015).
62. V. E. Baracos, L. Martin, M. Korc, D. C. Guttridge, K. C. H. Fearon, Cancer-associated cachexia. *Nat Rev Dis Primers* **4**, 17105 (2018).
63. K. C. Fearon, D. J. Glass, D. C. Guttridge, Cancer cachexia: mediators, signaling, and metabolic pathways. *Cell Metab* **16**, 153-166 (2012).
64. J. A. Ross, K. C. Fearon, Eicosanoid-dependent cancer cachexia and wasting. *Curr Opin Clin Nutr Metab Care* **5**, 241-248 (2002).
65. G. Zhang *et al.*, Tumor induces muscle wasting in mice through releasing extracellular Hsp70 and Hsp90. *Nat Commun* **8**, 589 (2017).
66. M. A. Egerman, D. J. Glass, Signaling pathways controlling skeletal muscle mass. *Crit Rev Biochem Mol Biol* **49**, 59-68 (2014).
67. K. T. Murphy, The pathogenesis and treatment of cardiac atrophy in cancer cachexia. *Am J Physiol Heart Circ Physiol* **310**, H466-477 (2016).
68. A. K. Biswas, S. Acharyya, Cancer-Associated Cachexia: A Systemic Consequence of Cancer Progression. *Annual Review of Cancer Biology* **4**, 391-411 (2020).
69. K. G. Burfeind, K. A. Michaelis, D. L. Marks, The central role of hypothalamic inflammation in the acute illness response and cachexia. *Semin Cell Dev Biol* **54**, 42-52 (2016).
70. K. Timper, J. C. Bruning, Hypothalamic circuits regulating appetite and energy homeostasis: pathways to obesity. *Dis Model Mech* **10**, 679-689 (2017).
71. J. M. Garcia *et al.*, Active ghrelin levels and active to total ghrelin ratio in cancer-induced cachexia. *J Clin Endocrinol Metab* **90**, 2920-2926 (2005).
72. K. M. Heppner *et al.*, Both acyl and des-acyl ghrelin regulate adiposity and glucose metabolism via central nervous system ghrelin receptors. *Diabetes* **63**, 122-131 (2014).
73. D. H. St-Pierre *et al.*, Relationship between ghrelin and energy expenditure in healthy young women. *J Clin Endocrinol Metab* **89**, 5993-5997 (2004).
74. P. E. Porporato *et al.*, Acylated and unacylated ghrelin impair skeletal muscle atrophy in mice. *J Clin Invest* **123**, 611-622 (2013).
75. J. M. Garcia, J. Friend, S. Allen, Therapeutic potential of anamorelin, a novel, oral ghrelin mimetic, in patients with cancer-related cachexia: a multicenter, randomized, double-blind, crossover, pilot study. *Support Care Cancer* **21**, 129-137 (2013).
76. J. M. Garcia *et al.*, Anamorelin for patients with cancer cachexia: an integrated analysis of two phase 2, randomised, placebo-controlled, double-blind trials. *Lancet Oncol* **16**, 108-116 (2015).
77. J. T. Dwarkasing *et al.*, Hypothalamic food intake regulation in a cancer-cachectic mouse model. *J Cachexia Sarcopenia Muscle* **5**, 159-169 (2014).
78. J. T. Dwarkasing *et al.*, Differences in food intake of tumour-bearing cachectic mice are associated with hypothalamic serotonin signalling. *J Cachexia Sarcopenia Muscle* **6**, 84-94 (2015).
79. E. R. Ropelle *et al.*, A central role for neuronal adenosine 5'-monophosphate-activated protein kinase in cancer-induced anorexia. *Endocrinology* **148**, 5220-5229 (2007).
80. G. Mastorakos, G. P. Chrousos, J. S. Weber, Recombinant interleukin-6 activates the hypothalamic-pituitary-adrenal axis in humans. *J Clin Endocrinol Metab* **77**, 1690-1694 (1993).
81. W. E. Nolten *et al.*, Effects of cytokines on the pituitary-adrenal axis in cancer patients. *J Interferon Res* **13**, 349-357 (1993).
82. B. D. Curti *et al.*, Endocrine effects of IL-1 alpha and beta administered in a phase I trial to patients with advanced cancer. *J Immunother Emphasis Tumor Immunol* **19**, 142-148 (1996).
83. P. J. Barnes, Anti-inflammatory actions of glucocorticoids: molecular mechanisms. *Clin Sci (Lond)* **94**, 557-572 (1998).
84. D. Qi, B. Rodrigues, Glucocorticoids produce whole body insulin resistance with changes in cardiac metabolism. *Am J Physiol Endocrinol Metab* **292**, E654-667 (2007).

85. A. J. Peckett, D. C. Wright, M. C. Riddell, The effects of glucocorticoids on adipose tissue lipid metabolism. *Metabolism* **60**, 1500-1510 (2011).
86. S. T. Russell, M. J. Tisdale, The role of glucocorticoids in the induction of zinc-alpha2-glycoprotein expression in adipose tissue in cancer cachexia. *Br J Cancer* **92**, 876-881 (2005).
87. C. C. de Theije *et al.*, Glucocorticoid Receptor Signaling Impairs Protein Turnover Regulation in Hypoxia-Induced Muscle Atrophy in Male Mice. *Endocrinology* **159**, 519-534 (2018).
88. T. P. Braun *et al.*, Muscle atrophy in response to cytotoxic chemotherapy is dependent on intact glucocorticoid signaling in skeletal muscle. *PLoS One* **9**, e106489 (2014).
89. G. Gayan-Ramirez, F. Vanderhoydonc, G. Verhoeven, M. Decramer, Acute treatment with corticosteroids decreases IGF-1 and IGF-2 expression in the rat diaphragm and gastrocnemius. *Am J Respir Crit Care Med* **159**, 283-289 (1999).
90. M. Imae, Z. Fu, A. Yoshida, T. Noguchi, H. Kato, Nutritional and hormonal factors control the gene expression of FoxOs, the mammalian homologues of DAF-16. *J Mol Endocrinol* **30**, 253-262 (2003).
91. C. G. Fenton *et al.*, Therapeutic glucocorticoids prevent bone loss but drive muscle wasting when administered in chronic polyarthritis. *Arthritis Res Ther* **21**, 182 (2019).
92. A. M. Cypess *et al.*, Identification and importance of brown adipose tissue in adult humans. *N Engl J Med* **360**, 1509-1517 (2009).
93. L. S. Sidossis *et al.*, Browning of Subcutaneous White Adipose Tissue in Humans after Severe Adrenergic Stress. *Cell Metab* **22**, 219-227 (2015).
94. M. Petruzzelli, E. F. Wagner, Mechanisms of metabolic dysfunction in cancer-associated cachexia. *Genes Dev* **30**, 489-501 (2016).
95. S. Kir *et al.*, PTH/PTHrP Receptor Mediates Cachexia in Models of Kidney Failure and Cancer. *Cell Metab* **23**, 315-323 (2016).
96. S. Kaur, C. Auger, M. G. Jeschke, Adipose Tissue Metabolic Function and Dysfunction: Impact of Burn Injury. *Front Cell Dev Biol* **8**, 599576 (2020).
97. K. L. Kliewer *et al.*, Adipose tissue lipolysis and energy metabolism in early cancer cachexia in mice. *Cancer Biol Ther* **16**, 886-897 (2015).
98. M. Petruzzelli *et al.*, A switch from white to brown fat increases energy expenditure in cancer-associated cachexia. *Cell Metab* **20**, 433-447 (2014).
99. S. Kir *et al.*, Tumour-derived PTH-related protein triggers adipose tissue browning and cancer cachexia. *Nature* **513**, 100-104 (2014).
100. S. K. Das *et al.*, Adipose triglyceride lipase contributes to cancer-associated cachexia. *Science* **333**, 233-238 (2011).
101. A. Carriere *et al.*, Browning of white adipose cells by intermediate metabolites: an adaptive mechanism to alleviate redox pressure. *Diabetes* **63**, 3253-3265 (2014).
102. P. Bostrom *et al.*, A PGC1-alpha-dependent myokine that drives brown-fat-like development of white fat and thermogenesis. *Nature* **481**, 463-468 (2012).
103. J. Laurencikiene *et al.*, Evidence for an important role of CIDEA in human cancer cachexia. *Cancer Res* **68**, 9247-9254 (2008).
104. M. Rohm *et al.*, An AMP-activated protein kinase-stabilizing peptide ameliorates adipose tissue wasting in cancer cachexia in mice. *Nat Med* **22**, 1120-1130 (2016).
105. M. Vujasinovic, R. Valente, M. Del Chiaro, J. Permert, J. M. Lohr, Pancreatic Exocrine Insufficiency in Pancreatic Cancer. *Nutrients* **9**, (2017).
106. L. V. Danai *et al.*, Altered exocrine function can drive adipose wasting in early pancreatic cancer. *Nature* **558**, 600-604 (2018).
107. M. A. Honors, K. P. Kinzig, The role of insulin resistance in the development of muscle wasting during cancer cachexia. *J Cachexia Sarcopenia Muscle* **3**, 5-11 (2012).
108. M. L. Asp, M. Tian, A. A. Wendel, M. A. Belury, Evidence for the contribution of insulin resistance to the development of cachexia in tumor-bearing mice. *Int J Cancer* **126**, 756-763 (2010).
109. M. L. Asp, M. Tian, K. L. Kliewer, M. A. Belury, Rosiglitazone delayed weight loss and anorexia while attenuating adipose depletion in mice with cancer cachexia. *Cancer Biol Ther* **12**, 957-965 (2011).
110. A. G. Oliveira, M. C. Gomes-Marcondes, Metformin treatment modulates the tumour-induced wasting effects in muscle protein metabolism minimising the cachexia in tumour-bearing rats. *BMC Cancer* **16**, 418 (2016).
111. J. M. Argiles, B. Stemmler, F. J. Lopez-Soriano, S. Busquets, Inter-tissue communication in cancer cachexia. *Nat Rev Endocrinol* **15**, 9-20 (2018).
112. C. P. Holroyde, T. G. Gabuzda, R. C. Putnam, P. Paul, G. A. Reichard, Altered glucose metabolism in metastatic carcinoma. *Cancer Res* **35**, 3710-3714 (1975).

113. C. P. Holroyde, C. L. Skutches, G. Boden, G. A. Reichard, Glucose metabolism in cachectic patients with colorectal cancer. *Cancer Res* **44**, 5910-5913 (1984).
114. D. E. Friesen, V. E. Baracos, J. A. Tuszynski, Modeling the energetic cost of cancer as a result of altered energy metabolism: implications for cachexia. *Theor Biol Med Model* **12**, 17 (2015).
115. J. M. Argiles, N. Campos, J. M. Lopez-Pedrosa, R. Rueda, L. Rodriguez-Manas, Skeletal Muscle Regulates Metabolism via Interorgan Crosstalk: Roles in Health and Disease. *J Am Med Dir Assoc* **17**, 789-796 (2016).
116. J. M. Argiles, F. J. Lopez-Soriano, The energy state of tumor-bearing rats. *J Biol Chem* **266**, 2978-2982 (1991).
117. A. Jones *et al.*, TSC22D4 is a molecular output of hepatic wasting metabolism. *EMBO Mol Med* **5**, 294-308 (2013).
118. M. Watanabe *et al.*, Bile acids induce energy expenditure by promoting intracellular thyroid hormone activation. *Nature* **439**, 484-489 (2006).
119. M. M. Thibaut *et al.*, Inflammation-induced cholestasis in cancer cachexia. *J Cachexia Sarcopenia Muscle* **12**, 70-90 (2021).
120. A. Bonetto *et al.*, Differential Bone Loss in Mouse Models of Colon Cancer Cachexia. *Front Physiol* **7**, 679 (2016).
121. D. J. DiGirolamo, D. P. Kiel, K. A. Esser, Bone and skeletal muscle: neighbors with close ties. *J Bone Miner Res* **28**, 1509-1518 (2013).
122. R. Sartori *et al.*, BMP signaling controls muscle mass. *Nat Genet* **45**, 1309-1318 (2013).
123. Y. Bren-Mattison, M. Hausburg, B. B. Olwin, Growth of limb muscle is dependent on skeletal-derived Indian hedgehog. *Dev Biol* **356**, 486-495 (2011).
124. H. Liang, S. Pun, T. J. Wronski, Bone anabolic effects of basic fibroblast growth factor in ovariectomized rats. *Endocrinology* **140**, 5780-5788 (1999).
125. R. A. Power, U. T. Iwaniec, K. A. Magee, N. G. Mitova-Caneva, T. J. Wronski, Basic fibroblast growth factor has rapid bone anabolic effects in ovariectomized rats. *Osteoporos Int* **15**, 716-723 (2004).
126. S. Yakar *et al.*, Circulating levels of IGF-1 directly regulate bone growth and density. *J Clin Invest* **110**, 771-781 (2002).
127. D. L. Waning *et al.*, Excess TGF-beta mediates muscle weakness associated with bone metastases in mice. *Nat Med* **21**, 1262-1271 (2015).
128. F. Pin *et al.*, RANKL Blockade Reduces Cachexia and Bone Loss Induced by Non-Metastatic Ovarian Cancer in Mice. *J Bone Miner Res*, (2021).
129. F. Armougom, M. Henry, B. Vialettes, D. Raccah, D. Raoult, Monitoring bacterial community of human gut microbiota reveals an increase in Lactobacillus in obese patients and Methanogens in anorexic patients. *PLoS One* **4**, e7125 (2009).
130. B. J. Varian *et al.*, Beneficial bacteria inhibit cachexia. *Oncotarget* **7**, 11803-11816 (2016).
131. L. B. Bindels *et al.*, Restoring specific lactobacilli levels decreases inflammation and muscle atrophy markers in an acute leukemia mouse model. *PLoS One* **7**, e37971 (2012).
132. L. B. Bindels *et al.*, Increased gut permeability in cancer cachexia: mechanisms and clinical relevance. *Oncotarget* **9**, 18224-18238 (2018).
133. L. B. Bindels *et al.*, Gut microbiota-derived propionate reduces cancer cell proliferation in the liver. *Br J Cancer* **107**, 1337-1344 (2012).
134. D. Dudgeon, V. E. Baracos, Physiological and functional failure in chronic obstructive pulmonary disease, congestive heart failure and cancer: a debilitating intersection of sarcopenia, cachexia and breathlessness. *Curr Opin Support Palliat Care* **10**, 236-241 (2016).
135. M. Olivan *et al.*, Theophylline is able to partially revert cachexia in tumour-bearing rats. *Nutr Metab (Lond)* **9**, 76 (2012).
136. A. Barkhudaryan, N. Scherbakov, J. Springer, W. Doehner, Cardiac muscle wasting in individuals with cancer cachexia. *ESC Heart Fail* **4**, 458-467 (2017).
137. M. S. Willis *et al.*, Doxorubicin Exposure Causes Subacute Cardiac Atrophy Dependent on the Striated Muscle-Specific Ubiquitin Ligase MuRF1. *Circ Heart Fail* **12**, e005234 (2019).
138. L. A. Gilliam, J. S. Moylan, L. A. Callahan, M. P. Sumandea, M. B. Reid, Doxorubicin causes diaphragm weakness in murine models of cancer chemotherapy. *Muscle Nerve* **43**, 94-102 (2011).
139. A. Hyltander, C. Drott, U. Korner, R. Sandstrom, K. Lundholm, Elevated energy expenditure in cancer patients with solid tumours. *Eur J Cancer* **27**, 9-15 (1991).
140. L. F. Shirazi, J. Bissett, F. Romeo, J. L. Mehta, Role of Inflammation in Heart Failure. *Curr Atheroscler Rep* **19**, 27 (2017).
141. S. Reuter, S. C. Gupta, M. M. Chaturvedi, B. B. Aggarwal, Oxidative stress, inflammation, and cancer: how are they linked? *Free Radic Biol Med* **49**, 1603-1616 (2010).

142. C. Muhlfeld *et al.*, Cancer induces cardiomyocyte remodeling and hypoinnervation in the left ventricle of the mouse heart. *PLoS One* **6**, e20424 (2011).
143. R. H. Ritchie, A. C. Rosenkranz, D. M. Kaye, B-type natriuretic peptide: endogenous regulator of myocardial structure, biomarker and therapeutic target. *Curr Mol Med* **9**, 814-825 (2009).
144. S. C. Burjonroppa *et al.*, Cancer patients with markedly elevated B-type natriuretic peptide may not have volume overload. *Am J Clin Oncol* **30**, 287-293 (2007).
145. P. Delafontaine, T. Yoshida, The Renin-Angiotensin System and the Biology of Skeletal Muscle: Mechanisms of Muscle Wasting in Chronic Disease States. *Trans Am Clin Climatol Assoc* **127**, 245-258 (2016).
146. C. A. Penafuerte *et al.*, Identification of neutrophil-derived proteases and angiotensin II as biomarkers of cancer cachexia. *Br J Cancer* **114**, 680-687 (2016).
147. D. Attaix *et al.*, The ubiquitin-proteasome system and skeletal muscle wasting. *Essays Biochem* **41**, 173-186 (2005).
148. S. Schiaffino, K. A. Dyar, S. Ciciliot, B. Blaauw, M. Sandri, Mechanisms regulating skeletal muscle growth and atrophy. *FEBS J* **280**, 4294-4314 (2013).
149. K. Mukund, S. Subramaniam, Skeletal muscle: A review of molecular structure and function, in health and disease. *Wiley Interdiscip Rev Syst Biol Med* **12**, e1462 (2020).
150. J. E. Morley, D. R. Thomas, M. M. Wilson, Cachexia: pathophysiology and clinical relevance. *Am J Clin Nutr* **83**, 735-743 (2006).
151. H. M. Argadine, N. J. Hellyer, C. B. Mantilla, W. Z. Zhan, G. C. Sieck, The effect of denervation on protein synthesis and degradation in adult rat diaphragm muscle. *J Appl Physiol (1985)* **107**, 438-444 (2009).
152. P. N. Quy, A. Kuma, P. Pierre, N. Mizushima, Proteasome-dependent activation of mammalian target of rapamycin complex 1 (mTORC1) is essential for autophagy suppression and muscle remodeling following denervation. *J Biol Chem* **288**, 1125-1134 (2013).
153. R. R. Kalyani, M. Corriere, L. Ferrucci, Age-related and disease-related muscle loss: the effect of diabetes, obesity, and other diseases. *Lancet Diabetes Endocrinol* **2**, 819-829 (2014).
154. S. Ali, J. M. Garcia, Sarcopenia, cachexia and aging: diagnosis, mechanisms and therapeutic options - a mini-review. *Gerontology* **60**, 294-305 (2014).
155. W. J. Evans, Reversing sarcopenia: how weight training can build strength and vitality. *Geriatrics* **51**, 46-47, 51-43; quiz 54 (1996).
156. M. Sandri, Protein breakdown in cancer cachexia. *Semin Cell Dev Biol* **54**, 11-19 (2016).
157. C. F. Bentzinger, Y. X. Wang, M. A. Rudnicki, Building muscle: molecular regulation of myogenesis. *Cold Spring Harb Perspect Biol* **4**, (2012).
158. J. M. Webster, L. Kempen, R. S. Hardy, R. C. J. Langen, Inflammation and Skeletal Muscle Wasting During Cachexia. *Front Physiol* **11**, 597675 (2020).
159. F. Penna *et al.*, Muscle wasting and impaired myogenesis in tumor bearing mice are prevented by ERK inhibition. *PLoS One* **5**, e13604 (2010).
160. S. Inaba, A. Hinohara, M. Tachibana, K. Tsujikawa, S. I. Fukada, Muscle regeneration is disrupted by cancer cachexia without loss of muscle stem cell potential. *PLoS One* **13**, e0205467 (2018).
161. F. W. Booth, B. S. Tseng, M. Fluck, J. A. Carson, Molecular and cellular adaptation of muscle in response to physical training. *Acta Physiol Scand* **162**, 343-350 (1998).
162. A. Musaro *et al.*, Localized Igf-1 transgene expression sustains hypertrophy and regeneration in senescent skeletal muscle. *Nat Genet* **27**, 195-200 (2001).
163. M. Murgia *et al.*, Ras is involved in nerve-activity-dependent regulation of muscle genes. *Nat Cell Biol* **2**, 142-147 (2000).
164. G. Pallafacchina, E. Calabria, A. L. Serrano, J. M. Kalhovde, S. Schiaffino, A protein kinase B-dependent and rapamycin-sensitive pathway controls skeletal muscle growth but not fiber type specification. *Proc Natl Acad Sci U S A* **99**, 9213-9218 (2002).
165. B. Blaauw *et al.*, Inducible activation of Akt increases skeletal muscle mass and force without satellite cell activation. *FASEB J* **23**, 3896-3905 (2009).
166. C. F. Bentzinger *et al.*, Skeletal muscle-specific ablation of raptor, but not of rictor, causes metabolic changes and results in muscle dystrophy. *Cell Metab* **8**, 411-424 (2008).
167. V. Risson *et al.*, Muscle inactivation of mTOR causes metabolic and dystrophin defects leading to severe myopathy. *J Cell Biol* **187**, 859-874 (2009).
168. J. S. You *et al.*, The role of raptor in the mechanical load-induced regulation of mTOR signaling, protein synthesis, and skeletal muscle hypertrophy. *FASEB J* **33**, 4021-4034 (2019).
169. Q. Zhang *et al.*, Lack of muscle mTOR kinase activity causes early onset myopathy and compromises whole-body homeostasis. *J Cachexia Sarcopenia Muscle* **10**, 35-53 (2019).

170. W. O. Kline, F. J. Panaro, H. Yang, S. C. Bodine, Rapamycin inhibits the growth and muscle-sparing effects of clenbuterol. *J Appl Physiol (1985)* **102**, 740-747 (2007).
171. J. Sorensen, Lung Cancer Cachexia: Can Molecular Understanding Guide Clinical Management? *Integr Cancer Ther* **17**, 1000-1008 (2018).
172. M. Sandri, Autophagy in skeletal muscle. *FEBS Lett* **584**, 1411-1416 (2010).
173. L. Galluzzi, F. Pietrocola, B. Levine, G. Kroemer, Metabolic control of autophagy. *Cell* **159**, 1263-1276 (2014).
174. N. Mizushima, A. Yamamoto, M. Matsui, T. Yoshimori, Y. Ohsumi, In vivo analysis of autophagy in response to nutrient starvation using transgenic mice expressing a fluorescent autophagosome marker. *Mol Biol Cell* **15**, 1101-1111 (2004).
175. I. Dikic, Z. Elazar, Mechanism and medical implications of mammalian autophagy. *Nat Rev Mol Cell Biol* **19**, 349-364 (2018).
176. S. von Haehling, S. D. Anker, Cachexia as a major underestimated and unmet medical need: facts and numbers. *J Cachexia Sarcopenia Muscle* **1**, 1-5 (2010).
177. L. Brocca *et al.*, FoxO-dependent atrogenes vary among catabolic conditions and play a key role in muscle atrophy induced by hindlimb suspension. *J Physiol* **595**, 1143-1158 (2017).
178. G. Milan *et al.*, Regulation of autophagy and the ubiquitin-proteasome system by the FoxO transcriptional network during muscle atrophy. *Nat Commun* **6**, 6670 (2015).
179. C. Mammucari *et al.*, FoxO3 controls autophagy in skeletal muscle in vivo. *Cell Metab* **6**, 458-471 (2007).
180. N. Shimizu *et al.*, Crosstalk between glucocorticoid receptor and nutritional sensor mTOR in skeletal muscle. *Cell Metab* **13**, 170-182 (2011).
181. E. Bertaggia, L. Coletto, M. Sandri, Posttranslational modifications control FoxO3 activity during denervation. *Am J Physiol Cell Physiol* **302**, C587-596 (2012).
182. A. W. Beharry *et al.*, HDAC1 activates FoxO and is both sufficient and required for skeletal muscle atrophy. *J Cell Sci* **127**, 1441-1453 (2014).
183. M. Sandri *et al.*, PGC-1alpha protects skeletal muscle from atrophy by suppressing FoxO3 action and atrophy-specific gene transcription. *Proc Natl Acad Sci U S A* **103**, 16260-16265 (2006).
184. J. J. Brault, J. G. Jespersen, A. L. Goldberg, Peroxisome proliferator-activated receptor gamma coactivator 1alpha or 1beta overexpression inhibits muscle protein degradation, induction of ubiquitin ligases, and disuse atrophy. *J Biol Chem* **285**, 19460-19471 (2010).
185. J. Yin *et al.*, Dkk3 dependent transcriptional regulation controls age related skeletal muscle atrophy. *Nat Commun* **9**, 1752 (2018).
186. F. M. Torti, B. Dieckmann, B. Beutler, A. Cerami, G. M. Ringold, A macrophage factor inhibits adipocyte gene expression: an in vitro model of cachexia. *Science* **229**, 867-869 (1985).
187. A. Zentella, K. Manogue, A. Cerami, Cachectin/TNF-mediated lactate production in cultured myocytes is linked to activation of a futile substrate cycle. *Cytokine* **5**, 436-447 (1993).
188. A. C. McPherron, A. M. Lawler, S. J. Lee, Regulation of skeletal muscle mass in mice by a new TGF-beta superfamily member. *Nature* **387**, 83-90 (1997).
189. H. Ding *et al.*, Activin A induces skeletal muscle catabolism via p38beta mitogen-activated protein kinase. *J Cachexia Sarcopenia Muscle* **8**, 202-212 (2017).
190. C. L. Mendias *et al.*, Transforming growth factor-beta induces skeletal muscle atrophy and fibrosis through the induction of atrogin-1 and scleraxis. *Muscle Nerve* **45**, 55-59 (2012).
191. R. Sartori *et al.*, Smad2 and 3 transcription factors control muscle mass in adulthood. *Am J Physiol Cell Physiol* **296**, C1248-1257 (2009).
192. C. E. Winbanks *et al.*, Follistatin-mediated skeletal muscle hypertrophy is regulated by Smad3 and mTOR independently of myostatin. *J Cell Biol* **197**, 997-1008 (2012).
193. X. Zhou *et al.*, Reversal of cancer cachexia and muscle wasting by ActRIIB antagonism leads to prolonged survival. *Cell* **142**, 531-543 (2010).
194. R. Sartori, V. Romanello, M. Sandri, Mechanisms of muscle atrophy and hypertrophy: implications in health and disease. *Nat Commun* **12**, 330 (2021).
195. D. Cai *et al.*, IKKbeta/NF-kappaB activation causes severe muscle wasting in mice. *Cell* **119**, 285-298 (2004).
196. R. C. Langen *et al.*, NF-kappaB activation is required for the transition of pulmonary inflammation to muscle atrophy. *Am J Respir Cell Mol Biol* **47**, 288-297 (2012).
197. C. Miao *et al.*, Pyrrolidine Dithiocarbamate (PDTC) Attenuates Cancer Cachexia by Affecting Muscle Atrophy and Fat Lipolysis. *Front Pharmacol* **8**, 915 (2017).
198. A. Mittal *et al.*, The TWEAK-Fn14 system is a critical regulator of denervation-induced skeletal muscle atrophy in mice. *J Cell Biol* **188**, 833-849 (2010).

199. P. K. Paul *et al.*, Targeted ablation of TRAF6 inhibits skeletal muscle wasting in mice. *J Cell Biol* **191**, 1395-1411 (2010).
200. D. C. Guttridge, M. W. Mayo, L. V. Madrid, C. Y. Wang, A. S. Baldwin, Jr., NF-kappaB-induced loss of MyoD messenger RNA: possible role in muscle decay and cachexia. *Science* **289**, 2363-2366 (2000).
201. R. C. Langen, A. M. Schols, M. C. Kelders, E. F. Wouters, Y. M. Janssen-Heininger, Inflammatory cytokines inhibit myogenic differentiation through activation of nuclear factor-kappaB. *FASEB J* **15**, 1169-1180 (2001).
202. R. C. Langen *et al.*, Muscle wasting and impaired muscle regeneration in a murine model of chronic pulmonary inflammation. *Am J Respir Cell Mol Biol* **35**, 689-696 (2006).
203. H. F. Kramer, L. J. Goodyear, Exercise, MAPK, and NF-kappaB signaling in skeletal muscle. *J Appl Physiol (1985)* **103**, 388-395 (2007).
204. S. Chiappalupi *et al.*, Targeting RAGE prevents muscle wasting and prolongs survival in cancer cachexia. *J Cachexia Sarcopenia Muscle* **11**, 929-946 (2020).
205. Y. P. Li *et al.*, TNF-alpha acts via p38 MAPK to stimulate expression of the ubiquitin ligase atrogin1/MAFbx in skeletal muscle. *FASEB J* **19**, 362-370 (2005).
206. W. Li, J. S. Moylan, M. A. Chambers, J. Smith, M. B. Reid, Interleukin-1 stimulates catabolism in C2C12 myotubes. *Am J Physiol Cell Physiol* **297**, C706-714 (2009).
207. T. K. Sin *et al.*, Cancer-Induced Muscle Wasting Requires p38beta MAPK Activation of p300. *Cancer Res* **81**, 885-897 (2021).
208. J. Hess, P. Angel, M. Schorpp-Kistner, AP-1 subunits: quarrel and harmony among siblings. *J Cell Sci* **117**, 5965-5973 (2004).
209. X. Liu, G. Manzano, D. H. Lovett, H. T. Kim, Role of AP-1 and RE-1 binding sites in matrix metalloproteinase-2 transcriptional regulation in skeletal muscle atrophy. *Biochem Biophys Res Commun* **396**, 219-223 (2010).
210. C. Schindler, D. E. Levy, T. Decker, JAK-STAT signaling: from interferons to cytokines. *J Biol Chem* **282**, 20059-20063 (2007).
211. A. Bonetto *et al.*, JAK/STAT3 pathway inhibition blocks skeletal muscle wasting downstream of IL-6 and in experimental cancer cachexia. *Am J Physiol Endocrinol Metab* **303**, E410-421 (2012).
212. K. A. Baltgalvis *et al.*, Muscle wasting and interleukin-6-induced atrogin-I expression in the cachectic Apc (Min/+) mouse. *Pflugers Arch* **457**, 989-1001 (2009).
213. V. Moresi, S. Adamo, L. Berghella, The JAK/STAT Pathway in Skeletal Muscle Pathophysiology. *Front Physiol* **10**, 500 (2019).
214. F. Haddad, F. Zaldivar, D. M. Cooper, G. R. Adams, IL-6-induced skeletal muscle atrophy. *J Appl Physiol (1985)* **98**, 911-917 (2005).
215. L. Zhang *et al.*, Stat3 activation links a C/EBPdelta to myostatin pathway to stimulate loss of muscle mass. *Cell Metab* **18**, 368-379 (2013).
216. K. A. Silva *et al.*, Inhibition of Stat3 activation suppresses caspase-3 and the ubiquitin-proteasome system, leading to preservation of muscle mass in cancer cachexia. *J Biol Chem* **290**, 11177-11187 (2015).
217. J. Fujita *et al.*, Anti-interleukin-6 receptor antibody prevents muscle atrophy in colon-26 adenocarcinoma-bearing mice with modulation of lysosomal and ATP-ubiquitin-dependent proteolytic pathways. *Int J Cancer* **68**, 637-643 (1996).
218. T. Tsujinaka *et al.*, Muscle undergoes atrophy in association with increase of lysosomal cathepsin activity in interleukin-6 transgenic mouse. *Biochem Biophys Res Commun* **207**, 168-174 (1995).
219. M. N. Goodman, Interleukin-6 induces skeletal muscle protein breakdown in rats. *Proc Soc Exp Biol Med* **205**, 182-185 (1994).
220. J. P. White *et al.*, Muscle mTORC1 suppression by IL-6 during cancer cachexia: a role for AMPK. *Am J Physiol Endocrinol Metab* **304**, E1042-1052 (2013).
221. C. Mammucari *et al.*, The mitochondrial calcium uniporter controls skeletal muscle trophism in vivo. *Cell Rep* **10**, 1269-1279 (2015).
222. J. L. Ruas *et al.*, A PGC-1alpha isoform induced by resistance training regulates skeletal muscle hypertrophy. *Cell* **151**, 1319-1331 (2012).
223. C. Tezze *et al.*, Age-Associated Loss of OPA1 in Muscle Impacts Muscle Mass, Metabolic Homeostasis, Systemic Inflammation, and Epithelial Senescence. *Cell Metab* **25**, 1374-1389 e1376 (2017).
224. B. N. VanderVeen, D. K. Fix, J. A. Carson, Disrupted Skeletal Muscle Mitochondrial Dynamics, Mitophagy, and Biogenesis during Cancer Cachexia: A Role for Inflammation. *Oxid Med Cell Longev* **2017**, 3292087 (2017).
225. J. L. Brown *et al.*, Mitochondrial degeneration precedes the development of muscle atrophy in progression of cancer cachexia in tumour-bearing mice. *J Cachexia Sarcopenia Muscle* **8**, 926-938 (2017).
226. G. Favaro *et al.*, DRP1-mediated mitochondrial shape controls calcium homeostasis and muscle mass. *Nat Commun* **10**, 2576 (2019).

227. F. Pin, M. E. Couch, A. Bonetto, Preservation of muscle mass as a strategy to reduce the toxic effects of cancer chemotherapy on body composition. *Curr Opin Support Palliat Care* **12**, 420-426 (2018).
228. H. W. Pogrebniak, W. Matthews, H. I. Pass, Chemotherapy amplifies production of tumor necrosis factor. *Surgery* **110**, 231-237 (1991).
229. A. Fanzani, A. Zanola, F. Rovetta, S. Rossi, M. F. Aleo, Cisplatin triggers atrophy of skeletal C2C12 myotubes via impairment of Akt signalling pathway and subsequent increment activity of proteasome and autophagy systems. *Toxicol Appl Pharmacol* **250**, 312-321 (2011).
230. R. N. Montalvo, V. Doerr, K. Min, H. H. Szeto, A. J. Smuder, Doxorubicin-induced oxidative stress differentially regulates proteolytic signaling in cardiac and skeletal muscle. *Am J Physiol Regul Integr Comp Physiol* **318**, R227-R233 (2020).
231. L. A. Gilliam, D. K. St Clair, Chemotherapy-induced weakness and fatigue in skeletal muscle: the role of oxidative stress. *Antioxid Redox Signal* **15**, 2543-2563 (2011).
232. L. A. A. Gilliam *et al.*, The anticancer agent doxorubicin disrupts mitochondrial energy metabolism and redox balance in skeletal muscle. *Free Radic Biol Med* **65**, 988-996 (2013).
233. L. A. Gilliam *et al.*, Doxorubicin acts via mitochondrial ROS to stimulate catabolism in C2C12 myotubes. *Am J Physiol Cell Physiol* **302**, C195-202 (2012).
234. A. J. Smuder, A. N. Kavazis, K. Min, S. K. Powers, Exercise protects against doxorubicin-induced oxidative stress and proteolysis in skeletal muscle. *J Appl Physiol (1985)* **110**, 935-942 (2011).
235. A. J. Smuder, A. N. Kavazis, M. B. Hudson, W. B. Nelson, S. K. Powers, Oxidation enhances myofibrillar protein degradation via calpain and caspase-3. *Free Radic Biol Med* **49**, 1152-1160 (2010).
236. T. A. Nissinen *et al.*, Systemic blockade of ACVR2B ligands prevents chemotherapy-induced muscle wasting by restoring muscle protein synthesis without affecting oxidative capacity or atrogenes. *Sci Rep* **6**, 32695 (2016).
237. J. J. Hulmi *et al.*, Prevention of chemotherapy-induced cachexia by ACVR2B ligand blocking has different effects on heart and skeletal muscle. *J Cachexia Sarcopenia Muscle* **9**, 417-432 (2018).
238. B. J. Crielaard, T. Lammers, S. Rivella, Targeting iron metabolism in drug discovery and delivery. *Nat Rev Drug Discov* **16**, 400-423 (2017).
239. K. J. Waldron, J. C. Rutherford, D. Ford, N. J. Robinson, Metalloproteins and metal sensing. *Nature* **460**, 823-830 (2009).
240. S. V. Torti, F. M. Torti, Iron and cancer: more ore to be mined. *Nat Rev Cancer* **13**, 342-355 (2013).
241. C. Andreini, V. Putignano, A. Rosato, L. Banci, The human iron-proteome. *Metallomics* **10**, 1223-1231 (2018).
242. F. W. Outten, E. C. Theil, Iron-based redox switches in biology. *Antioxid Redox Signal* **11**, 1029-1046 (2009).
243. D. Galaris, A. Barbouti, K. Pantopoulos, Iron homeostasis and oxidative stress: An intimate relationship. *Biochim Biophys Acta Mol Cell Res* **1866**, 118535 (2019).
244. T. Nakamura, I. Naguro, H. Ichijo, Iron homeostasis and iron-regulated ROS in cell death, senescence and human diseases. *Biochim Biophys Acta Gen Subj* **1863**, 1398-1409 (2019).
245. M. W. Hentze, M. U. Muckenthaler, N. C. Andrews, Balancing acts: molecular control of mammalian iron metabolism. *Cell* **117**, 285-297 (2004).
246. M. U. Muckenthaler, S. Rivella, M. W. Hentze, B. Galy, A Red Carpet for Iron Metabolism. *Cell* **168**, 344-361 (2017).
247. S. Swaminathan, V. A. Fonseca, M. G. Alam, S. V. Shah, The role of iron in diabetes and its complications. *Diabetes Care* **30**, 1926-1933 (2007).
248. S. V. Torti, D. H. Manz, B. T. Paul, N. Blanchette-Farra, F. M. Torti, Iron and Cancer. *Annu Rev Nutr* **38**, 97-125 (2018).
249. A. J. Cross *et al.*, A prospective study of red and processed meat intake in relation to cancer risk. *PLoS Med* **4**, e325 (2007).
250. N. Tasevska *et al.*, A prospective study of meat, cooking methods, meat mutagens, heme iron, and lung cancer risks. *Am J Clin Nutr* **89**, 1884-1894 (2009).
251. S. C. Larsson, A. Wolk, Red and processed meat consumption and risk of pancreatic cancer: meta-analysis of prospective studies. *Br J Cancer* **106**, 603-607 (2012).
252. P. Paluszkiewicz, K. Smolinska, I. Debinska, W. A. Turski, Main dietary compounds and pancreatic cancer risk. The quantitative analysis of case-control and cohort studies. *Cancer Epidemiol* **36**, 60-67 (2012).
253. J. Guo, W. Wei, L. Zhan, Red and processed meat intake and risk of breast cancer: a meta-analysis of prospective studies. *Breast Cancer Res Treat* **151**, 191-198 (2015).
254. L. M. Ferrucci *et al.*, Intake of meat, meat mutagens, and iron and the risk of breast cancer in the Prostate, Lung, Colorectal, and Ovarian Cancer Screening Trial. *Br J Cancer* **101**, 178-184 (2009).
255. A. J. Cross *et al.*, A large prospective study of meat consumption and colorectal cancer risk: an investigation of potential mechanisms underlying this association. *Cancer Res* **70**, 2406-2414 (2010).

256. N. M. Bastide, F. H. Pierre, D. E. Corpet, Heme iron from meat and risk of colorectal cancer: a meta-analysis and a review of the mechanisms involved. *Cancer Prev Res (Phila)* **4**, 177-184 (2011).
257. N. M. Bastide *et al.*, A central role for heme iron in colon carcinogenesis associated with red meat intake. *Cancer Res* **75**, 870-879 (2015).
258. G. G. Kuhnle *et al.*, Diet-induced endogenous formation of nitroso compounds in the GI tract. *Free Radic Biol Med* **43**, 1040-1047 (2007).
259. P. Steinberg, Red Meat-Derived Nitroso Compounds, Lipid Peroxidation Products and Colorectal Cancer. *Foods* **8**, (2019).
260. R. G. Stevens, B. I. Graubard, M. S. Micozzi, K. Neriishi, B. S. Blumberg, Moderate elevation of body iron level and increased risk of cancer occurrence and death. *Int J Cancer* **56**, 364-369 (1994).
261. M. Elmberg *et al.*, Cancer risk in patients with hereditary hemochromatosis and in their first-degree relatives. *Gastroenterology* **125**, 1733-1741 (2003).
262. S. Fargion, L. Valenti, A. L. Fracanzani, Hemochromatosis gene (HFE) mutations and cancer risk: expanding the clinical manifestations of hereditary iron overload. *Hepatology* **51**, 1119-1121 (2010).
263. K. M. Musallam, M. D. Cappellini, J. C. Wood, A. T. Taher, Iron overload in non-transfusion-dependent thalassemia: a clinical perspective. *Blood Rev* **26 Suppl 1**, S16-19 (2012).
264. K. Merk *et al.*, The incidence of cancer among blood donors. *Int J Epidemiol* **19**, 505-509 (1990).
265. L. R. Zacharski *et al.*, Decreased cancer risk after iron reduction in patients with peripheral arterial disease: results from a randomized trial. *J Natl Cancer Inst* **100**, 996-1002 (2008).
266. Y. Kohgo, K. Ikuta, T. Ohtake, Y. Torimoto, J. Kato, Body iron metabolism and pathophysiology of iron overload. *Int J Hematol* **88**, 7-15 (2008).
267. A. Yiannikourides, G. O. Latunde-Dada, A Short Review of Iron Metabolism and Pathophysiology of Iron Disorders. *Medicines (Basel)* **6**, (2019).
268. D. Chiabrando, F. Vinchi, V. Fiorito, S. Mercurio, E. Tolosano, Heme in pathophysiology: a matter of scavenging, metabolism and trafficking across cell membranes. *Front Pharmacol* **5**, 61 (2014).
269. D. M. Ward, J. Kaplan, Ferroportin-mediated iron transport: expression and regulation. *Biochim Biophys Acta* **1823**, 1426-1433 (2012).
270. B. K. Fuqua, C. D. Vulpe, G. J. Anderson, Intestinal iron absorption. *J Trace Elem Med Biol* **26**, 115-119 (2012).
271. Y. Suryo Rahmanto, S. Bal, K. H. Loh, Y. Yu, D. R. Richardson, Melanotransferrin: search for a function. *Biochim Biophys Acta* **1820**, 237-243 (2012).
272. M. R. Food, E. O. Sekyere, D. R. Richardson, The soluble form of the membrane-bound transferrin homologue, melanotransferrin, inefficiently donates iron to cells via nonspecific internalization and degradation of the protein. *Eur J Biochem* **269**, 4435-4445 (2002).
273. L. Rosa, A. Cutone, M. S. Lepanto, R. Paesano, P. Valenti, Lactoferrin: A Natural Glycoprotein Involved in Iron and Inflammatory Homeostasis. *Int J Mol Sci* **18**, (2017).
274. D. R. Richardson, E. H. Morgan, The transferrin homologue, melanotransferrin (p97), is rapidly catabolized by the liver of the rat and does not effectively donate iron to the brain. *Biochim Biophys Acta* **1690**, 124-133 (2004).
275. L. A. Lambert, Molecular evolution of the transferrin family and associated receptors. *Biochim Biophys Acta* **1820**, 244-255 (2012).
276. P. P. Ward, M. Mendoza-Meneses, G. A. Cunningham, O. M. Conneely, Iron status in mice carrying a targeted disruption of lactoferrin. *Mol Cell Biol* **23**, 178-185 (2003).
277. E. Nemeth *et al.*, Hepcidin regulates cellular iron efflux by binding to ferroportin and inducing its internalization. *Science* **306**, 2090-2093 (2004).
278. I. De Domenico, D. M. Ward, J. Kaplan, Hepcidin and ferroportin: the new players in iron metabolism. *Semin Liver Dis* **31**, 272-279 (2011).
279. E. Rossi, Hepcidin--the iron regulatory hormone. *Clin Biochem Rev* **26**, 47-49 (2005).
280. A. Pagani, A. Nai, L. Silvestri, C. Camaschella, Hepcidin and Anemia: A Tight Relationship. *Front Physiol* **10**, 1294 (2019).
281. L. Kautz *et al.*, Identification of erythroferrone as an erythroid regulator of iron metabolism. *Nat Genet* **46**, 678-684 (2014).
282. M. M. Seldin, J. M. Peterson, M. S. Byerly, Z. Wei, G. W. Wong, Myonectin (CTRP15), a novel myokine that links skeletal muscle to systemic lipid homeostasis. *J Biol Chem* **287**, 11968-11980 (2012).
283. R. S. Ohgami *et al.*, Identification of a ferrireductase required for efficient transferrin-dependent iron uptake in erythroid cells. *Nat Genet* **37**, 1264-1269 (2005).
284. N. C. Andrews, The iron transporter DMT1. *Int J Biochem Cell Biol* **31**, 991-994 (1999).
285. D. Trinder, E. Baker, Transferrin receptor 2: a new molecule in iron metabolism. *Int J Biochem Cell Biol* **35**, 292-296 (2003).

286. V. Fiorito, D. Chiabrando, S. Petrillo, F. Bertino, E. Tolosano, The Multifaceted Role of Heme in Cancer. *Front Oncol* **9**, 1540 (2019).
287. G. C. Shaw *et al.*, Mitoferrin is essential for erythroid iron assimilation. *Nature* **440**, 96-100 (2006).
288. P. N. Paradkar, K. B. Zumbrennen, B. H. Paw, D. M. Ward, J. Kaplan, Regulation of mitochondrial iron import through differential turnover of mitoferrin 1 and mitoferrin 2. *Mol Cell Biol* **29**, 1007-1016 (2009).
289. W. E. Dowdle *et al.*, Selective VPS34 inhibitor blocks autophagy and uncovers a role for NCOA4 in ferritin degradation and iron homeostasis in vivo. *Nat Cell Biol* **16**, 1069-1079 (2014).
290. C. P. Anderson, M. Shen, R. S. Eisenstein, E. A. Leibold, Mammalian iron metabolism and its control by iron regulatory proteins. *Biochim Biophys Acta* **1823**, 1468-1483 (2012).
291. K. Volz, The functional duality of iron regulatory protein 1. *Curr Opin Struct Biol* **18**, 106-111 (2008).
292. N. Takahashi-Makise, D. M. Ward, J. Kaplan, On the mechanism of iron sensing by IRP2: new players, new paradigms. *Nat Chem Biol* **5**, 874-875 (2009).
293. M. W. Hentze, M. U. Muckenthaler, B. Galy, C. Camaschella, Two to tango: regulation of Mammalian iron metabolism. *Cell* **142**, 24-38 (2010).
294. H. Ye, T. A. Rouault, Human iron-sulfur cluster assembly, cellular iron homeostasis, and disease. *Biochemistry* **49**, 4945-4956 (2010).
295. R. Lill, Function and biogenesis of iron-sulphur proteins. *Nature* **460**, 831-838 (2009).
296. J. G. Quigley *et al.*, Identification of a human heme exporter that is essential for erythropoiesis. *Cell* **118**, 757-766 (2004).
297. S. B. Keel *et al.*, A heme export protein is required for red blood cell differentiation and iron homeostasis. *Science* **319**, 825-828 (2008).
298. C. Glorieux, P. B. Calderon, Catalase, a remarkable enzyme: targeting the oldest antioxidant enzyme to find a new cancer treatment approach. *Biol Chem* **398**, 1095-1108 (2017).
299. L. Forsberg, L. Lyrenas, U. de Faire, R. Morgenstern, A common functional C-T substitution polymorphism in the promoter region of the human catalase gene influences transcription factor binding, reporter gene transcription and is correlated to blood catalase levels. *Free Radic Biol Med* **30**, 500-505 (2001).
300. K. Liu *et al.*, Two common functional catalase gene polymorphisms (rs1001179 and rs794316) and cancer susceptibility: evidence from 14,942 cancer cases and 43,285 controls. *Oncotarget* **7**, 62954-62965 (2016).
301. C. D. Wang *et al.*, The Role of Catalase C262T Gene Polymorphism in the Susceptibility and Survival of Cancers. *Sci Rep* **6**, 26973 (2016).
302. D. A. Wink, L. A. Ridnour, S. P. Hussain, C. C. Harris, The reemergence of nitric oxide and cancer. *Nitric Oxide* **19**, 65-67 (2008).
303. S. K. Choudhari, M. Chaudhary, S. Bagde, A. R. Gadbail, V. Joshi, Nitric oxide and cancer: a review. *World J Surg Oncol* **11**, 118 (2013).
304. C. A. Rouzer, L. J. Marnett, Cyclooxygenases: structural and functional insights. *J Lipid Res* **50 Suppl**, S29-34 (2009).
305. B. Liu, L. Qu, S. Yan, Cyclooxygenase-2 promotes tumor growth and suppresses tumor immunity. *Cancer Cell Int* **15**, 106 (2015).
306. N. Hashemi Goradel, M. Najafi, E. Salehi, B. Farhood, K. Mortezaee, Cyclooxygenase-2 in cancer: A review. *J Cell Physiol* **234**, 5683-5699 (2019).
307. M. Cardenas-Rodriguez, A. Chatzi, K. Tokatlidis, Iron-sulfur clusters: from metals through mitochondria biogenesis to disease. *J Biol Inorg Chem* **23**, 509-520 (2018).
308. T. A. Rouault, Biogenesis of iron-sulfur clusters in mammalian cells: new insights and relevance to human disease. *Dis Model Mech* **5**, 155-164 (2012).
309. S. Schmucker *et al.*, Mammalian frataxin: an essential function for cellular viability through an interaction with a preformed ISCU/NFS1/ISD11 iron-sulfur assembly complex. *PLoS One* **6**, e16199 (2011).
310. C. L. Tsai, D. P. Barondeau, Human frataxin is an allosteric switch that activates the Fe-S cluster biosynthetic complex. *Biochemistry* **49**, 9132-9139 (2010).
311. J. Bridwell-Rabb, A. M. Winn, D. P. Barondeau, Structure-function analysis of Friedreich's ataxia mutants reveals determinants of frataxin binding and activation of the Fe-S assembly complex. *Biochemistry* **50**, 7265-7274 (2011).
312. T. L. Stemmler, E. Lesuisse, D. Pain, A. Dancis, Frataxin and mitochondrial FeS cluster biogenesis. *J Biol Chem* **285**, 26737-26743 (2010).
313. R. C. Hider, X. L. Kong, Glutathione: a key component of the cytoplasmic labile iron pool. *Biometals* **24**, 1179-1187 (2011).
314. W. Qi, J. A. Cowan, Mechanism of glutaredoxin-ISU [2Fe-2S] cluster exchange. *Chem Commun (Camb)* **47**, 4989-4991 (2011).

315. S. Bekri *et al.*, Human ABC7 transporter: gene structure and mutation causing X-linked sideroblastic anemia with ataxia with disruption of cytosolic iron-sulfur protein maturation. *Blood* **96**, 3256-3264 (2000).
316. S. W. Alvarez *et al.*, NFS1 undergoes positive selection in lung tumours and protects cells from ferroptosis. *Nature* **551**, 639-643 (2017).
317. I. Guccini *et al.*, Frataxin participates to the hypoxia-induced response in tumors. *Cell Death Dis* **2**, e123 (2011).
318. A. Bansal, M. C. Simon, Glutathione metabolism in cancer progression and treatment resistance. *J Cell Biol* **217**, 2291-2298 (2018).
319. J. R. Colca *et al.*, Identification of a novel mitochondrial protein ("mitoNEET") cross-linked specifically by a thiazolidinedione photoprobe. *Am J Physiol Endocrinol Metab* **286**, E252-260 (2004).
320. S. E. Wiley, A. N. Murphy, S. A. Ross, P. van der Geer, J. E. Dixon, MitoNEET is an iron-containing outer mitochondrial membrane protein that regulates oxidative capacity. *Proc Natl Acad Sci U S A* **104**, 5318-5323 (2007).
321. E. F. Binder, L. N. Robins, Cognitive impairment and length of hospital stay in older persons. *J Am Geriatr Soc* **38**, 759-766 (1990).
322. N. C. Chang, M. Nguyen, M. Germain, G. C. Shore, Antagonism of Beclin 1-dependent autophagy by BCL-2 at the endoplasmic reticulum requires NAF-1. *EMBO J* **29**, 606-618 (2010).
323. C. M. Kusminski *et al.*, MitoNEET-driven alterations in adipocyte mitochondrial activity reveal a crucial adaptive process that preserves insulin sensitivity in obesity. *Nat Med* **18**, 1539-1549 (2012).
324. M. E. Roberts *et al.*, Identification of disulfide bond formation between MitoNEET and glutamate dehydrogenase 1. *Biochemistry* **52**, 8969-8971 (2013).
325. R. Mittler *et al.*, NEET Proteins: A New Link Between Iron Metabolism, Reactive Oxygen Species, and Cancer. *Antioxid Redox Signal* **30**, 1083-1095 (2019).
326. B. Chen *et al.*, CISD2 associated with proliferation indicates negative prognosis in patients with hepatocellular carcinoma. *Int J Clin Exp Pathol* **8**, 13725-13738 (2015).
327. L. Liu *et al.*, CISD2 expression is a novel marker correlating with pelvic lymph node metastasis and prognosis in patients with early-stage cervical cancer. *Med Oncol* **31**, 183 (2014).
328. A. F. Salem, D. Whitaker-Menezes, A. Howell, F. Sotgia, M. P. Lisanti, Mitochondrial biogenesis in epithelial cancer cells promotes breast cancer tumor growth and confers autophagy resistance. *Cell Cycle* **11**, 4174-4180 (2012).
329. M. Darash-Yahana *et al.*, Breast cancer tumorigenicity is dependent on high expression levels of NAF-1 and the lability of its Fe-S clusters. *Proc Natl Acad Sci U S A* **113**, 10890-10895 (2016).
330. Y. S. Sohn *et al.*, NAF-1 and mitoNEET are central to human breast cancer proliferation by maintaining mitochondrial homeostasis and promoting tumor growth. *Proc Natl Acad Sci U S A* **110**, 14676-14681 (2013).
331. J. W. Rensvold *et al.*, Complementary RNA and protein profiling identifies iron as a key regulator of mitochondrial biogenesis. *Cell Rep* **3**, 237-245 (2013).
332. J. Stiban, M. So, L. S. Kaguni, Iron-Sulfur Clusters in Mitochondrial Metabolism: Multifaceted Roles of a Simple Cofactor. *Biochemistry (Mosc)* **81**, 1066-1080 (2016).
333. A. H. Robbins, C. D. Stout, The structure of aconitase. *Proteins* **5**, 289-312 (1989).
334. A. H. Robbins, C. D. Stout, Structure of activated aconitase: formation of the [4Fe-4S] cluster in the crystal. *Proc Natl Acad Sci U S A* **86**, 3639-3643 (1989).
335. J. Talib, M. J. Davies, Exposure of aconitase to smoking-related oxidants results in iron loss and increased iron response protein-1 activity: potential mechanisms for iron accumulation in human arterial cells. *J Biol Inorg Chem* **21**, 305-317 (2016).
336. P. R. Gardner, I. Fridovich, Superoxide sensitivity of the Escherichia coli aconitase. *J Biol Chem* **266**, 19328-19333 (1991).
337. D. Han *et al.*, Sites and mechanisms of aconitase inactivation by peroxynitrite: modulation by citrate and glutathione. *Biochemistry* **44**, 11986-11996 (2005).
338. F. Ciccarone *et al.*, Aconitase 2 inhibits the proliferation of MCF-7 cells promoting mitochondrial oxidative metabolism and ROS/FoxO1-mediated autophagic response. *Br J Cancer* **122**, 182-193 (2020).
339. N. Wilkinson, K. Pantopoulos, The IRP/IRE system in vivo: insights from mouse models. *Front Pharmacol* **5**, 176 (2014).
340. V. Yankovskaya *et al.*, Architecture of succinate dehydrogenase and reactive oxygen species generation. *Science* **299**, 700-704 (2003).
341. A. Lemarie, S. Grimm, Mutations in the heme b-binding residue of SDHC inhibit assembly of respiratory chain complex II in mammalian cells. *Mitochondrion* **9**, 254-260 (2009).
342. C. Bardella, P. J. Pollard, I. Tomlinson, SDH mutations in cancer. *Biochim Biophys Acta* **1807**, 1432-1443 (2011).
343. A. J. Gill, Succinate dehydrogenase (SDH) and mitochondrial driven neoplasia. *Pathology* **44**, 285-292 (2012).

344. C. Ricketts *et al.*, Germline SDHB mutations and familial renal cell carcinoma. *J Natl Cancer Inst* **100**, 1260-1262 (2008).
345. C. J. Ricketts *et al.*, Succinate dehydrogenase kidney cancer: an aggressive example of the Warburg effect in cancer. *J Urol* **188**, 2063-2071 (2012).
346. E. Dalla Pozza *et al.*, Regulation of succinate dehydrogenase and role of succinate in cancer. *Semin Cell Dev Biol* **98**, 4-14 (2020).
347. R. D. Guzy, B. Sharma, E. Bell, N. S. Chandel, P. T. Schumacker, Loss of the SdhB, but Not the SdhA, subunit of complex II triggers reactive oxygen species-dependent hypoxia-inducible factor activation and tumorigenesis. *Mol Cell Biol* **28**, 718-731 (2008).
348. P. L. Tseng *et al.*, Decreased succinate dehydrogenase B in human hepatocellular carcinoma accelerates tumor malignancy by inducing the Warburg effect. *Sci Rep* **8**, 3081 (2018).
349. L. B. Sullivan, D. Y. Gui, M. G. Vander Heiden, Altered metabolite levels in cancer: implications for tumour biology and cancer therapy. *Nat Rev Cancer* **16**, 680-693 (2016).
350. D. R. Winge, Sealing the mitochondrial respirasome. *Mol Cell Biol* **32**, 2647-2652 (2012).
351. W. Xu, T. Barrientos, N. C. Andrews, Iron and copper in mitochondrial diseases. *Cell Metab* **17**, 319-328 (2013).
352. P. E. Porporato, N. Filigheddu, J. M. B. Pedro, G. Kroemer, L. Galluzzi, Mitochondrial metabolism and cancer. *Cell Res* **28**, 265-280 (2018).
353. S. E. Weinberg, N. S. Chandel, Targeting mitochondria metabolism for cancer therapy. *Nat Chem Biol* **11**, 9-15 (2015).
354. L. Dong, J. Neuzil, Targeting mitochondria as an anticancer strategy. *Cancer Commun (Lond)* **39**, 63 (2019).
355. D. J. Netz *et al.*, Eukaryotic DNA polymerases require an iron-sulfur cluster for the formation of active complexes. *Nat Chem Biol* **8**, 125-132 (2011).
356. O. Stehling *et al.*, MMS19 assembles iron-sulfur proteins required for DNA metabolism and genomic integrity. *Science* **337**, 195-199 (2012).
357. K. Gari *et al.*, MMS19 links cytoplasmic iron-sulfur cluster assembly to DNA metabolism. *Science* **337**, 243-245 (2012).
358. V. D. Paul, R. Lill, Biogenesis of cytosolic and nuclear iron-sulfur proteins and their role in genome stability. *Biochim Biophys Acta* **1853**, 1528-1539 (2015).
359. A. G. Baranovskiy, H. M. Siebler, Y. I. Pavlov, T. H. Tahirov, Iron-Sulfur Clusters in DNA Polymerases and Primases of Eukaryotes. *Methods Enzymol* **599**, 1-20 (2018).
360. S. K. Jozwiakowski, S. Kummer, K. Gari, Human DNA polymerase delta requires an iron-sulfur cluster for high-fidelity DNA synthesis. *Life Sci Alliance* **2**, (2019).
361. R. A. Finch *et al.*, Triapine (3-aminopyridine-2-carboxaldehyde- thiosemicarbazone): A potent inhibitor of ribonucleotide reductase activity with broad spectrum antitumor activity. *Biochem Pharmacol* **59**, 983-991 (2000).
362. K. P. Hoyes, R. C. Hider, J. B. Porter, Cell cycle synchronization and growth inhibition by 3-hydroxypyridin-4-one iron chelators in leukemia cell lines. *Cancer Res* **52**, 4591-4599 (1992).
363. C. E. Cooper *et al.*, The relationship of intracellular iron chelation to the inhibition and regeneration of human ribonucleotide reductase. *J Biol Chem* **271**, 20291-20299 (1996).
364. V. Khodaverdian *et al.*, Deferiprone: Pan-selective Histone Lysine Demethylase Inhibition Activity and Structure Activity Relationship Study. *Sci Rep* **9**, 4802 (2019).
365. T. Nishino, K. Okamoto, The role of the [2Fe-2s] cluster centers in xanthine oxidoreductase. *J Inorg Biochem* **82**, 43-49 (2000).
366. G. L. Wang, G. L. Semenza, Desferrioxamine induces erythropoietin gene expression and hypoxia-inducible factor 1 DNA-binding activity: implications for models of hypoxia signal transduction. *Blood* **82**, 3610-3615 (1993).
367. A. Nandal *et al.*, Activation of the HIF prolyl hydroxylase by the iron chaperones PCBP1 and PCBP2. *Cell Metab* **14**, 647-657 (2011).
368. G. L. Semenza, HIF-1: mediator of physiological and pathophysiological responses to hypoxia. *J Appl Physiol (1985)* **88**, 1474-1480 (2000).
369. A. G. Frey *et al.*, Iron chaperones PCBP1 and PCBP2 mediate the metallation of the dinuclear iron enzyme deoxyhypusine hydroxylase. *Proc Natl Acad Sci U S A* **111**, 8031-8036 (2014).
370. V. V. Vu *et al.*, Human deoxyhypusine hydroxylase, an enzyme involved in regulating cell growth, activates O2 with a nonheme diiron center. *Proc Natl Acad Sci U S A* **106**, 14814-14819 (2009).
371. M. H. Park, The post-translational synthesis of a polyamine-derived amino acid, hypusine, in the eukaryotic translation initiation factor 5A (eIF5A). *J Biochem* **139**, 161-169 (2006).
372. E. Nemeth, T. Ganz, Anemia of inflammation. *Hematol Oncol Clin North Am* **28**, 671-681, vi (2014).
373. A. Pietrangelo *et al.*, STAT3 is required for IL-6-gp130-dependent activation of hepcidin in vivo. *Gastroenterology* **132**, 294-300 (2007).

374. E. Nemeth *et al.*, IL-6 mediates hypoferremia of inflammation by inducing the synthesis of the iron regulatory hormone hepcidin. *J Clin Invest* **113**, 1271-1276 (2004).
375. G. Nicolas *et al.*, The gene encoding the iron regulatory peptide hepcidin is regulated by anemia, hypoxia, and inflammation. *J Clin Invest* **110**, 1037-1044 (2002).
376. E. Nemeth *et al.*, Hepcidin, a putative mediator of anemia of inflammation, is a type II acute-phase protein. *Blood* **101**, 2461-2463 (2003).
377. I. Buck, F. Morceau, C. Grigorakaki, M. Dicato, M. Diederich, Linking anemia to inflammation and cancer: the crucial role of TNFalpha. *Biochem Pharmacol* **77**, 1572-1579 (2009).
378. P. Lee, H. Peng, T. Gelbart, L. Wang, E. Beutler, Regulation of hepcidin transcription by interleukin-1 and interleukin-6. *Proc Natl Acad Sci U S A* **102**, 1906-1910 (2005).
379. P. Matak *et al.*, Activated macrophages induce hepcidin expression in HuH7 hepatoma cells. *Haematologica* **94**, 773-780 (2009).
380. I. Theurl *et al.*, Autocrine formation of hepcidin induces iron retention in human monocytes. *Blood* **111**, 2392-2399 (2008).
381. F. B. Sow *et al.*, Expression and localization of hepcidin in macrophages: a role in host defense against tuberculosis. *J Leukoc Biol* **82**, 934-945 (2007).
382. C. Peyssonnaux *et al.*, TLR4-dependent hepcidin expression by myeloid cells in response to bacterial pathogens. *Blood* **107**, 3727-3732 (2006).
383. D. H. Bach, H. J. Park, S. K. Lee, The Dual Role of Bone Morphogenetic Proteins in Cancer. *Mol Ther Oncolytics* **8**, 1-13 (2018).
384. M. Scimeca, E. Bonanno, New highlight in breast cancer development: the key role of hepcidin and iron metabolism. *Ann Transl Med* **6**, S56 (2018).
385. C. M. Ciniselli *et al.*, Plasma hepcidin in early-stage breast cancer patients: no relationship with interleukin-6, erythropoietin and erythroferrone. *Expert Rev Proteomics* **12**, 695-701 (2015).
386. R. Orlandi *et al.*, Hepcidin and ferritin blood level as noninvasive tools for predicting breast cancer. *Ann Oncol* **25**, 352-357 (2014).
387. Q. Chen *et al.*, Increased hepcidin expression in non-small cell lung cancer tissue and serum is associated with clinical stage. *Thorac Cancer* **5**, 14-24 (2014).
388. S. Y. Sato K, Inoue S et al., Serum hepcidin and iron are associated with non-small cell lung cancer stage. *European Respiratory Journal* (2016).
389. H. W. Hann *et al.*, Prognostic importance of serum ferritin in patients with Stages III and IV neuroblastoma: the Childrens Cancer Study Group experience. *Cancer Res* **45**, 2843-2848 (1985).
390. H. W. Hann, B. Lange, M. W. Stahlhut, K. A. McGlynn, Prognostic importance of serum transferrin and ferritin in childhood Hodgkin's disease. *Cancer* **66**, 313-316 (1990).
391. S. Koyama *et al.*, Serum ferritin level is a prognostic marker in patients with peripheral T-cell lymphoma. *Int J Lab Hematol* **39**, 112-117 (2017).
392. S. Lee, A. Song, W. Eo, Serum Ferritin as a Prognostic Biomarker for Survival in Relapsed or Refractory Metastatic Colorectal Cancer. *J Cancer* **7**, 957-964 (2016).
393. H. Ito *et al.*, Serum ferritin levels in patients with cervical cancer. *Obstet Gynecol* **55**, 358-362 (1980).
394. D. M. Marcus, N. Zinberg, Measurement of serum ferritin by radioimmunoassay: results in normal individuals and patients with breast cancer. *J Natl Cancer Inst* **55**, 791-795 (1975).
395. A. A. Alkhateeb, J. R. Connor, The significance of ferritin in cancer: anti-oxidation, inflammation and tumorigenesis. *Biochim Biophys Acta* **1836**, 245-254 (2013).
396. S. V. Torti, F. M. Torti, Iron and cancer: 2020 Vision. *Cancer Res*, (2020).
397. Y. Shen *et al.*, Transferrin receptor 1 in cancer: a new sight for cancer therapy. *Am J Cancer Res* **8**, 916-931 (2018).
398. J. P. Brown, R. G. Woodbury, C. E. Hart, I. Hellstrom, K. E. Hellstrom, Quantitative analysis of melanoma-associated antigen p97 in normal and neoplastic tissues. *Proc Natl Acad Sci U S A* **78**, 539-543 (1981).
399. K. Dus-Szachniewicz *et al.*, Pattern of Melanotransferrin Expression in Human Colorectal Tissues: An Immunohistochemical Study on Potential Clinical Application. *Anticancer Res* **35**, 6551-6561 (2015).
400. S. Shaheduzzaman *et al.*, Silencing of Lactotransferrin expression by methylation in prostate cancer progression. *Cancer Biol Ther* **6**, 1088-1095 (2007).
401. A. Ieni *et al.*, Immunoexpression of lactoferrin in triple-negative breast cancer patients: A proposal to select a less aggressive subgroup. *Oncol Lett* **13**, 3205-3209 (2017).
402. H. Tsuda *et al.*, Cancer prevention by bovine lactoferrin: from animal studies to human trial. *Biometals* **23**, 399-409 (2010).

403. T. M. Moastafa, D. El-Sissy Ael, G. K. El-Saeed, M. S. Koura, Study on the Therapeutic Benefit on Lactoferrin in Patients with Colorectal Cancer Receiving Chemotherapy. *Int Sch Res Notices* **2014**, 184278 (2014).
404. A. Calzolari *et al.*, Transferrin receptor 2 is frequently expressed in human cancer cell lines. *Blood Cells Mol Dis* **39**, 82-91 (2007).
405. A. Calzolari *et al.*, Transferrin receptor 2 is frequently and highly expressed in glioblastomas. *Transl Oncol* **3**, 123-134 (2010).
406. A. Calzolari *et al.*, TfR2 localizes in lipid raft domains and is released in exosomes to activate signal transduction along the MAPK pathway. *J Cell Sci* **119**, 4486-4498 (2006).
407. X. Xue *et al.*, Iron Uptake via DMT1 Integrates Cell Cycle with JAK-STAT3 Signaling to Promote Colorectal Tumorigenesis. *Cell Metab* **24**, 447-461 (2016).
408. J. Boult *et al.*, Overexpression of cellular iron import proteins is associated with malignant progression of esophageal adenocarcinoma. *Clin Cancer Res* **14**, 379-387 (2008).
409. P. Xing *et al.*, Roles of low-density lipoprotein receptor-related protein 1 in tumors. *Chin J Cancer* **35**, 6 (2016).
410. C. Ma *et al.*, CD163-positive cancer cells are potentially associated with high malignant potential in clear cell renal cell carcinoma. *Med Mol Morphol* **51**, 13-20 (2018).
411. Z. Cheng, D. Zhang, B. Gong, P. Wang, F. Liu, CD163 as a novel target gene of STAT3 is a potential therapeutic target for gastric cancer. *Oncotarget* **8**, 87244-87262 (2017).
412. I. Shabo, O. Stal, H. Olsson, S. Dore, J. Svanvik, Breast cancer expression of CD163, a macrophage scavenger receptor, is related to early distant recurrence and reduced patient survival. *Int J Cancer* **123**, 780-786 (2008).
413. S. Garvin, H. Oda, L. G. Arnesson, A. Lindstrom, I. Shabo, Tumor cell expression of CD163 is associated to postoperative radiotherapy and poor prognosis in patients with breast cancer treated with breast-conserving surgery. *J Cancer Res Clin Oncol* **144**, 1253-1263 (2018).
414. M. H. Hiyama K, Tamura M, Shimokawa, Hiyama, Kaneko, Nagano, Hyodo, Tanaka, Miwa, Ogawa, Nakanishi and Tamai, Cancer cells uptake porphyrins via heme carrier protein 1. *Journal of Porphyrins and Phthalocyanines* **17**, (2013).
415. T. B. Aydemir, R. J. Cousins, The Multiple Faces of the Metal Transporter ZIP14 (SLC39A14). *J Nutr* **148**, 174-184 (2018).
416. J. B. Cowland, N. Borregaard, Molecular characterization and pattern of tissue expression of the gene for neutrophil gelatinase-associated lipocalin from humans. *Genomics* **45**, 17-23 (1997).
417. Z. Tong *et al.*, Neutrophil gelatinase-associated lipocalin as a survival factor. *Biochem J* **391**, 441-448 (2005).
418. C. A. Fernandez *et al.*, The matrix metalloproteinase-9/neutrophil gelatinase-associated lipocalin complex plays a role in breast tumor growth and is present in the urine of breast cancer patients. *Clin Cancer Res* **11**, 5390-5395 (2005).
419. L. R. Devireddy, C. Gazin, X. Zhu, M. R. Green, A cell-surface receptor for lipocalin 24p3 selectively mediates apoptosis and iron uptake. *Cell* **123**, 1293-1305 (2005).
420. R. A. M. Brown *et al.*, Altered Iron Metabolism and Impact in Cancer Biology, Metastasis, and Immunology. *Front Oncol* **10**, 476 (2020).
421. J. Moreaux, A. Kassambara, D. Hose, B. Klein, STEAP1 is overexpressed in cancers: a promising therapeutic target. *Biochem Biophys Res Commun* **429**, 148-155 (2012).
422. T. G. Grunewald, H. Bach, A. Cossarizza, I. Matsumoto, The STEAP protein family: versatile oxidoreductases and targets for cancer immunotherapy with overlapping and distinct cellular functions. *Biol Cell* **104**, 641-657 (2012).
423. A. J. Patel, R. Som, eComment. The evidence for stress ulcer prophylaxis in patients undergoing cardiac surgery. *Interact Cardiovasc Thorac Surg* **14**, 628 (2012).
424. T. Wu *et al.*, Expression of Ferritin Light Chain (FTL) Is Elevated in Glioblastoma, and FTL Silencing Inhibits Glioblastoma Cell Proliferation via the GADD45/JNK Pathway. *PLoS One* **11**, e0149361 (2016).
425. S. I. Shpyleva *et al.*, Role of ferritin alterations in human breast cancer cells. *Breast Cancer Res Treat* **126**, 63-71 (2011).
426. A. Salatino *et al.*, H-Ferritin Affects Cisplatin-Induced Cytotoxicity in Ovarian Cancer Cells through the Modulation of ROS. *Oxid Med Cell Longev* **2019**, 3461251 (2019).
427. F. Zhang, W. Wang, Y. Tsuji, S. V. Torti, F. M. Torti, Post-transcriptional modulation of iron homeostasis during p53-dependent growth arrest. *J Biol Chem* **283**, 33911-33918 (2008).
428. Y. Fukuda *et al.*, Upregulated heme biosynthesis, an exploitable vulnerability in MYCN-driven leukemogenesis. *JCI Insight* **2**, (2017).
429. J. Hooda *et al.*, Enhanced heme function and mitochondrial respiration promote the progression of lung cancer cells. *PLoS One* **8**, e63402 (2013).
430. S. Sohoni *et al.*, Elevated Heme Synthesis and Uptake Underpin Intensified Oxidative Metabolism and Tumorigenic Functions in Non-Small Cell Lung Cancer Cells. *Cancer Res* **79**, 2511-2525 (2019).

431. J. Shen *et al.*, Iron metabolism regulates p53 signaling through direct heme-p53 interaction and modulation of p53 localization, stability, and function. *Cell Rep* **7**, 180-193 (2014).
432. G. Canesin *et al.*, Scavenging of Labile Heme by Hemopexin Is a Key Checkpoint in Cancer Growth and Metastases. *Cell Rep* **32**, 108181 (2020).
433. S. K. Chiang, S. E. Chen, L. C. Chang, A Dual Role of Heme Oxygenase-1 in Cancer Cells. *Int J Mol Sci* **20**, (2018).
434. M. Nitti *et al.*, HO-1 Induction in Cancer Progression: A Matter of Cell Adaptation. *Antioxidants (Basel)* **6**, (2017).
435. G. Chen, C. Fillebeen, J. Wang, K. Pantopoulos, Overexpression of iron regulatory protein 1 suppresses growth of tumor xenografts. *Carcinogenesis* **28**, 785-791 (2007).
436. R. D. Horniblow *et al.*, BRAF mutations are associated with increased iron regulatory protein-2 expression in colorectal tumorigenesis. *Cancer Sci* **108**, 1135-1143 (2017).
437. Z. Deng, D. H. Manz, S. V. Torti, F. M. Torti, Iron-responsive element-binding protein 2 plays an essential role in regulating prostate cancer cell growth. *Oncotarget* **8**, 82231-82243 (2017).
438. W. Wang *et al.*, IRP2 regulates breast tumor growth. *Cancer Res* **74**, 497-507 (2014).
439. M. J. Kerins, A. Ooi, The Roles of NRF2 in Modulating Cellular Iron Homeostasis. *Antioxid Redox Signal* **29**, 1756-1773 (2018).
440. S. Wu, H. Lu, Y. Bai, Nrf2 in cancers: A double-edged sword. *Cancer Med* **8**, 2252-2267 (2019).
441. M. Rojo de la Vega, E. Chapman, D. D. Zhang, NRF2 and the Hallmarks of Cancer. *Cancer Cell* **34**, 21-43 (2018).
442. K. A. O'Donnell *et al.*, Activation of transferrin receptor 1 by c-Myc enhances cellular proliferation and tumorigenesis. *Mol Cell Biol* **26**, 2373-2386 (2006).
443. A. Rolfs, I. Kvietikova, M. Gassmann, R. H. Wenger, Oxygen-regulated transferrin expression is mediated by hypoxia-inducible factor-1. *J Biol Chem* **272**, 20055-20062 (1997).
444. C. N. Lok, P. Ponka, Identification of a hypoxia response element in the transferrin receptor gene. *J Biol Chem* **274**, 24147-24152 (1999).
445. D. Xue, C. X. Zhou, Y. B. Shi, H. Lu, X. Z. He, Decreased expression of ferroportin in prostate cancer. *Oncol Lett* **10**, 913-916 (2015).
446. D. G. Ward *et al.*, Increased hepcidin expression in colorectal carcinogenesis. *World J Gastroenterol* **14**, 1339-1345 (2008).
447. R. Toshiyama *et al.*, Association of iron metabolic enzyme hepcidin expression levels with the prognosis of patients with pancreatic cancer. *Oncol Lett* **15**, 8125-8133 (2018).
448. Z. K. Pinnix *et al.*, Ferroportin and iron regulation in breast cancer progression and prognosis. *Sci Transl Med* **2**, 43ra56 (2010).
449. Z. Gu *et al.*, Decreased ferroportin promotes myeloma cell growth and osteoclast differentiation. *Cancer Res* **75**, 2211-2221 (2015).
450. B. Zhao *et al.*, Role of hepcidin and iron metabolism in the onset of prostate cancer. *Oncol Lett* **15**, 9953-9958 (2018).
451. M. J. Brookes *et al.*, Modulation of iron transport proteins in human colorectal carcinogenesis. *Gut* **55**, 1449-1460 (2006).
452. S. J. Dixon *et al.*, Ferroptosis: an iron-dependent form of nonapoptotic cell death. *Cell* **149**, 1060-1072 (2012).
453. M. M. Gaschler, B. R. Stockwell, Lipid peroxidation in cell death. *Biochem Biophys Res Commun* **482**, 419-425 (2017).
454. F. Ursini, M. Maiorino, C. Gregolin, The selenoenzyme phospholipid hydroperoxide glutathione peroxidase. *Biochim Biophys Acta* **839**, 62-70 (1985).
455. A. Hinman *et al.*, Vitamin E hydroquinone is an endogenous regulator of ferroptosis via redox control of 15-lipoxygenase. *PLoS One* **13**, e0201369 (2018).
456. R. Skouta *et al.*, Ferrostatins inhibit oxidative lipid damage and cell death in diverse disease models. *J Am Chem Soc* **136**, 4551-4556 (2014).
457. S. Doll *et al.*, FSP1 is a glutathione-independent ferroptosis suppressor. *Nature* **575**, 693-698 (2019).
458. S. Ma, E. S. Henson, Y. Chen, S. B. Gibson, Ferroptosis is induced following siramesine and lapatinib treatment of breast cancer cells. *Cell Death Dis* **7**, e2307 (2016).
459. M. Gao *et al.*, Ferroptosis is an autophagic cell death process. *Cell Res* **26**, 1021-1032 (2016).
460. V. S. Viswanathan *et al.*, Dependency of a therapy-resistant state of cancer cells on a lipid peroxidase pathway. *Nature* **547**, 453-457 (2017).
461. M. J. Hangauer *et al.*, Drug-tolerant persister cancer cells are vulnerable to GPX4 inhibition. *Nature* **551**, 247-250 (2017).

462. B. Hassannia, P. Vandenabeele, T. Vanden Berghe, Targeting Ferroptosis to Iron Out Cancer. *Cancer Cell* **35**, 830-849 (2019).
463. J. Li *et al.*, Ferroptosis: past, present and future. *Cell Death Dis* **11**, 88 (2020).
464. P. Danhier *et al.*, Cancer metabolism in space and time: Beyond the Warburg effect. *Biochim Biophys Acta Bioenerg* **1858**, 556-572 (2017).
465. M. Serra, A. Columbano, U. Ammarah, M. Mazzone, A. Menga, Understanding Metal Dynamics Between Cancer Cells and Macrophages: Competition or Synergism? *Front Oncol* **10**, 646 (2020).
466. M. Costa da Silva *et al.*, Iron Induces Anti-tumor Activity in Tumor-Associated Macrophages. *Front Immunol* **8**, 1479 (2017).
467. C. M. Thielmann *et al.*, Iron accumulation in tumor-associated macrophages marks an improved overall survival in patients with lung adenocarcinoma. *Sci Rep* **9**, 11326 (2019).
468. S. J. F. Cronin, C. J. Woolf, G. Weiss, J. M. Penninger, The Role of Iron Regulation in Immunometabolism and Immune-Related Disease. *Front Mol Biosci* **6**, 116 (2019).
469. C. Mertens *et al.*, Macrophage-derived lipocalin-2 transports iron in the tumor microenvironment. *Oncoimmunology* **7**, e1408751 (2018).
470. M. Jung *et al.*, Lipocalin 2 from macrophages stimulated by tumor cell-derived sphingosine 1-phosphate promotes lymphangiogenesis and tumor metastasis. *Sci Signal* **9**, ra64 (2016).
471. D. Kir *et al.*, Cell-permeable iron inhibits vascular endothelial growth factor receptor-2 signaling and tumor angiogenesis. *Oncotarget* **7**, 65348-65363 (2016).
472. L. Wu, Y. Du, J. Lok, E. H. Lo, C. Xing, Lipocalin-2 enhances angiogenesis in rat brain endothelial cells via reactive oxygen species and iron-dependent mechanisms. *J Neurochem* **132**, 622-628 (2015).
473. Y. W. Kim, T. V. Byzova, Oxidative stress in angiogenesis and vascular disease. *Blood* **123**, 625-631 (2014).
474. S. Akatsuka *et al.*, Fenton reaction induced cancer in wild type rats recapitulates genomic alterations observed in human cancer. *PLoS One* **7**, e43403 (2012).
475. L. S. Horniblow R, Beggs A, Iqbal T, Tselepis C, Epigenetic dna methylation modifications following chronic iron exposure to colonocytes in vitro. *Gut*, (2017).
476. S. Luanpitpong *et al.*, Regulation of lung cancer cell migration and invasion by reactive oxygen species and caveolin-1. *J Biol Chem* **285**, 38832-38840 (2010).
477. L. Hu *et al.*, NGAL decreases E-cadherin-mediated cell-cell adhesion and increases cell motility and invasion through Rac1 in colon carcinoma cells. *Lab Invest* **89**, 531-548 (2009).
478. I. P. Pogribny *et al.*, Modulation of intracellular iron metabolism by iron chelation affects chromatin remodeling proteins and corresponding epigenetic modifications in breast cancer cells and increases their sensitivity to chemotherapeutic agents. *Int J Oncol* **42**, 1822-1832 (2013).
479. S. X. Liang, D. R. Richardson, The effect of potent iron chelators on the regulation of p53: examination of the expression, localization and DNA-binding activity of p53 and the transactivation of WAF1. *Carcinogenesis* **24**, 1601-1614 (2003).
480. Z. Deng, D. H. Manz, S. V. Torti, F. M. Torti, Effects of Ferroportin-Mediated Iron Depletion in Cells Representative of Different Histological Subtypes of Prostate Cancer. *Antioxid Redox Signal* **30**, 1043-1061 (2019).
481. S. Song *et al.*, Wnt inhibitor screen reveals iron dependence of beta-catenin signaling in cancers. *Cancer Res* **71**, 7628-7639 (2011).
482. W. Zhang *et al.*, Deferoxamine enhances cell migration and invasion through promotion of HIF-1alpha expression and epithelial-mesenchymal transition in colorectal cancer. *Oncol Rep* **31**, 111-116 (2014).
483. H. Ludwig, E. Muldur, G. Endler, W. Hubl, Prevalence of iron deficiency across different tumors and its association with poor performance status, disease status and anemia. *Ann Oncol* **24**, 1886-1892 (2013).
484. C. Camaschella, A. Nai, L. Silvestri, Iron metabolism and iron disorders revisited in the hepcidin era. *Haematologica* **105**, 260-272 (2020).
485. N. H. Gehring, M. W. Hentze, K. Pantopoulos, Inactivation of both RNA binding and aconitase activities of iron regulatory protein-1 by quinone-induced oxidative stress. *J Biol Chem* **274**, 6219-6225 (1999).
486. R. Bellelli *et al.*, NCOA4 Deficiency Impairs Systemic Iron Homeostasis. *Cell Rep* **14**, 411-421 (2016).
487. J. Liu *et al.*, Mitochondrial Dysfunction Launches Dexamethasone-Induced Skeletal Muscle Atrophy via AMPK/FOXO3 Signaling. *Mol Pharm* **13**, 73-84 (2016).
488. B. Zhao *et al.*, Mitochondrial dysfunction activates the AMPK signaling and autophagy to promote cell survival. *Genes Dis* **3**, 82-87 (2016).
489. T. Fukawa *et al.*, Excessive fatty acid oxidation induces muscle atrophy in cancer cachexia. *Nat Med* **22**, 666-671 (2016).
490. F. F. Dutra, M. T. Bozza, Heme on innate immunity and inflammation. *Front Pharmacol* **5**, 115 (2014).

491. P. Robach *et al.*, Strong iron demand during hypoxia-induced erythropoiesis is associated with down-regulation of iron-related proteins and myoglobin in human skeletal muscle. *Blood* **109**, 4724-4731 (2007).
492. H. Li *et al.*, Iron regulatory protein deficiency compromises mitochondrial function in murine embryonic fibroblasts. *Sci Rep* **8**, 5118 (2018).
493. B. Galy *et al.*, Iron regulatory proteins secure mitochondrial iron sufficiency and function. *Cell Metab* **12**, 194-201 (2010).
494. E. G. Meyron-Holtz *et al.*, Genetic ablations of iron regulatory proteins 1 and 2 reveal why iron regulatory protein 2 dominates iron homeostasis. *EMBO J* **23**, 386-395 (2004).
495. T. Barrientos *et al.*, Metabolic Catastrophe in Mice Lacking Transferrin Receptor in Muscle. *EBioMedicine* **2**, 1705-1717 (2015).
496. L. J. Scott, Ferric Carboxymaltose: A Review in Iron Deficiency. *Drugs* **78**, 479-493 (2018).
497. G. Marone, S. Poto, R. Giugliano, D. Celestino, S. Bonini, Control mechanisms of human basophil releasability. *J Allergy Clin Immunol* **78**, 974-980 (1986).
498. Y. Peng *et al.*, Muscle atrophy induced by overexpression of ALAS2 is related to muscle mitochondrial dysfunction. *Skelet Muscle* **11**, 9 (2021).
499. S. Levi, E. Rovida, The role of iron in mitochondrial function. *Biochim Biophys Acta* **1790**, 629-636 (2009).
500. J. W. Rensvold, K. A. Krautkramer, J. A. Dowell, J. M. Denu, D. J. Pagliarini, Iron Deprivation Induces Transcriptional Regulation of Mitochondrial Biogenesis. *J Biol Chem* **291**, 20827-20837 (2016).
501. G. F. Allen, R. Toth, J. James, I. G. Ganley, Loss of iron triggers PINK1/Parkin-independent mitophagy. *EMBO Rep* **14**, 1127-1135 (2013).
502. T. W. Bastian, W. C. von Hohenberg, M. K. Georgieff, L. M. Lanier, Chronic Energy Depletion due to Iron Deficiency Impairs Dendritic Mitochondrial Motility during Hippocampal Neuron Development. *J Neurosci* **39**, 802-813 (2019).
503. V. Romanello *et al.*, Mitochondrial fission and remodelling contributes to muscle atrophy. *EMBO J* **29**, 1774-1785 (2010).
504. A. R. Palla *et al.*, Inhibition of prostaglandin-degrading enzyme 15-PGDH rejuvenates aged muscle mass and strength. *Science* **371**, (2021).
505. M. Beltra, F. Pin, R. Ballaro, P. Costelli, F. Penna, Mitochondrial Dysfunction in Cancer Cachexia: Impact on Muscle Health and Regeneration. *Cells* **10**, (2021).
506. D. Neyroud, R. L. Nosacka, A. R. Judge, R. T. Hepple, Colon 26 adenocarcinoma (C26)-induced cancer cachexia impairs skeletal muscle mitochondrial function and content. *J Muscle Res Cell Motil* **40**, 59-65 (2019).
507. J. M. Argiles, C. C. Fontes-Oliveira, M. Toledo, F. J. Lopez-Soriano, S. Busquets, Cachexia: a problem of energetic inefficiency. *J Cachexia Sarcopenia Muscle* **5**, 279-286 (2014).
508. C. A. Finch *et al.*, Iron deficiency in the rat. Physiological and biochemical studies of muscle dysfunction. *J Clin Invest* **58**, 447-453 (1976).
509. J. J. Maguire, K. J. Davies, P. R. Dallman, L. Packer, Effects of dietary iron deficiency of iron-sulfur proteins and bioenergetic functions of skeletal muscle mitochondria. *Biochim Biophys Acta* **679**, 210-220 (1982).
510. H. Oexle, E. Gnaiger, G. Weiss, Iron-dependent changes in cellular energy metabolism: influence on citric acid cycle and oxidative phosphorylation. *Biochim Biophys Acta* **1413**, 99-107 (1999).
511. P. A. Leermakers *et al.*, Iron deficiency-induced loss of skeletal muscle mitochondrial proteins and respiratory capacity; the role of mitophagy and secretion of mitochondria-containing vesicles. *FASEB J* **34**, 6703-6717 (2020).
512. V. Romanello, M. Sandri, Mitochondrial Quality Control and Muscle Mass Maintenance. *Front Physiol* **6**, 422 (2015).
513. J. Abrigo, F. Simon, D. Cabrera, C. Vilos, C. Cabello-Verrugio, Mitochondrial Dysfunction in Skeletal Muscle Pathologies. *Curr Protein Pept Sci* **20**, 536-546 (2019).
514. N. A. Stephens *et al.*, Intramyocellular lipid droplets increase with progression of cachexia in cancer patients. *J Cachexia Sarcopenia Muscle* **2**, 111-117 (2011).
515. M. R. Davis *et al.*, Enhanced expression of lipogenic genes may contribute to hyperglycemia and alterations in plasma lipids in response to dietary iron deficiency. *Genes Nutr* **7**, 415-425 (2012).
516. D. Zhou *et al.*, Iron overload is related to muscle wasting in patients with cachexia of gastric cancer: using quantitative proteome analysis. *Med Oncol* **37**, 113 (2020).
517. M. Assi, F. Derbre, L. Lefeuvre-Orfila, A. Rebillard, Antioxidant supplementation accelerates cachexia development by promoting tumor growth in C26 tumor-bearing mice. *Free Radic Biol Med* **91**, 204-214 (2016).
518. J. W. S. Jahng *et al.*, Iron overload inhibits late stage autophagic flux leading to insulin resistance. *EMBO Rep* **20**, e47911 (2019).
519. Y. Li *et al.*, Transferrin receptor 1 plays an important role in muscle development and denervation-induced muscular atrophy. *Neural Regen Res* **16**, 1308-1316 (2021).

520. H. Ding *et al.*, Transferrin receptor 1 ablation in satellite cells impedes skeletal muscle regeneration through activation of ferroptosis. *J Cachexia Sarcopenia Muscle* **12**, 746-768 (2021).
521. K. Higashida, S. Inoue, N. Nakai, Iron deficiency attenuates protein synthesis stimulated by branched-chain amino acids and insulin in myotubes. *Biochem Biophys Res Commun* **531**, 112-117 (2020).
522. C. Shang *et al.*, Iron chelation inhibits mTORC1 signaling involving activation of AMPK and REDD1/Bnip3 pathways. *Oncogene* **39**, 5201-5213 (2020).
523. A. Watson, C. Lipina, H. J. McArdle, P. M. Taylor, H. S. Hundal, Iron depletion suppresses mTORC1-directed signalling in intestinal Caco-2 cells via induction of REDD1. *Cell Signal* **28**, 412-424 (2016).
524. J. M. Fernandez-Real, A. Lopez-Bermejo, W. Ricart, Cross-talk between iron metabolism and diabetes. *Diabetes* **51**, 2348-2354 (2002).
525. K. L. Klempa, W. T. Willis, R. Chengson, P. R. Dallman, G. A. Brooks, Iron deficiency decreases gluconeogenesis in isolated rat hepatocytes. *J Appl Physiol (1985)* **67**, 1868-1872 (1989).
526. Y. Gao *et al.*, Adipocyte iron regulates leptin and food intake. *J Clin Invest* **125**, 3681-3691 (2015).
527. E. A. Jankowska *et al.*, Effects of intravenous iron therapy in iron-deficient patients with systolic heart failure: a meta-analysis of randomized controlled trials. *Eur J Heart Fail* **18**, 786-795 (2016).
528. R. Larsen *et al.*, A central role for free heme in the pathogenesis of severe sepsis. *Sci Transl Med* **2**, 51ra71 (2010).
529. V. Fiorito *et al.*, The heme synthesis-export system regulates the tricarboxylic acid cycle flux and oxidative phosphorylation. *Cell Rep* **35**, 109252 (2021).
530. S. Lyoumi *et al.*, Heme and acute inflammation role in vivo of heme in the hepatic expression of positive acute-phase reactants in rats. *Eur J Biochem* **261**, 190-196 (1999).
531. F. A. Wagener *et al.*, Heme is a potent inducer of inflammation in mice and is counteracted by heme oxygenase. *Blood* **98**, 1802-1811 (2001).
532. B. N. Porto *et al.*, Heme induces neutrophil migration and reactive oxygen species generation through signaling pathways characteristic of chemotactic receptors. *J Biol Chem* **282**, 24430-24436 (2007).
533. A. P. Monteiro *et al.*, Leukotriene B4 mediates neutrophil migration induced by heme. *J Immunol* **186**, 6562-6567 (2011).
534. S. Xiong, L. Dong, L. Cheng, Neutrophils in cancer carcinogenesis and metastasis. *J Hematol Oncol* **14**, 173 (2021).
535. S. K. Wculek, I. Malanchi, Neutrophils support lung colonization of metastasis-initiating breast cancer cells. *Nature* **528**, 413-417 (2015).
536. R. Sartori, P. Gregorevic, M. Sandri, TGFbeta and BMP signaling in skeletal muscle: potential significance for muscle-related disease. *Trends Endocrinol Metab* **25**, 464-471 (2014).
537. E. Wyart *et al.*, Metabolic Alterations in a Slow-Paced Model of Pancreatic Cancer-Induced Wasting. *Oxid Med Cell Longev* **2018**, 6419805 (2018).
538. A. Murata *et al.*, Superior Mesenteric Artery-Pancreaticoduodenal Arcade Bypass Grafting for Repair of Inferior Pancreaticoduodenal Artery Aneurysm with Celiac Axis Occlusion. *Ann Vasc Dis* **11**, 153-157 (2018).
539. P. R. Sinclair, N. Gorman, J. M. Jacobs, Measurement of heme concentration. *Curr Protoc Toxicol* **Chapter 8**, Unit 8 3 (2001).
540. B. Rothermel *et al.*, A protein encoded within the Down syndrome critical region is enriched in striated muscles and inhibits calcineurin signaling. *J Biol Chem* **275**, 8719-8725 (2000).

Acknowledgements

Many people contributed to this work and I cannot thank them enough. I would like to express my sincerest gratitude to everyone who ever helped, taught, or supported me, scientifically or personally, during these four years.

First, I would like to thank my supervisor Paolo Ettore Porporato for giving me the opportunity to join his lab where I enjoyed the freedom of thoughts, for the guidance, encouragements, and everlasting enthusiasm.

Many thanks my lab fellows who always cheer me up. I am especially grateful to Alessio Menga for his tremendous contribution, unconditional generosity, and friendly yet professional suggestions. Thanks a lot to Elisabeth, who shared the main project presented herein with me, for the patience, scientific, and personal exchanges. Thanks to Valentina for being always available to help, the recipes and motivational messages, and for proofreading this work. Thanks to Erica for the positivity, enthusiasm, and calling me each time for coffee breaks.

I have been very lucky to share the office/bench with people who provided invaluable technical suggestions: Ming, Marie-Claire, Jean, Federico, Jigen, Giovanna, Matteo, and Lidia. Also, thanks to Miriam Mistretta for taking care of the FLVCR breeding, and Laura Conti for FACS analysis.

I would also like to thank the outstanding folks in VIMM-Padova, where I had the chance to visit during my PhD: Especially Roberta (whose perseverance is particularly admirable) and Camilla, for their incredible kindness and patience.

I have met great friends and flatmates in Torino: Guohua, Mika, Sarah, Huayi, Sophie, Abhishek, Anna and Ruth. Thanks for the ceaseless support and for making me feel home, I will remember fondly our time discovering Italy and our culinary experiments done together.

人生の価値は、何を得るかではなく、何を残すかにある。

Torino, December 20th 2021